Chapter 21

ATMOSPHERIC COMPOSITION

Section 21.1 G.P. Anderson, H.S. Muench
Section 21.2 R.E. Good
Section 21.3 C.R. Philbrick
Section 21.4 W. Swider

The thin envelope of gas that surrounds the earth has evolved into the present state routinely accepted as our atmosphere. While the evolutionary history of the atmosphere has been studied by several scientists, this chapter deals only with our current understanding of the gas species present. The density and temperature structure and the nomenclature adopted to describe it have been discussed in Chapters 14 through 16.

The atmosphere can be viewed as a giant photochemical and dynamical experiment where aeronomers try, with limited snapshot glimpses, to understand and model its complexities. Nitrogen and oxygen in molecular and atomic forms contribute 99% of the total atmospheric composition to altitudes near 500 km. However, it is the minor species which comprise less than 1% of the atmosphere that are most important in establishing the chemical and dynamical behavior of the atmosphere. The minor species of interest include all forms of the molecules that result following dissociation by sunlight of not only the major species but also the less abundant molecules containing hydrogen and carbon. The noble gases also contribute to the sum of the minor species and provide inert tracers for examining the dynamical processes in the upper atmosphere. Sources such as meteorites, interplanetary dust, and the solar wind contribute additional minor species to the top of the atmosphere. Tropospheric clouds, aerosols, ocean spray, anthropogenic sources, and industrial pollution contribute sources of minor species from below. Within the past 10 to 15 years, the potential impact of manmade pollution in modifying the bulk properties of the atmosphere has been realized. The excited states of several significant minor species must be examined separately because of the special importance they have on particular chemical processes.

The role of the minor species in the atmosphere is most important to the following topics:

1. Absorbing and shielding the earth's surface from solar ultraviolet radiation
2. Establishing the radiation balance by absorption and emission of infrared radiation which establishes the thermal structure of the atmosphere
3. Absorption of the extreme ultraviolet radiation which leads, through ion chemistry, to the formation of the D, E, and F regions of the ionosphere

During the past 10 years significant advances in mass spectrometry, optical spectrometry, radiometry, and interferometry have rapidly improved our knowledge of the atmospheric composition. The region between 50 and 140 km can be directly sampled only by rocket borne instruments, but recent advances in remote sounding techniques are beginning to provide additional data of a more synoptic nature in this region. The lower altitudes can be probed by aircraft and balloons while the higher altitudes have been examined during the past 20 years by satellite instruments.

21.1 ATMOSPHERIC OZONE, BELOW 50 KM

Ozone, a minor, variable constituent of the atmosphere, is recognized as a dominant influence on both the present and past character of the earth's environment. It contributes less than 0.0001% to the total atmospheric mass, yet is the critical blocking filter for dangerous high energy solar radiation between 0.2 and 0.3 μm. The ozone redistributes this absorbed ultraviolet energy into the stratospheric thermal structure through collisional heating. Coincident with its absorption properties, ozone also emits radiation at longer wavelengths, serving as an effective cooling agent. Because ozone is chemically responsive to the concentrations of other minor constituents, some of which may be manmade, it has received much scientific and public attention.

Ozone (O_3) is composed of three atoms of oxygen and is gaseous under conditions found in the earth's atmosphere. The bent triatomic structure leads directly to its rich rotation-vibration infrared signature. Actual concentrations vary con-

siderably in time and space; the vertical distribution is dominated by the occurrence of a deep stratospheric layer with maximum values of 5×10^{12} m^{-3} [Krueger and Minzner, 1976]. Since this layer is embedded within the exponential decrease in total atmospheric concentration, ozone is often reported in units of mixing ratio. Typical mixing ratios of 0.03 to 0.10 parts per million by mass (ppmm) are found throughout the troposphere, with an abrupt increase beginning only at the tropopause. A stratospheric maximum mixing ratio of approximately 12 ppmm occurs near 35 km (Figure 21-1 [Dütsch, 1978]). (Note: Data referenced in Dütsch [1978] have been graciously supplied to AFGL by Professor Dütsch and were the basis for Figures 21-1, 21-10 and 21-11.)

The gas is a very powerful oxidant, readily attacking organic compounds (particularly double-bonded structures such as natural rubber) and will harm sensitive plant and animal tissue. Most life forms are tolerant to normal surface ozone amounts, but unusually high doses, even for brief periods, will produce damage [CRC, 1969; Parent, 1978]. For example, humans begin to smell ozone as concentrations increase above levels of 0.03 to 0.06 ppmm, and they might notice some discomfort at 0.05 to 0.1 ppmm. When doses exceed 0.6 to 0.8 ppmm, as might occur under extreme conditions near the ground or at jet aircraft altitudes, a two-hour exposure will produce strong irritation (reversible) to the pulmonary system and will lower resistance to infection. Doses of 15 ppmm are fatal to laboratory animals and will produce severe pneumonia-like illness in humans. Such high concentrations, although frequent in the middle atmosphere, will not occur naturally in the habitable environment.

Units for Atmospheric Ozone: Published reports on atmospheric ozone vary in their units for describing ozone content. The choice depends on the measuring technique as well as the intended user. Vertically integrated or total ozone is normally presented in "Dobson Units;" 1 DU equals 1 milli-atmosphere-centimeter (m-atm-cm), the equivalent vertical depth of pure ozone under standard temperature and pressure. The vertical ozone distribution is sometimes expressed in DU/km, but more frequently is presented as a mixing ratio, partial pressure, mass density, or number density. Units such as micrograms (μg), parts-per-million (ppm), and nanobars (nbar) are used to avoid including powers of ten. Some definitions and conversions are shown in Table 21-1.

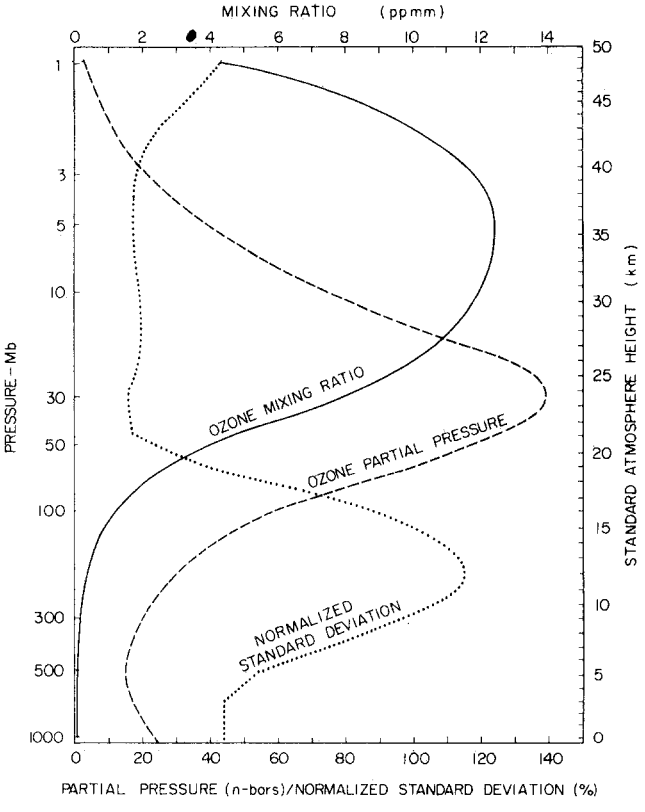

Figure 21-1. Global annual mean vertical distribution of ozone mixing ratio, ozone partial pressure, and normalized standard deviation.

21.1.1 Production

Atmospheric ozone originates primarily from photochemical reactions in the stratosphere, although some minor local tropospheric sources, both natural and anthropogenic, exist. The simplest stratospheric model for ozone production (first postulated by Sidney Chapman in 1930 [Chapman, 1930]) hypothesizes an equilibrium among the major forms of oxygen: O_2, O and O_3; the latter two are referred to collectively as "odd" oxygen. Molecular oxygen provides a resevoir of O atoms through photodissociation:

$$O_2 + h\nu \rightarrow O + O$$

where $h\nu$ is the quantized representation of the available solar ultraviolet energy; (h = Planck's constant and ν = frequency of the photon.* The atomic oxygen rapidly combines with the abundant O_2 in a three-body collision to form ozone:

$$O + O_2 + M \rightarrow O_3 + M.$$

The third reactant (M), most likely N_2 or O_2, is necessary for energy and momentum balance. The primary control to this ozone formation sequence is destruction through photodissociation:

*The frequency of solar energy required for photodissociation, ν, is specifically dependent on the structure of the molecule. To bring about O_2 dissociation, a photon has sufficient energy only at wavelengths less than 0.24 μm; for O_3, energy associated with wavelengths between 0.2 and 0.3 μm is most efficient, although other narrow wavelength intervals contribute. For more detail on the molecular physics governing absorption and photodissociation in the atmosphere, see, for example, Goody [1964].

Table 21-1. Ozone units definitions and conversions.

Ozone Parameter	Symbol	Typical Values
Total Ozone	Ω	305 DU or 0.305 atm-cm NTP
Mass Mixing Ratio	r_{3m}	5 ppmm or 5×10^{-6} g O_3/g air
Volume Mixing Ratio	r_{3v}	3 ppmv or 3×10^{-6} cm^3 O_3/cm^3 air
Partial Pressure	P_3	80 nbars or 80 μmb
Number Density	N_3	26×10^{17} molecules O_3/m^3
Mass Density	ρ_3	210 μg/m^3 or 2.1×10^{-7} kg/m^3

$$r_{3v}\ (\text{ppmv}) = 0.604\ r_{3m}\ (\mu\text{g/g}) = P_3\ (\text{nbar})/P(\text{mb}) = \frac{N_3\ T(\text{K})}{7.248 \times 10^{18}\ P(\text{mb})}$$

$$\rho\ (\mu\text{g/m}^3) = 7.97 \times 10^{17}\ N_3\ (\text{molecules/m}^3) = 21.41\ \Delta\Omega/\Delta Z(\text{DU/km})$$

$$P_3\ (\text{nbar}) = 1.732 \times 10^{-3}\ \rho_3\ (\mu\text{g/m}^3)\ T\ (\text{Kelvin})$$

$$\Delta\Omega = 0.790\ P_3\ \ln(P_a/P_b)\ \text{for a layer bounded by } P_a \text{ and } P_b$$

$$O_3 + h\nu \rightarrow O + O_2.$$

Direct recombination of O and O_3 or O and O is slow.

The observed diurnal modulation in ozone densities at and above the stratopause is a direct response to the loss of the photodissociative Chapman reactions at sunset. The photochemical balance between the odd oxygen species is abruptly shifted toward O_3, producing nighttime increases of approximately 10% at 50 km and 50% at 60 km [Herman, 1979; Lean, 1982; Allen et al., 1984].

The simple Chapman scheme predicts an ozone distribution with a properly located stratospheric maximum; however, the magnitudes of the calculated concentrations are generally higher than the measured amounts. Reactions with and among other trace constituents, including oxides of nitrogen, hydrogen, and chlorine, significantly alter the ozone photochemical balance [Crutzen, 1971; Molina and Rowland, 1974; Nicolet, 1975]. The full chemical description is so complex that the number of recognized reactions now exceeds one hundred and is continually being updated. (See for example NASA/JPL [1982] or Anderson et al. [1985].) The catalytic gas phase nature of many of these reactions has the net effect of accelerating the conversion of O and O_3 to O_2. For example, in the upper stratosphere the hydroxyl (OH) radical can react with ozone to form hydrogen dioxide (HO_2) plus molecular oxygen [Thrush, 1980]. The HO_2 rapidly combines with atomic oxygen, reforming OH and molecular oxygen. This cycle is written in chemical notation as

$$\begin{aligned} OH + O_3 &\rightarrow HO_2 + O_2 \\ HO_2 + O &\rightarrow OH + O_2 \\ \text{NET:}\quad O + O_3 &\rightarrow 2O_2 \end{aligned}$$

Similar catalytic reactions (where OH may be replaced by nitrogen or chlorine radicals) strongly modify stratospheric O_3 concentrations and are dominant in the tropospheric ozone chemistry [Fishman, 1985].

External modifications to the steady-state distribution of any of the catalytic constituents can perturb the momentary or longer-lived equilibrium ozone concentrations. For instance, mixing ratios near the stratopause respond to propagating planetary waves because of the strong temperature dependence of the hydrogen reactions [Barnett et al., 1975]. In addition, the occurrence of solar proton events has been associated with a marked, though temporary, reduction in ozone near the polar stratopause, initiated by downward transport of catalytically active nitric oxide from the mesosphere [Crutzen et al., 1975; Heath et al., 1977; Peters et al., 1981; Solomon et al., 1983]. It is, of course, the effects of long term anthropogenic deposition of catalytic reactants that remains a major concern. Photolysis of chlorofluorocarbons (for example, CCL_2F_2, CCl_2F), used primarily as refrigerants and aerosol spray carriers, provides an increasing stratospheric source of ClO [Stolarski and Cicerone, 1974; Rowland and Molina, 1975]. Since no other effective removal mechanism has been established for these compounds [NAS, 1979], their release at the surface is followed by slow but eventual (~10 years) diffusion and transport into the stratosphere. Ultraviolet solar energy then frees the ClO, initiating the potential reaction schemes with ozone and other constituents. Additional anthropogenic modification to the ozone balance, both in the troposphere and stratosphere, can be expected from the release of nitrogen and carbon compounds related to engine exhausts, fertilizers, biomass burning, and atmospheric nuclear testing [WMO, 1981; Angell and Korshover, 1983]. The extent and magnitude of ozone modulation directly attributed to man has not yet been firmly established theoretically nor experimentally. See Sections 21.1.4 and 21.1.7 for further discussion.

21.1.2 Transport

In the upper stratosphere the photochemical reaction rates are sufficiently fast that ozone equilibrium will usually be approached within hours. However, lower in the atmosphere dynamic processes begin to compete and eventually

dominate [Hartmann, 1978]. A simplified explanation for the loss of photochemical control of O_3 lower in the stratosphere is the disappearance of the ultraviolet sunlight necessary for dissociation of both O_2 and O_3. The ozone and molecular oxygen above 30 km remove almost 90% of the selective energy, reducing both the instantaneous source ($O_2 + h\nu$) and the sink ($O_3 + h\nu$) of odd oxygen. Photochemical reactions affecting ozone, including diurnal modulations, do occur in the troposphere; however, the source molecules are primarily those capable of responding to visible and near-ultraviolet light.

The relatively complete conversion to dynamic control, with ozone acting as a conserved tracer for the atmospheric motions, occurs by approximately 25 km [Cunnold et al., 1980]. The altitude and thickness of the transition zone between the photochemical and dynamic regimes varies with latitude and season, depending largely on the solar geometry and the strength and frequency of planetary wave disturbances. The transition zone is important because much of the poleward transport of ozone is thought to occur in this region [Garcia and Hartmann, 1980].

Eventually, ozone formed photochemically in the upper stratosphere reaches the tropopause and passes into the troposphere. The major exchange mechanism occurs in the vicinity of the midlatitude jet stream [Danielsen et al, 1970; Danielsen and Hipskind, 1980], although its efficiency is not well established. So little immediate blending occurs that measurements of ozone within a complex tropopause fold (Figures 21-2a and 21-2b) can determine whether air samples are of stratospheric or tropospheric origins [Shapiro et al., 1980; Roe, 1981]. Once in the troposphere, the lifetime for ozone is only a few days, since it is rapidly destroyed upon contact with the earth's surface. The removal is most efficient on vegetation, taking tens of minutes, but significant destruction also occurs over oceans, lakes, and even snow [Calbally, 1980].

In addition to its buffer role between the major stratospheric ozone sources and the ultimate surface destruction,

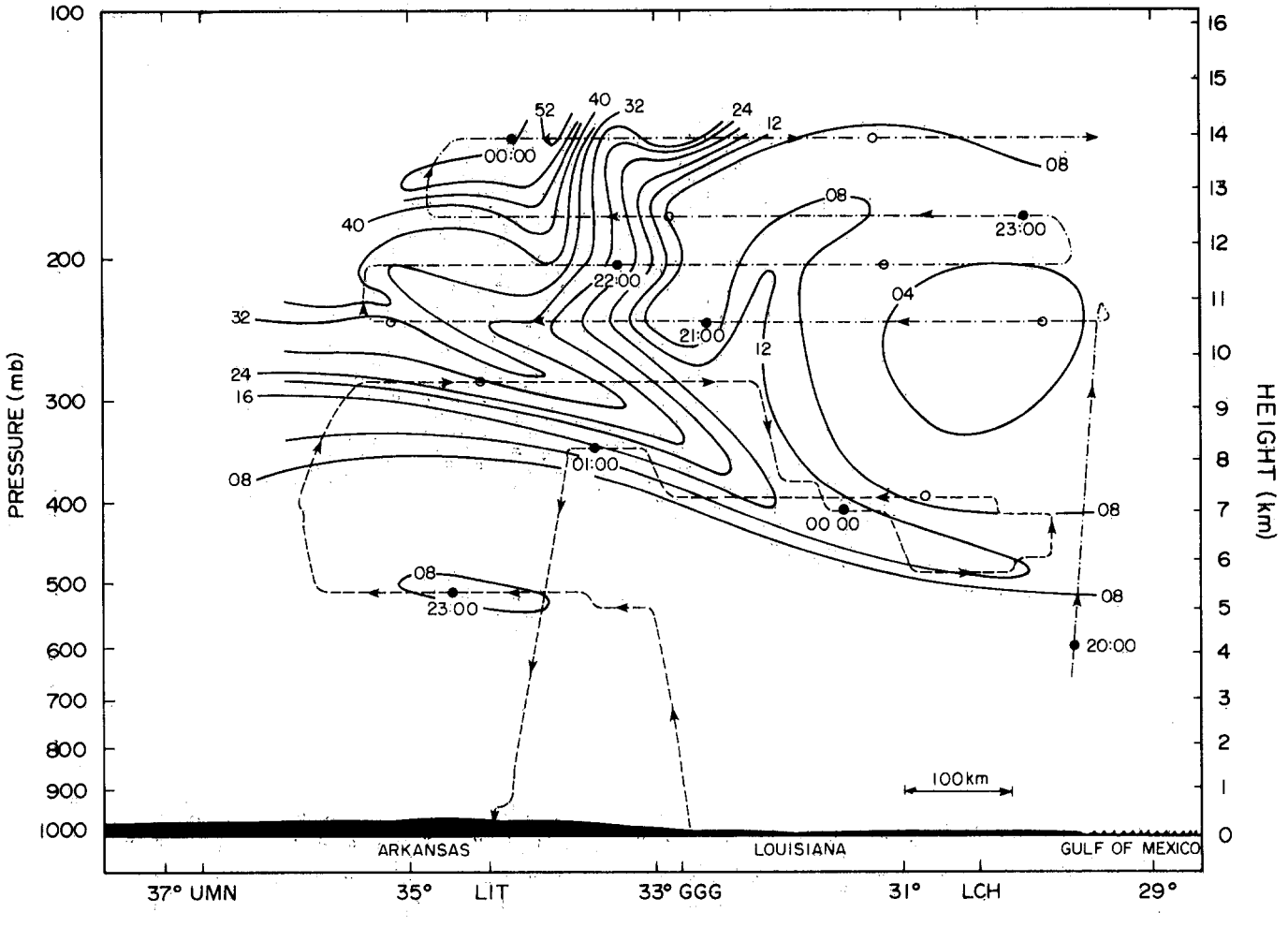

Figure 21-2a. Vertical cross section of ozone concentration (parts per hundred million) from western Missouri to western Louisiana. Analysis based on aircraft observations from 2000 GMT, 16 March 1978 to 0100 GMT, 17 March 1978 illustrates sloping "tongue" of ozone-rich air between 5 and 10 km [after Shapiro et al., 1980].

the troposphere is also an *in situ* chemically active environment. High temperature combustion in power plants, automobiles, and forest fires releases oxides of nitrogen, carbon, and other gases that near-ultraviolet sunlight can dissociate [Crutzen et al., 1975]. If gaseous organic compounds (such as petroleum fumes) are also present, the ozone equilibrium levels are significantly enhanced. These locally-increased concentrations contribute to the photochemical smogs found downwind of major cities. In addition, non-urban tropospheric chemistry can provide a globally-varying, non-anthropogenic *in situ* ozone source [Fishman et al., 1979; Liu et al., 1980]. The magnitude of this natural O_3 production is modified by the availability of such minor constituents as methane (from anaerobic metabolism [Ehhalt and Schmidt, 1978]), CO (from natural combustion sources [Persson, 1974], vegetation [Zimmerman et al., 1978], and NO (from lightning discharges [Noxon, 1976]). Direct O_3 photolysis is also enhanced by cloud and molecular scattering [Thompson, 1984]. Logan et al., [1981] have estimated some of the global pollutant budgets as almost evenly divided between anthropogenic and natural contributions. The balance varies with hemisphere, season, local weather, and chemical environments.

Because much research effort is being expended in understanding the tropospheric/stratospheric ozone cycle and its relation to man, comprehensive reviews of its chemistry and dynamics are published frequently. See, for instance, Brasseur [1982]; Brasseur and Solomon [1984]; *The Stratosphere, 1981* [WMO, 1981]; Logan et al., [1981]; *The NASA Assessment Report* [1984]; Whitten [1985]; Bojkov [1984].

21.1.3 Ozone Measurement

The complex control mechanisms—dynamic, radiative, and photochemical—that govern the global distribution of ozone prohibit a simple prediction of any local ozone en-

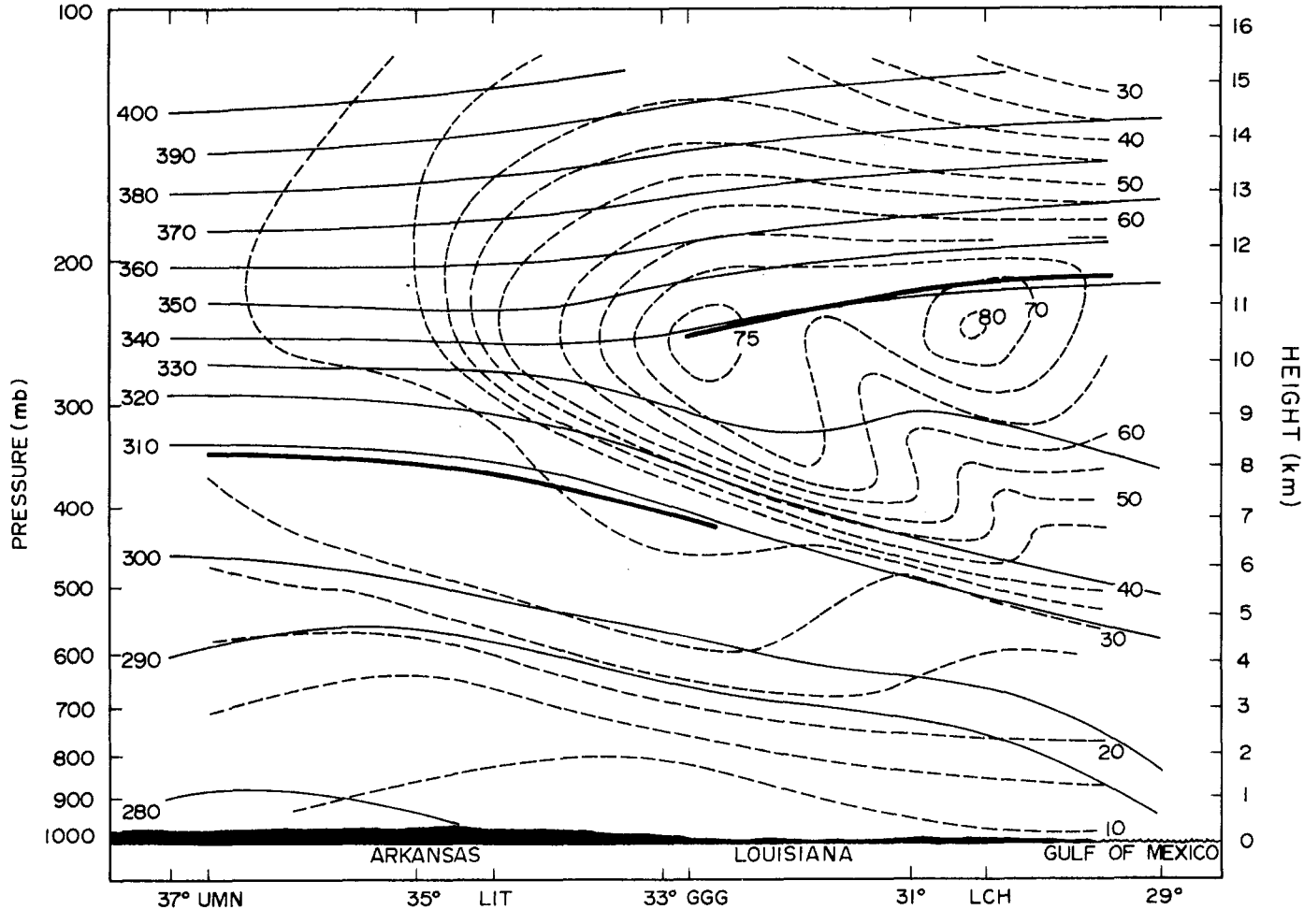

Figure 21-2b. Vertical cross section of potential temperature (thin solid lines), wind speed (dashed lines), and tropopause (heavy line) corresponding to previous figure. Potential temperature and static stability of air in the ozone tongue is characteristic of lower stratosphere air normally found north of the jet stream [after Shapiro et al., 1980].

vironment (see Section 21.1.7 on modeling efforts). A large complement of measurement techniques has been developed for both integrated column and vertical profile definition. The distinction is important because the total ozone overburden serves as the absorbing buffer for the solar radiation, while the vertical distribution governs energy deposition. Instrumentation based on the molecular, optical, and/or chemical properties of ozone has been adapted to ground and space platforms, including aircraft, balloons, rockets, and satellites.

In particular, the optical properties of ozone, both in the ultraviolet and infrared, provide rich instrumental applications. Spectral measurements of the differential absorption in the UV Hartley (0.2 to 0.3 μm) and Huggins (0.3 to 0.35 μm) bands are employed routinely. Beginning in the 1930s, ground station networks [Dobson, 1930; Dütsch, 1973] have been inferring atmospheric total ozone from observed variations in the measured solar irradiance within these wavelength intervals ("Unkehr/Dobson" and "M83" measurements). Observations of the zenith angle modulation of that same irradiance provide broad resolution (5–10 km) vertical structure information [Mateer, 1965].

Satellite instrumentation has created the opportunity for global coverage, a particular advantage when examining a constituent as variable as O_3 [Krueger et al., 1980]. Both total column and/or vertical distributions have been inferred from UV Hartley and Huggins band measurements [Anderson et al., 1969; Heath et al., 1973; Rusch et al., 1983]. These same absorption techniques, when used on balloons and rockets [Krueger, 1973; Mentall et al., 1980; Lean, 1982] provide an invaluable calibration test for the sounding networks. (For information on general mathematical formulations and algorithms for inversion of remotely-sensed atmospheric data, see for example Twomey [1977], Deepak [1977], Rodgers [1976], or Gordley and Russell [1981]).

Another satellite-based ultraviolet system infers ozone distributions by observing the occultation of a light source (solar or stellar) crossing the earth's horizon [Hays and Roble, 1973; Aiken et al., 1982; Millier et al., 1981]. For this method the vertical resolution is 4 to 6 km. Ultraviolet lasers have also been used to remotely probe the ozone layer from the ground (with potential satellite applications [Remsberg and Gordley, 1978]); the synchronous, atmospherically reflected laser signal [Pelon and Megie, 1982] provides both altitude (that is, distance from the source) and density information. An *in situ* application of ozone's ultraviolet absorption properties, used primarily on large balloons and rockets, includes both source and detector separated by a chamber filled with a local air sample [Ainsworth and Hagemeyer, 1980; Profitt and McLaughlin, 1983; National Academy Report, 1982; Robbins 1980]. Pumping efficiency then governs the vertical resolution (< 20 m, see Figure 21-12).

Infrared systems to measure atmospheric ozone employ the thermal emission of the triatomic molecule, usually in the strong vibration-rotation band near 9.6 μm. Infrared rocket and satellite instruments have determined both total ozone [Prabhakara et al., 1970; Lovill et al., 1978; Crosby et al., 1980] and vertical profiles [Gille et al., 1980b; Remsberg et al., 1984; Stair et al., 1984] using nadir (vertical) or limb viewing, respectively. The thermal dependence of the emission requires simultaneous temperature sounding; however, it is independent of solar insolation, providing full diurnal coverage. Vertical resolution is approximately 5 km throughout the stratosphere and lower mesosphere (12–65 km).

The longer wavelength (infrared, millimeter, and microwave) emission/absorption properties of the ozone molecule (see Harries [1980] for a general discussion) are also atmospherically useful. The shape and equivalent width of the spectrally-isolated lines provide independent measures of both density and pressure. In particular, the emission spectrum in the wavelength interval 50–300 Ghz (1–6 mm), as measured from the ground [Parrish, 1981] has been proposed for inclusion in the standard global sounding network. Similarly, molecular line parameters have been measured in absorption against the solar background spectrum [Farmer et al., 1980; Louisnard et al., 1983; Weinrab et al., 1984].

Fluorescence radiation at 1.27 μm, emanating from ozone photolysis ($O_3 + h\nu \rightarrow O_2 + O$), has been measured on a limited number of high-altitude rocket experiments [Weeks et al., 1978]. More recently this experiment, as part of an instrument complement on a spinning satellite, has measured global O_3 mixing ratio profiles up to 90 km [Thomas et al., 1983].

Small *in situ* chemical detectors (which record iodide or chemiluminescent reactions to the presence of ozone) are frequently used as portable ground and aircraft sensors or as expendable balloon and rocket-borne ozonesondes [Regener, 1960; Komhyr, 1971; Hilsenrath, 1980]. Their calibration is demanding, often requiring normalization of the profile to some other measurement; however, fine scale vertical structure (<50 m) measurements can be achieved at low cost. Mass spectrometers, because of their size and complexity, are not used routinely as sondes; they can be mounted on either aircraft or balloons and provide detailed *in situ* observations, including altitude profiles of isotopic abundances [Mauersberger, 1981].

A summary of the instrument systems currently being used for climatological analyses of ozone in the stratosphere and troposphere is presented in Table 21-2. The values for relative accuracy are based on instrument intercomparisons as well as observational consistency. They do not include the systematic differences (6%–8%) found between the total column ozone measured by Dobson ground-based instruments, which are considered the standard, and the ozone measured both by the back-scattered UV and infrared satellite instruments. The accuracies stated for the electrochemical and chemiluminescent sondes have been enhanced by an independent measurement of total ozone as part of

Table 21-2. Major data sources for atmospheric ozone below 50 km.

Type of Observation	Period	Obs./Mo.	Vertical Range	Vertical Resolution	Horizontal Resolution	Relative Accuracy	Comments
1. World Ozone Network (a)							
Dobson Spectrophotometer	1930–84 +	700	0–60 km	(Total Ozone)	Point	±3%	Cross-calibration of instruments difficult
M83 Instruments (filter)	1960–84 +	250	0–00 km	(Total Ozone)	Point	±8%	Problems with filter stability
Dobson Spectrophotometer-Umkehr	1935–84 +	60	0–60 km	6 km	Point	±6%	Requires clear sunrise or sunset
Electro-chemical Ozonesondes	1965–84 +	30	0–30 km	0.3	Point	±3%	Pump efficiency problems above 25 km
2. AFGL North America Network (b)							
Chemiluminescent Ozonesonde	1962–64	40	0–30 km	0 km	Point	±8%	Problems with chemiluminescent materials
3. NASA-OGO4 (BUV) (c)	1967–69	1000	30–50 km	7 km		±10%	Monthly means (daytime only)
4. NASA Nimbus 4 Satelite System (c)							
Back-Scattered Ultraviolet (BUV)	1970–77	18 000	0–60 km	(Total Ozone)	200 km	±3%	Excellent global coverage (daytime only)
Back-Scattered Ultraviolet (BUV)	1970–77	1800	22–60 km	7 km		±6%	Excellent global coverage (daytime only)
IR Interferometer Spectrometer (IRIB)	1971–72	40 000	0–60 km	(Total Ozone)	100 km	±3%	Excellent global coverage (day and night)
5. USAF DMSP Satellites, F1-F4 (d)							
Infra-Red Spectrometer	1977–80	3 000 000	0–60 km	(Total Ozone)	100 km	±7%	Cross-path scanning, excellent coverage, day and night
6. NASA Nimbus 7 Satellite System (c)							
Solar Back-Scattered UV (SBUV)	1978–84 +	32 000	0–60 km	(Total Ozone)	200 km	±3%	Excellent global coverage (daytime only)
Solar Back-Scattered UV (SBUV)	1978–84 +	32 000	22-60 km	7 km	200 km	±6%	Excellent global coverage (daytime only)
Limb IR Monitor of Stratosphere (LIMS)	1978–79	32 000	12-60 km	4 km	200 km	±7%	Excellent day-night coverage, requires cryogenics
Total Ozone Mapping Spectrometer (TOMS)	1978–84 +	1 200 000	0-60 km	(Total Ozone)	60 km	±3%	Cross-path scanning, daily global coverage
7. Solar Mesospheric Explorer (SME) (c)							
Back Scattered Ultraviolet (BUV)	1982–84 +	30 000	30–60 km	7 km	200 km	±5%	Global covering,
Near Infrared	1982–84 +	30 000	30–60 km	7 km	200 km	±5%	limb scanning (daytime only) Global covering, limb scanning (daytime only)

Data Sources.
(a) Archived at World Ozone Data Centre, Atmosphere Environment Service, 4905 Dufferin St., Downsview, Ontario, Canada M3H5T4a (Data published bimonthly in *Ozone Data For The World*)
(b) Archived at NOAA Environmental Data and Information Center, National Climatic Center, Federal Building, Asheville NC 28801
(c) Archived at National Space Science Data Center, Goddard Space Flight Center, Code 601, Greenbelt MD 20771
(d) For information: Dr. J. Lovell, PO Box 808, Lawrence Livermore Laboratories, Livermore CA 94550

the calibration. Further details on ozone instrumentation may be found in *The Stratosphere 1981* [WMO, 1981] or more recent reviews.

21.1.4 Total Ozone: Its Global Distribution and Variability

The most complete ozone data set is that for total ozone. Ground-based measurements have been made for over 40 years and a global network (albeit coarse) has existed for 25 years [London et al., 1976]. With the introduction of satellite sensors (see Table 21-2), the frequency, spatial coverage, and relative accuracy of such soundings have all been improved [Hilsenrath and Schlesinger, 1979]. Combined ground and satellite determinations allow the formulation of climatologies that describe the distribution and variability of total ozone on scales ranging from hours to years.

Hemispheric contour plots of the annually averaged column amounts of ozone and their normalized standard deviations are shown in Figures 21-3a and 21-3b. The distributions graphically demonstrate the impact of global dynamics on ozone in the troposphere and lower stratosphere (the contributions from these lowest altitudes to the total column is approximately 70%). Subsequently, the features of any total ozone distribution correlate well with those of similarly formulated maps of standard meteorological data near the tropopause [Miller et al., 1979]. For example, the structure in Figure 21-3 is negatively correlated with the annual mean height of the tropopause [Dobson, 1963]. The hemispheric asymmetries that persist in these annual means are primarily

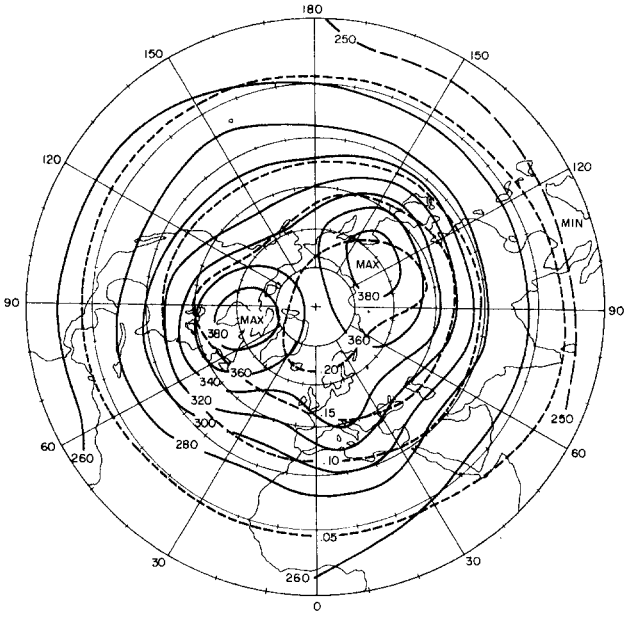

Figure 21-3a. Total ozone northern hemisphere, annual mean (m atm cm).Dashed lines indicate normalized standard deviation.

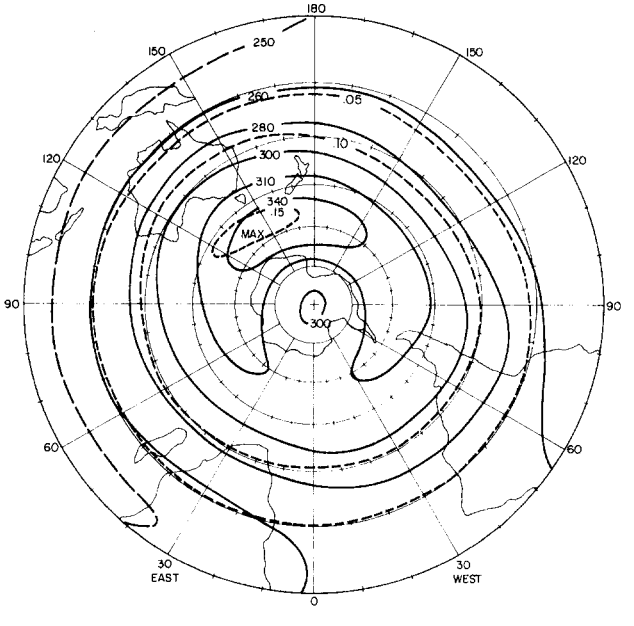

Figure 21-3b. Total ozone southern hemisphere, annual mean (m atm cm). Dashed lines indicate normalized standard deviation.

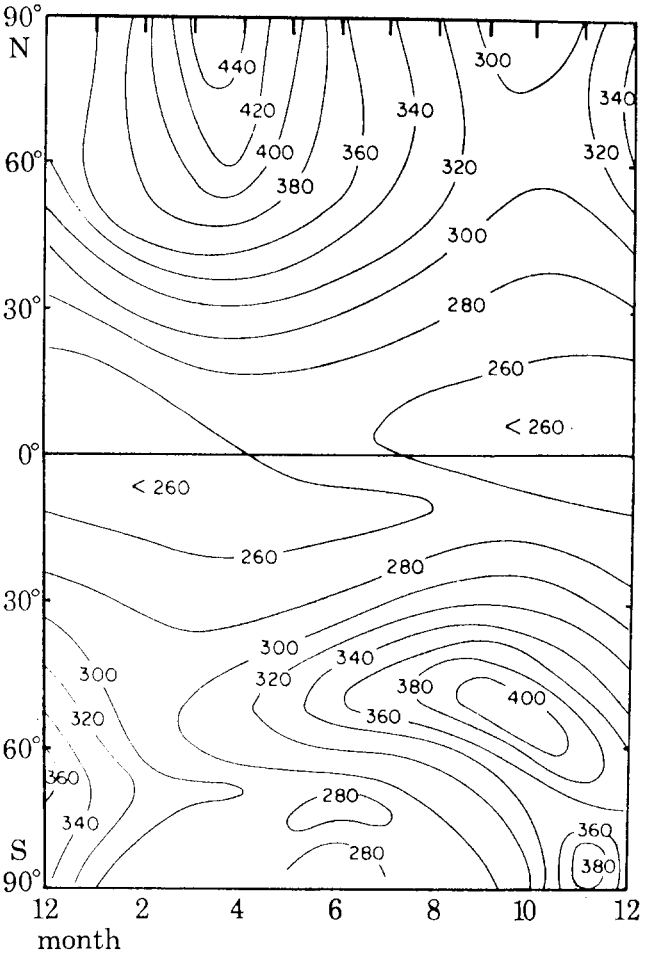

Figure 21-4. The observed zonally averaged distribution of total ozone (m atm cm). The low latitude minima and the hemispheric differences immediately reveal the importance of the dynamics of transport processes.

a consequence of geographically-stable, planetary-scale winter weather patterns [Hartmann, 1977]. See Holton [1980] for a more complete description of the controling dynamic processes.

The local variability in total ozone can be very large and, again, highly correlated with the instantaneous (synoptic) global weather system. Similarities between the features of the daily, satellite-derived total ozone measurements and the standard synoptic height maps of the 200 mb pressure surfaces have been observed [Shapiro et al., 1982]. If instantaneous O_3 column amounts can be rigorously related to the global tracking of planetary waves, the pertinent satellite data could be added to the meteorological inputs for weather prediction.

Total ozone climatology exhibits natural variations in both amplitude and period, ranging from daily to interannual, and perhaps even solar cycle [Wilcox et al., 1977; London and Reber, 1979]. The dominant influence on the variability is seasonal, as depicted in Figure 21-4. A harmonic analysis of ground (or satellite) data bases provides insight into the latitudinal dependence (Figure 21-5). At middle and high latitudes the annual period dominates, with additional power in the aperiodic component. Near the equator the total variability is small, allowing the statistical identification of semi-annual, annual, and quasi-biennial (26 month) waves [Angell and Korshover, 1983]. Anthropogenic modification of total ozone has yet to be established [Reinsel, 1981; Bloomfield et al., 1983]; its magnitude, as predicted by theoretical calculations, would be very small (a decrease of <0.1%/year, Logan et al., 1978; Penner, 1982; Wuebbles et al., 1983; NASA Academy Report, 1984), but over long time scales could be dramatic. Given ozone's large variability plus current instrumental limitations (both precision and intercalibration: see Table 21-2) man's influence is not yet detectable.

21.1.5 Vertical Profiles

The modified "Chapman" photochemical mechanism is sufficient to describe the basic vertical distribution of ozone; its dominant feature, as discussed previously, is the pronounced ozone layer, a region in the stratosphere of maximum concentrations (actually resulting from complex photochemical production and subsequent transport). However, measurable amounts of O_3 also occur throughout the troposphere and into the mesosphere. The climatological variability within this framework is similar to that for the total column, with additional complications from the altitude-dependent chemistry and dynamics.

An annual, globally-averaged vertical distribution (as in Figure 21-1) has a broad peak in mixing ratio (ppmm) near 35 km (note that the choice of units governs the definition of the maximum). The normalized standard deviation of the composite profile suggests that the variability is greatest near 12 km and 45 km (related respectively to dynamics at the tropopause and chemical responses to thermal and/or solar disturbances below the stratopause). The annual variances in Figure 21-1 are minimized by the geographical dominance

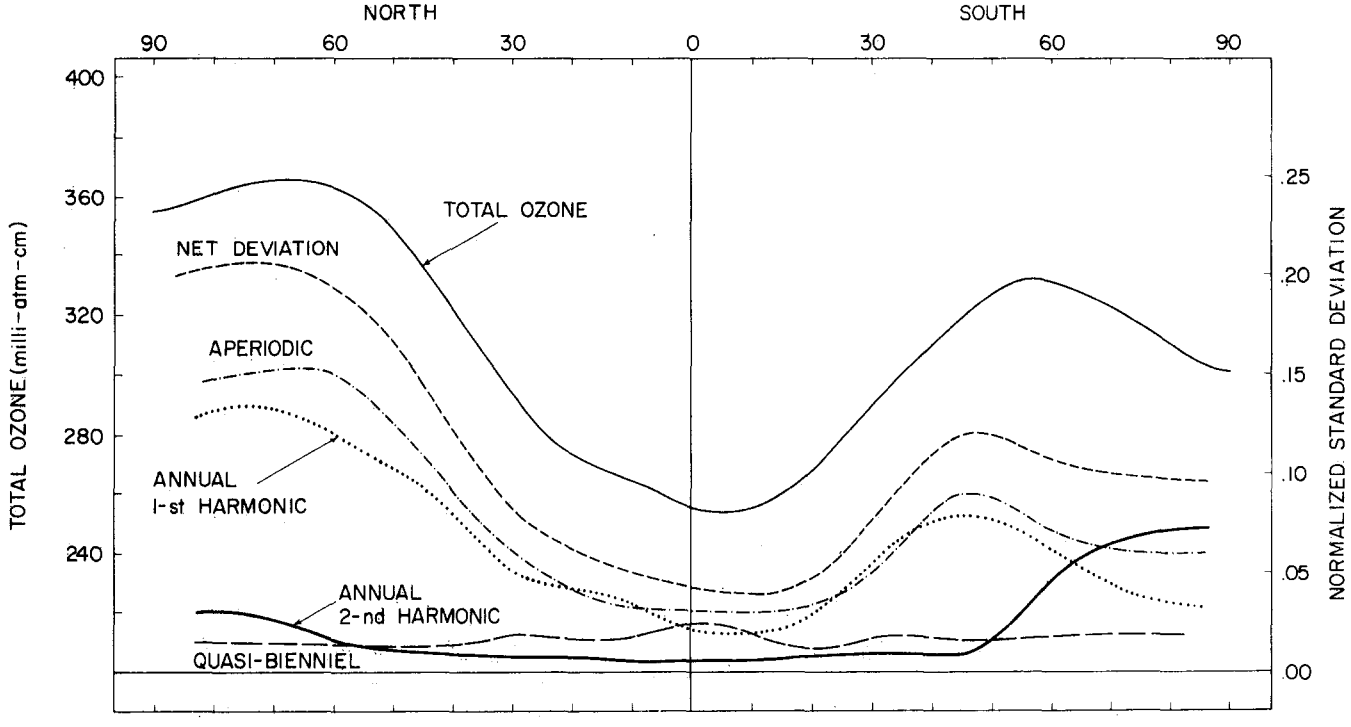

Figure 21-5. Meridional profile of total ozone and the components of temporal variability.

of large areas of relatively stable ozone profiles in the summer and low latitude; winter and equinoctial profiles actually exhibit much greater natural excursions over both long (seasonal) and short (hours to days) time scales.

As with total ozone, the first order variations about a basic vertical distribution can be ascribed to seasonal effects [Dütsch, 1978; Klenk et al., 1983]. Systematic satellite measurements provide the opportunity to examine these annual progressions as a function of latitude, particularly at and above 10 mb (approximately 30 km). For instance, sample one-month zonal mean distributions for 1979 (Figures 21-6a, b, c, d), based on satellite-derived, backscattered ultraviolet data [McPeters et al., 1984], encompass the seasonal features of the middle and upper stratosphere. Towards the winter pole the mixing ratio contours maximize at increasingly higher altitudes (often above 40–45 km, that is, 2–3 mb), in response to weaker photodissociation and stronger transport. The summer hemisphere, however, exhibits a stably located maximum. This imbalance reverses hemispheres with the seasons and is symmetric at the equinoxes. A statistical analysis of a similar data set for the years 1970–71, in combination with balloon measurements [Klenk et al., 1983], suggests that the zonal mean variance can be typically reduced to a four-parameter function (including latitude and day of the year) for selected pressure levels. The 1971 seasonally-dependent profiles for high,

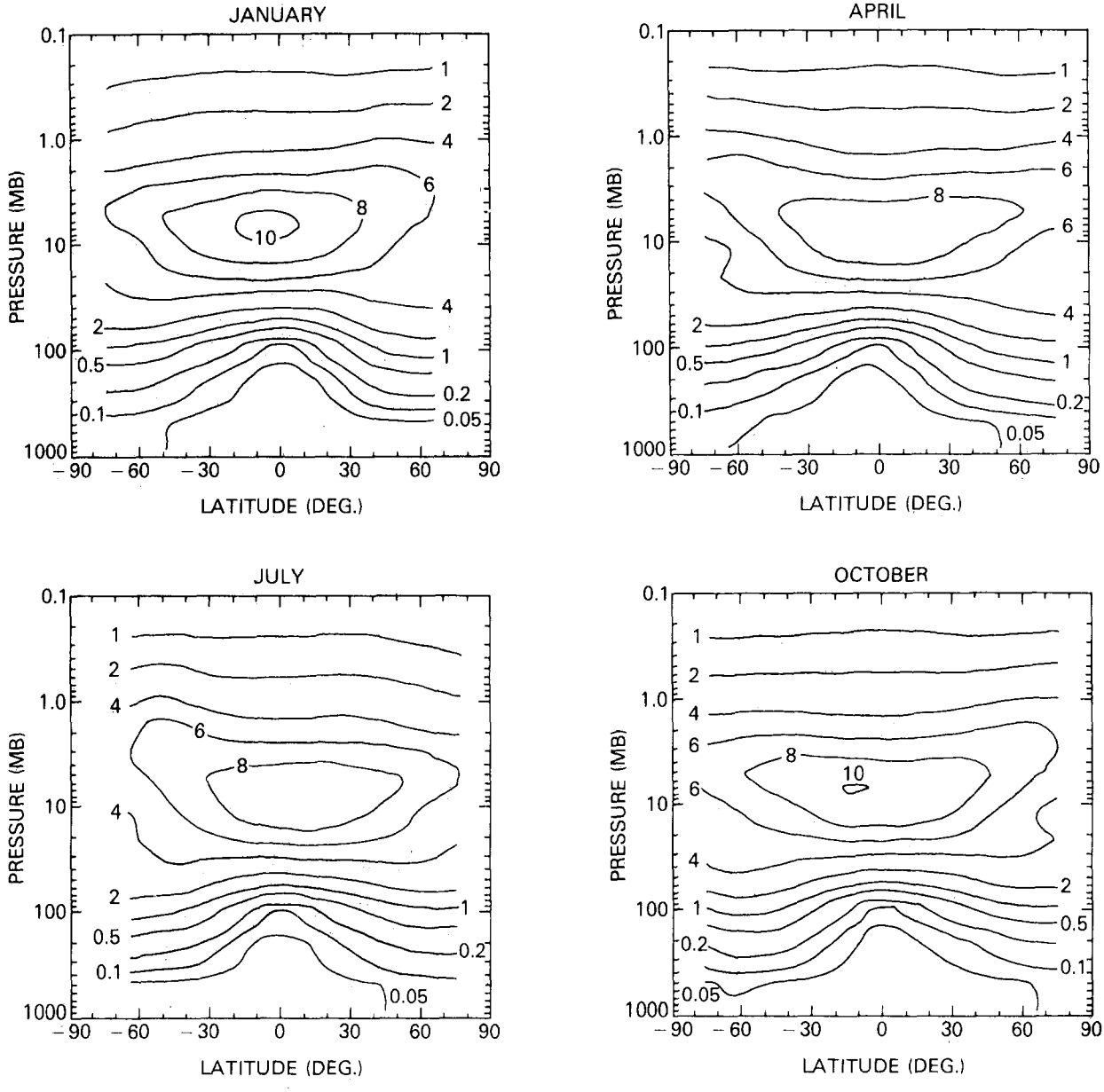

Figure 21-6. Latitude-height cross sections of the ozone mixing ratio (ppmv) for the months of (a) January, (b) April, (c) July, and (d) October. All profile measurements within 10° latitude zones were averaged each month. [McPeters et al., 1984].

middle, and low latitude intervals appear in Figures 21-7, 21-8, and 21-9.

A meridional cross section of annually-averaged ozone partial pressure was computed from approximately 15 years of ozonesonde ascents and Uhmkehr observations [Dütsch, 1978] and is presented in Figure 21-10. The pattern of partial pressure (solid lines) closely parallels the location of the tropopause, and the percent variability about the mean (dashed lines) is greatest where the slope of the tropopause is greatest—the region of midlatitude storm activity. The amplitude of the annual cycle (expressed as percent) is presented in Figure 21-11, together with the month of maximum value. In general, largest seasonal changes are near the tropopause with a peak in the spring season. Large seasonal changes are also found above 45 km at polar latitudes due to the effects of the annual temperature cycle on ozone photochemistry.

In addition to the seasonally-controlled annual cycle, other natural periods can also be extracted from the climatological profiles. The quasibiennial oscillation appears at low latitudes (mirroring the total ozone behavior) and is most apparent near the mixing ratio maximum [Angell and Korshover, 1983]. At 40 to 45 km there is a weak indication of a solar rotation response [Gille et al., 1984] which is again statistically separable only at low latitudes where the profiles exhibit the most stability. A semiannual oscillation in ozone mixing ratio has been identified over a broad range of pressures (1–30 mb) and latitudes [Maeda, 1984].

The day-to-day longitudinal distribution is not well represented by the zonal means. In general, the hemispheric weather patterns that influence total ozone can be identified in the vertical profiles; the details, however, depend on the atmospheric level being sounded. In the troposphere, O_3 is usually a reliable tracer for weather conditions, but it is also subject to *in situ* chemical reactions [Fishman, 1985]. Near the tropopause and in the lower stratosphere, planetary scale wave patterns are accurately replicated in the ozone field

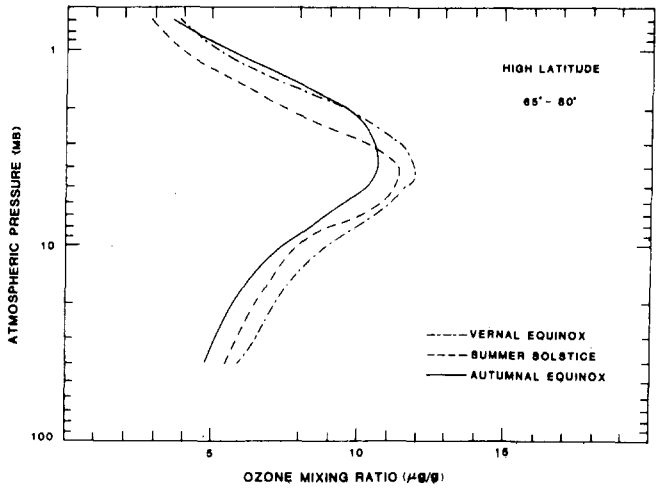

Figure 21-8. As in Figure 21-7 but for high latitude region 65°–80°.

[Gille et al., 1980b; Remsberg et al., 1984]. In the upper stratosphere the ozone concentrations begin to be modulated directly by the temperature sensitivity of the controlling chemistry [Barnett et al., 1975].

Preliminary climatological averages of ozone mixing ratios on constant pressure surfaces have been compiled for a range of time periods, from daily to seasonal, annual and interannual (in the stratosphere, see Remsberg et al., [1984], Barth et al., [1983], Nagatani and Miller [1984]; in the troposphere, see Bojkov [1983]). The complex structure of these climatologies is an integral response to the total atmospheric environment, including the instantaneous and gradient behavior (temporal and geographic) of temperature, transport parameters, and other minor constituent concentrations. Satellite platforms and field programs are currently being designed to address these complexities with complementary instrumentation (for instance, the Upper Atmosphere Research Satellite mission scheduled for the late 1980s [NASA Research Summaries, 1984]).

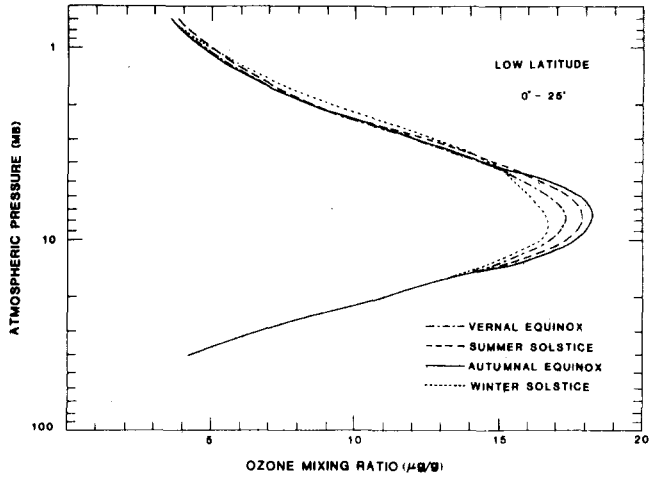

Figure 21-7. Ozone mixing ratio versus atmospheric pressure for the low latitude region <25° [Klenk et al., 1983].

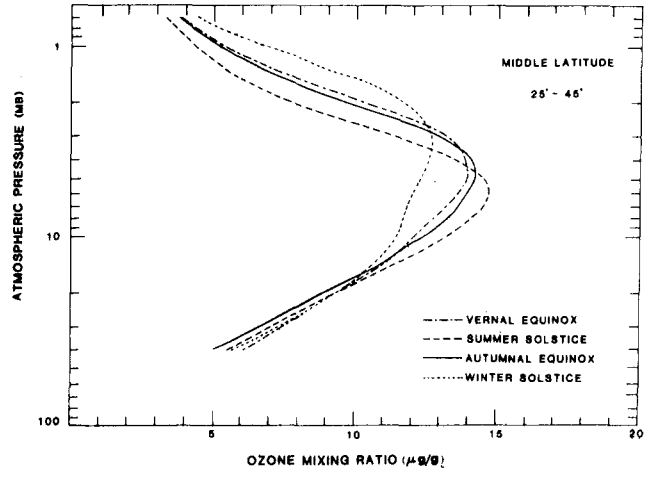

Figure 21-9. As in Figure 21-7 but for the middle latitude region 25°–45°.

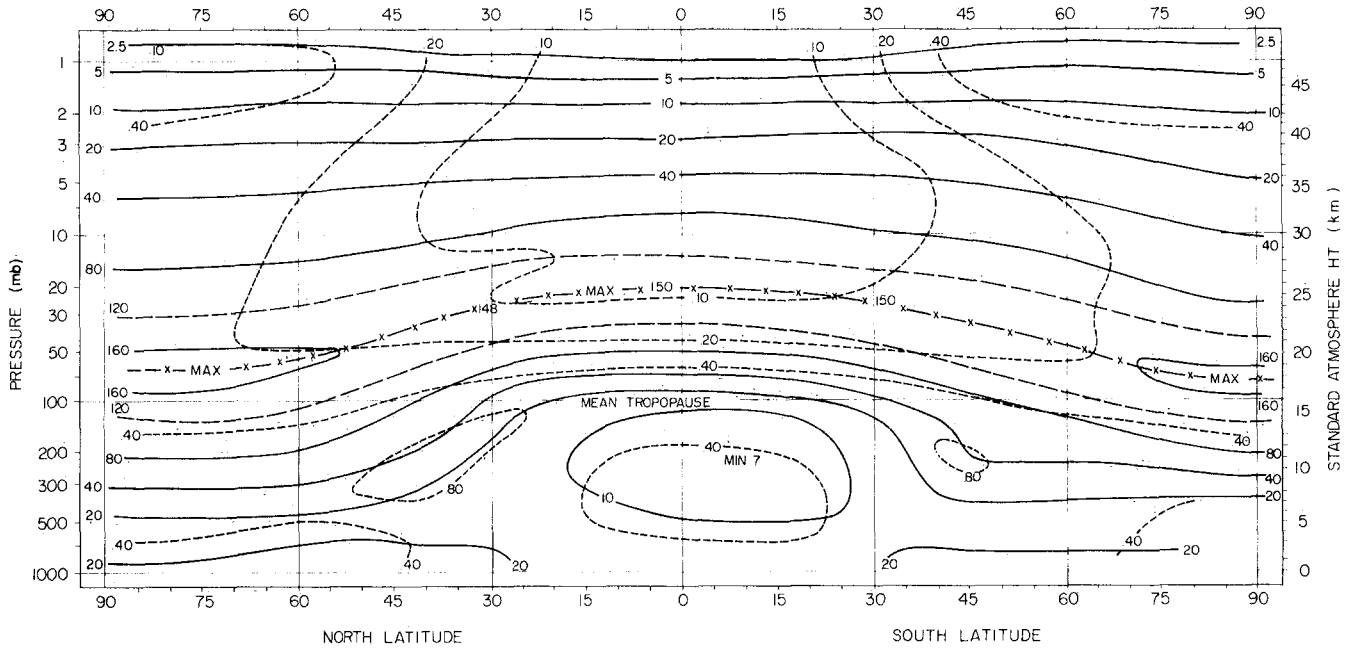

Figure 21-10. Pole-to-pole cross section of annual zonally averaged ozone (nbar) and normalized standard deviation (%).

21.1.6 Spatial and Temporal Scales of Ozone Variability

Satellite instrumentation cannot provide sufficient resolution (temporal, vertical, or horizontal) to describe modulations brought about by small-scale thermal waves and turbulence. This smaller scale ozone variability (Figure 21-12) as measured by *in situ* aircraft, balloon, and rocket data, appears as narrow horizontal layers (a kilometer or less in thickness) often extending for hundreds of kilometers along and tens of kilometers perpendicular to the flow [Dütsch, 1969]. These features can sometimes be directly related to tropopause folding, but even minor dynamic perturbations can lead to such turbulent stratification in a hydrostatically stable atmosphere [Dewan, 1981]. This structure in the ozone distribution, although prevalent, is not detectable from re-

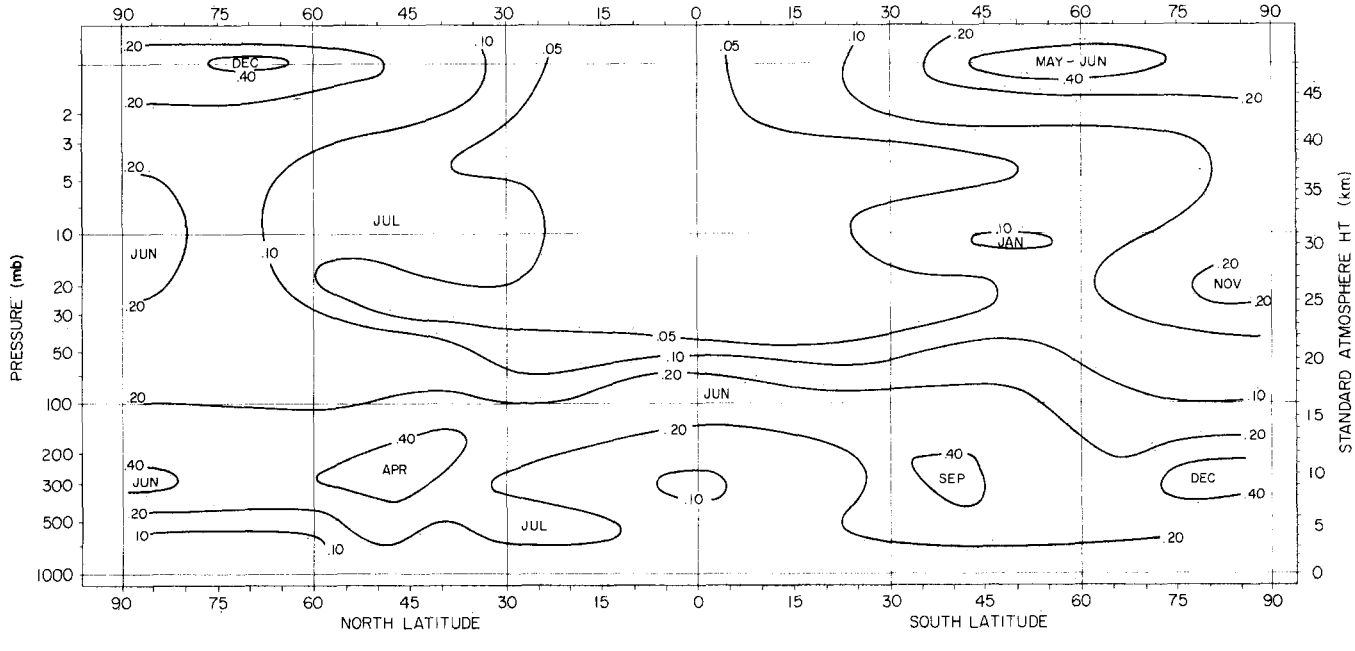

Figure 21-11. Pole-to-pole cross section of seasonal ozone variability (%) and time of maximum.

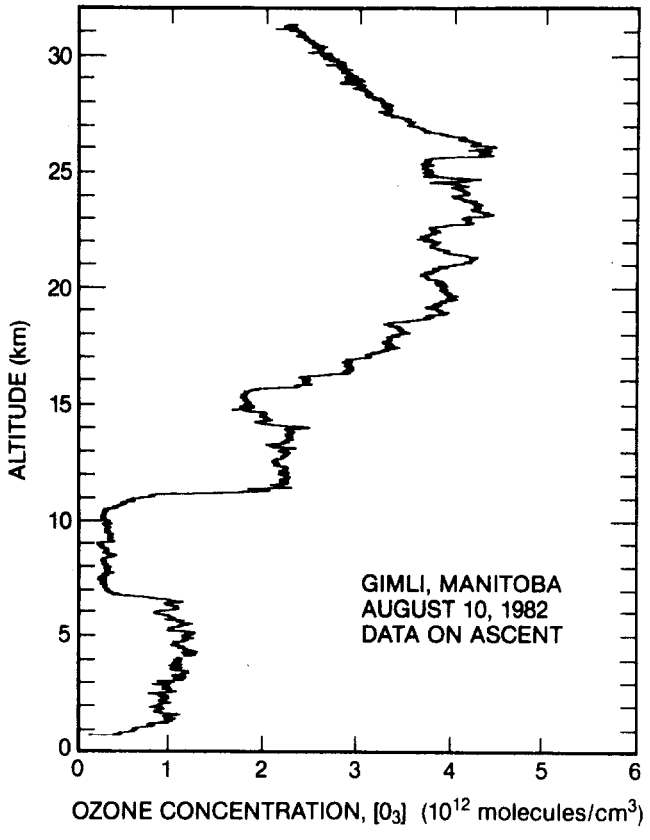

Figure 21-12. Vertical ozone ascent on 10 Aug 1982 over Gimli, Manitoba (3200 m) based on sampling at 5 m (1 s) intervals, illustrating thin layers of relatively high ozone concentration [Profitt and McLaughlin, 1983].

mote platforms (see Section 21.1.3 on measurement techniques). Measurements of both total ozone (ground-based) and local concentrations (*in situ* aircraft sampling at 11 km) have been used to estimate their respective degree of autocorrelation with east-west distance (Figure 21-13). The 11 km autocorrelation decays more rapidly, indicating a greater sensitivity to small scale motions; total ozone is

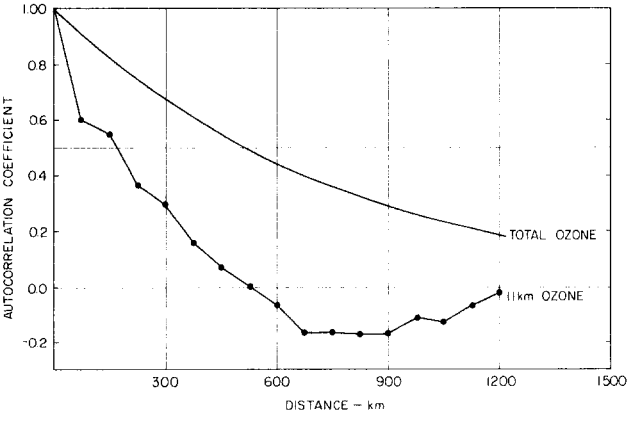

Figure 12-13. Variation of autocorrelation of total ozone with distance (E-W) in mid latitudes.

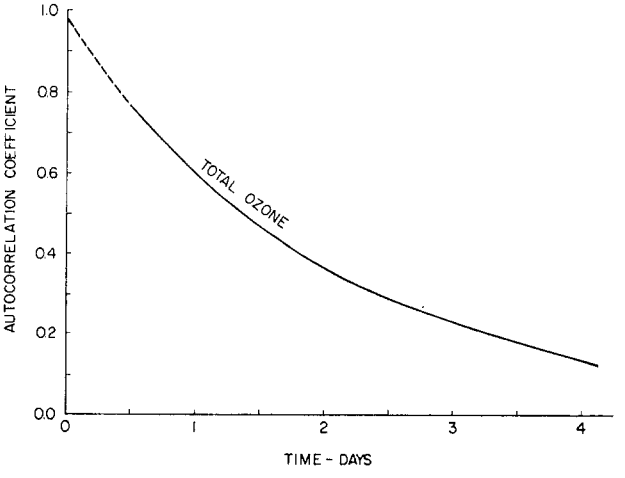

Figure 21-14. Decay of autocorrelation of total ozone with time.

associated with thicker atmospheric layers controlled by large scale dynamics. The time variation of the autocorrelation for total ozone (Figure 21-14) shows significant contributions from both long (seasonal) and short periods [Wilcox, 1978].

21.1.7 Mathematical Models

Mathematical descriptions of the atmospheric ozone layer date back to the original scheme of Chapman [1930]. However, as the natural variability in both total column abundance and vertical distribution were recognized, the need for more extensive modeling efforts becomes apparent. This requires balancing complex chemical schemes with an understanding of the feedbacks between ozone and the radiative-dynamic environments. The current formulations encompassing one, two, and three dimensional models, do not focus strictly on the ozone layer, but rather attempt to parametrize broader aspects of the surrounding atmosphere. [See the NASA Assessment Report, 1984 for a more complete discussion.]

The simplest conceptual models (other than simulations of local volume or laboratory environments) are one dimensional, with altitude or pressure as the vertical coordinate [Sze et al., 1980]. Because of the large number of individual chemical reactions necessary for atmospheric description [NASA/JPL, 1982], models typically divide the minor constituents into "families" [Wofsy and McElroy, 1974]. For example, molecular concentrations of NO or NO_2 are not calculated separately within the original mathematical formulation. Instead, a solution for the whole group of nitrogen-oxygen compounds (known as NO_x's) is found first; other standard families include the O_x (oxygen-oxygen), HO_x (hydrogen-oxygen), and ClO_x (chlorine-oxygen) compounds. Temporal modulations (with scales ranging from minutes to years) can be accomodated in 1-D models; broader applications include sophisticated parametrization of clouds,

radiative transfer, vertical transport, and exchange mechanisms.

Two-dimensional models can now include most of the photochemical and some of the temporal precision of the 1-D cases [Gidel et al., 1983]. The second dimension parametrizes the latitudinal gradients that exist on a global scale. The zonal mean temperature structure is incorporated either as input or internal calculation. There are various mathematical approaches adopted in 2-D models, including boundary conditions, radiative balance, integration timesteps, solution methods, etc. (see Table 2.14 in *The Stratosphere 1981* [WMO, 1981]). One of the most critical assumptions, however, is the method of approximating the eddy (non-zonal) motions, both in the horizontal and vertical directions. Pragmatic solutions have centered on "diffusion" coefficients which take the form of three dimensional tensors (K-theory, as proposed by Reed and German [1965]). An alternative mechanistic description, where at least part of eddy modulation is considered quasi-harmonic, has also been formulated [Garcia and Solomon, 1982].

The value of two dimensional models lies in their ability to replicate zonally-averaged measurements. They successfully reproduce the seasonal excursions of both the mean "total" ozone (Figure 21-3) and the mixing ratio maximum (Figure 21-6). Because they can incorporate time-dependent mechanisms (such as proposed solar rotation and solar cycle variability or minor constituent fluctuations [Garcia et al., 1984]), they have been used in conjunction with one dimensional models to investigate possible trends in ozone concentration. Prediction capability, however, is tied to the reliability of the input assumptions (including dynamic parametrization, reaction rates, and the atmospheric measurements against which they are evaluated). As an example of "model-related" sensitivities, the one dimensional models models formulated in 1979 forecast a potential 16%–18% anthropogenically-caused decrease in column O_3 by the year 2020. Models in 1982–83 predict a possible overall decrease of 2%–4% but with a strong altitude dependence and possible nonlinear response [Maugh, 1984; NASA Assessment Report, 1984]. The differences are related to updated determinations of critical chemical "constants", including the temperature and pressure dependence of reaction rates and absorption coefficients. Obviously, a definitive answer on the future of the ozone layer cannot yet be established, but 1 and 2-D models will facilitate the mathematical exploration of the possibilities.

Three dimensional models attempt to realistically simulate the fluid-dynamic, radiative, and photochemical characteristics of the atmosphere. The two general types of grid models (with variables proportional to latitude, longitude, and height) are similar to those used for large-scale meteorological forecasting. The global circulation models (GCMs) employ a comprehensive set of equations governing the radiation field, 3-D motions on a sphere, and at least part of the chemistry [Fels et al., 1980]. The lower boundary conditions can extend down to the solid-earth orography (including driving regons such as the Tibetan plateau) or are predicated on a modulated tropopause, initiating global stratospheric motions wth tropospheric forcing. The mechanistic models (MMs) parametrize general planetary characteristics (artificial ocean-continent boundaries, for instance), sacrificing realistic accuracy for increased flexibility. They have been used to simulate stratospheric warmings and their perturbing effect upon the whole global ozone distribution [Lordi et al., 1980; Hsu, 1981].

The horizontal and vertical resolution requirements for adequate three-dimensional representation of the physical processes affecting ozone are less rigid than those for tropospheric meteorological predictions. However, the grid sizes still serve as a limiting factor for computation speed and flexibility. These models are costly for trend predictions, but do provide the forum for physical understanding of climatological behavior and transport. For a fuller discussion, see *The Stratosphere 1981* [WMO, 1981] or more recent reviews.

21.2 MINOR CONSTITUENTS IN THE STRATOSPHERE

The existence of the stratosphere was discovered at the turn of the century by unmanned balloon measurements which found the temperature increased with altitude. The first understanding of the stratosphere occurred when Dobson suggested the heating was the result of UV absorption by ozone in the late 1920s. Chapman's pioneering photochemical explanation of the stratosphere in the 1930s remained the definitive description into the 1950s. The explosive research and recognition of the complex chemical nature of the stratosphere began inauspiciously in the late 1960s with the fear that supersonic transports (SSTs) would cause irreparable damage to the earth's environment. It is now recognized that the stratosphere has a very complex chemical composition generated from natural and man made sources. Furthermore, anthropogenic sources may lead to future changes of the stratosphere. The description that follows is not complete and must be updated and corrected as new information becomes available. A series of reports by government agencies and committees indicates the world wide interest in environmental protection and on-going stratospheric research - SCEP [1970], CIAP [1974], COMESA [1975], COVOS [1976], NAS [1975, 1979], DOE [1979], UNEP [1979, 1980], NASA [1977, 1979], FAA [1979], and WMO [1982]. These reports contain excellent summaries of minor constituents and theoretical and model explanations. Each succeeding years report contains new or revised information. Journal reviews of the stratosphere [Cicerone, 1975; Hudson, 1979; Murgatroyd, 1982; and Solomon, 1983] contain succinct descriptions of the minor con-

stituents. Emphasis has now shifted from measurements to developing a better understanding of the mechanisms and chemical processes identified earlier.

Neutral minor constituents of the stratosphere can be grouped into large categories of radicals, sources of radicals, sinks of radicals, and sources for the formation of aerosols. The radicals are conveniently divided into groups of odd oxygen—$O(^3P)$, $O(^1D)$, $O_2(^1\delta)$, $O_2(^1\Sigma)$, O_3; odd hydrogen —OH, HO_2, H_2O_2; odd nitrogen—NO, NO_2, HNO_3, N_2O5, HO_2, NO_2; and odd halogens—Cl, ClO, F, Br, BrO, HCl, HF, $ClONO_2$. The precursors or sources of the radicals are constituents such as N_2O, CH_4, H_2O, SF_6, CO_2, H_2, CCl_4, CH_3CCl_3, CH_3Cl, C_2HCl_3, CCl_3F, CCl_2F_2 and other chlorofluoromethanes (CFMs), some of which are introduced into the troposphere at mixing ratios greater than 100 pptv; these represent the major source of chlorine in the stratosphere. Stratospheric NO_x derives from nitrous dioxide (N_2O) transported from the ground. Large solar proton events could contribute appreciable amounts of NO in the upper stratosphere. The products of radical–radical reactions, which are generally inert, serve as sinks for the radicals. They also form shortlived storage from which radicals can be released by photolysis or oxidation. The major sinks are HCl, HNO_3, HNO_4, $ClONO_2$, H_2O_2, O_3, HO_2, NO_2, HOCl, N_2O_5, $COCl_2$, COFCl and HF. The minor constituents that are believed important as sources for aerosol growth are H_2SO_4, SO_2, COS and NH_3.

The following description of the minor constituents (Sections 21.2.1 through 21.2.9) has been excerpted from the World Meteorological Organization publication "The Stratosphere 1981 Theory and Measurements" with the permission of NASA. Even though this information can be found in a more detailed form in the original publication, it has been included in this chapter to provide the reader with the basic facts of stratospheric composition and a more complete picture of "Atmospheric Composition" as a whole.

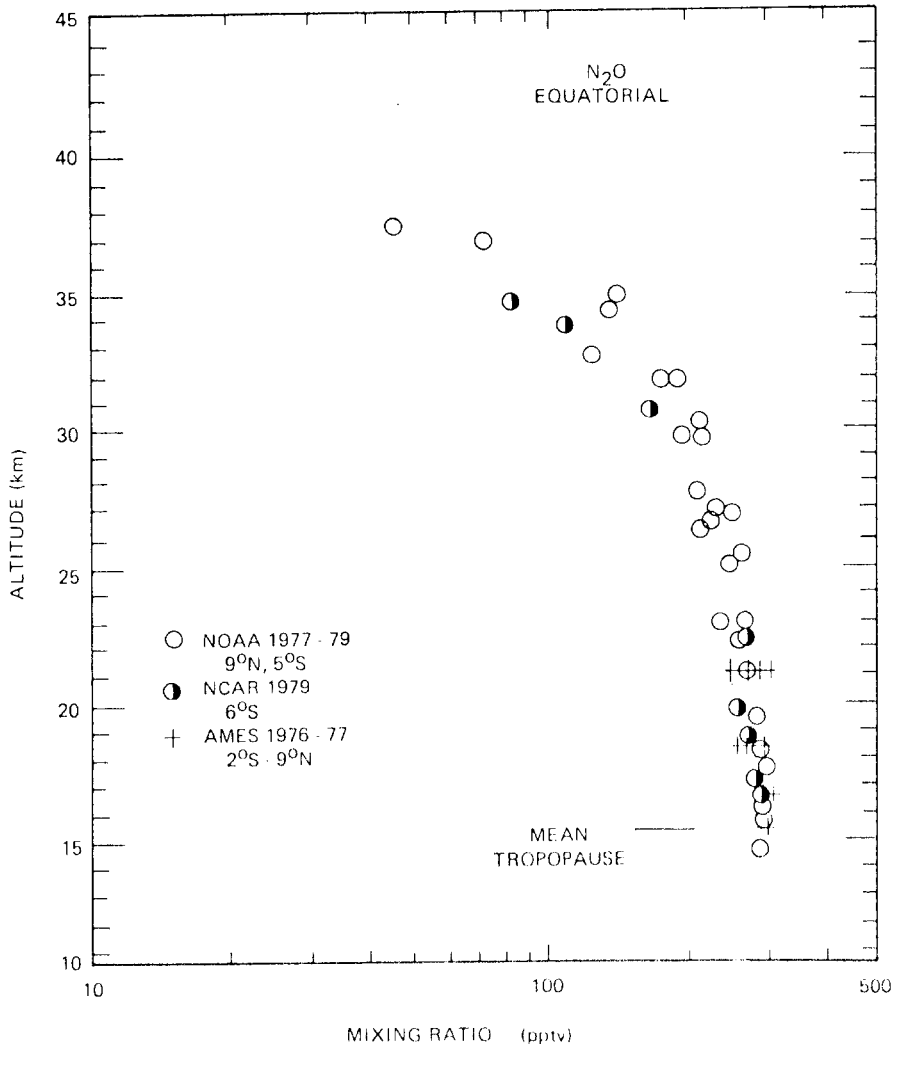

Figure 21-15. Measurements of N_2O as a function of altitude in the equatorial region.

21.2.1 Nitrous Oxide, FC-11, FC-12, and Methyl Chloride (N_2O, CCl_3F, CCl_2F_2 and CH_3Cl)

Since 1975 a number of measurements have been made of the stratospheric concentrations of N_2O, CCl_3F and CCl_2F_2. Four field programs have been particularly extensive, all involving laboratory analysis by gas chromatography of air samples collected by balloon-borne samplers. The few measurements made by *in situ* balloon-borne infrared techniques [Farmer et al., 1980] are consistent with these data. The four research groups are

NOAA Goldan et al. [1980, 1981]. Balloon-borne evacuated grab samples.

NCAR Heidt et al. [1975]. Balloon-borne cryosampler.

KFA Volz et al. [1981]. Balloon-borne cryosampler.

Ames Tyson et al. [1978]; Vedder et al. [1978]; Inn et al. [1979]; Vedder et al. [1981]. Balloon and aircraft-borne cryosampler.

The results from three of these groups, compared over narrow latitude bands, are shown for equatorial latitudes in Figures 21-15, 21-16, 21-17 and mid-latitudes in Figures 21-18 through 21-23. They are in good agreement with one another. The two single altitude profiles obtained by infrared techniques at 32°N and 30°S also fall in between the trends shown in Figures 21-18 through 21-23. The data for CCl_3F and CCl_2F_2 have been corrected for the well-established secular increase in each using tropospheric measurements.

The vertical profile of CH_3Cl as obtained from gas chromatographic measurements on cryogenic samples from balloon flights over Southern France (44°N) is shown in Figure 21-24. The data, although largely scattered, clearly show a very rapid decrease from 600 ppt at the tropopause to about 20 to 40 ppt at 30 km indicating the short lifetime of CH_3Cl.

21.2.2 Carbon-Containing Species

21.2.2.1 Carbon Dioxide (CO_2). Vertical profiles of CO_2 have been measured routinely at NCAR using a volumetric technique, achieving a precision of ± 3 ppm. About the same precision has been achieved at the KFA using gas-chromatography. The precision of the gas-chromatographic measurements has recently been improved to ± 0.5 ppm [Volz et al., 1981]. Additional measurements have been made by Bischof et al. [1980] using the infrared absorption technique, and by Mauersberger and Finstad (1980) using a balloon-borne mass spectrometric method.

The individual profiles of CO_2 are plotted in Figure 21-25. As can be seen, the older volumetric and GC-data show a large scatter but no significant gradients of the CO_2 mixing ratio in the stratosphere. However, from the more recent data [Volz et al., 1981] and from the measurements by Bischof et al. [1980], a weak but significant gradient is observed in the lower stratosphere, namely the CO_2 mixing ratio is found to decrease by about 6 to 7 ppm between the tropopause and 20 km altitude.

21.2.2.2 Carbon Monoxide (CO). Although the experimental data are extremely limited, the measurements cover

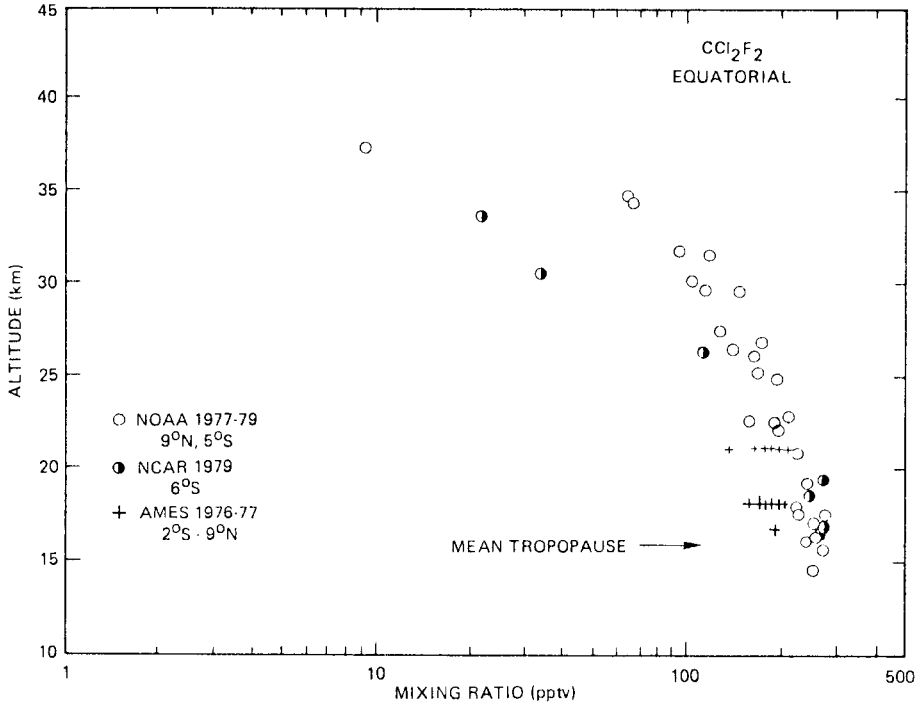

Figure 21-16. Measurements of CF_2Cl_2 (FC-12) as a function of altitude in the equatorial region.

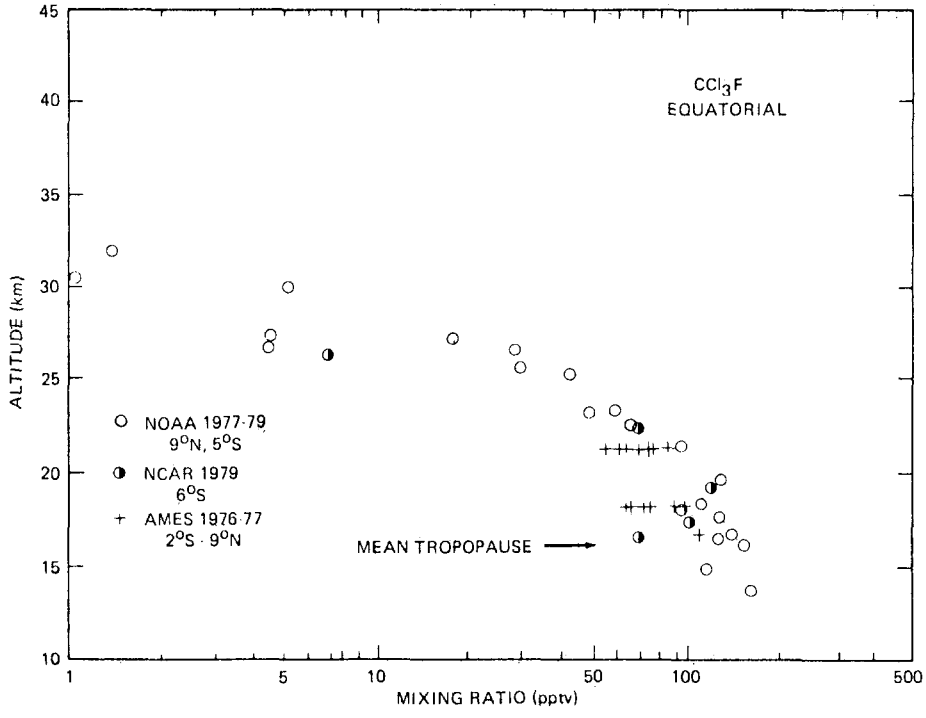

Figure 21-17. Measurements of CCl_3F (FC-11) as a function of altitude in the equatorial region.

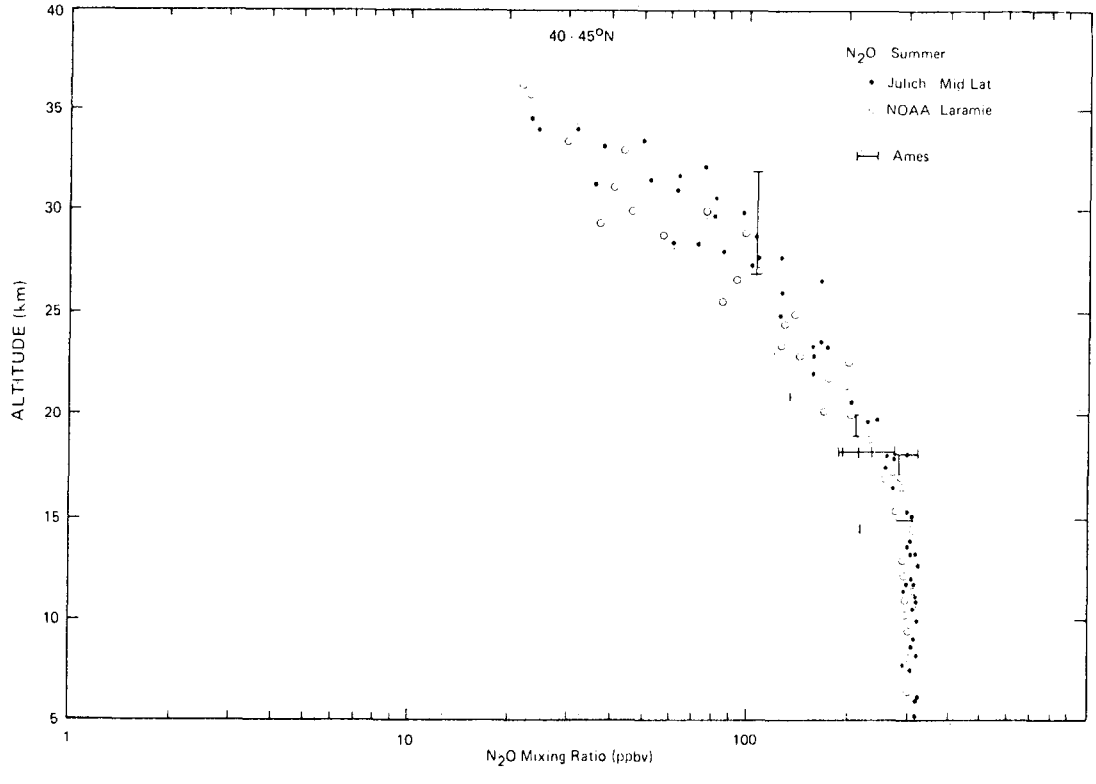

Figure 21-18. Midlatitude summer vertical profile of N_2O.

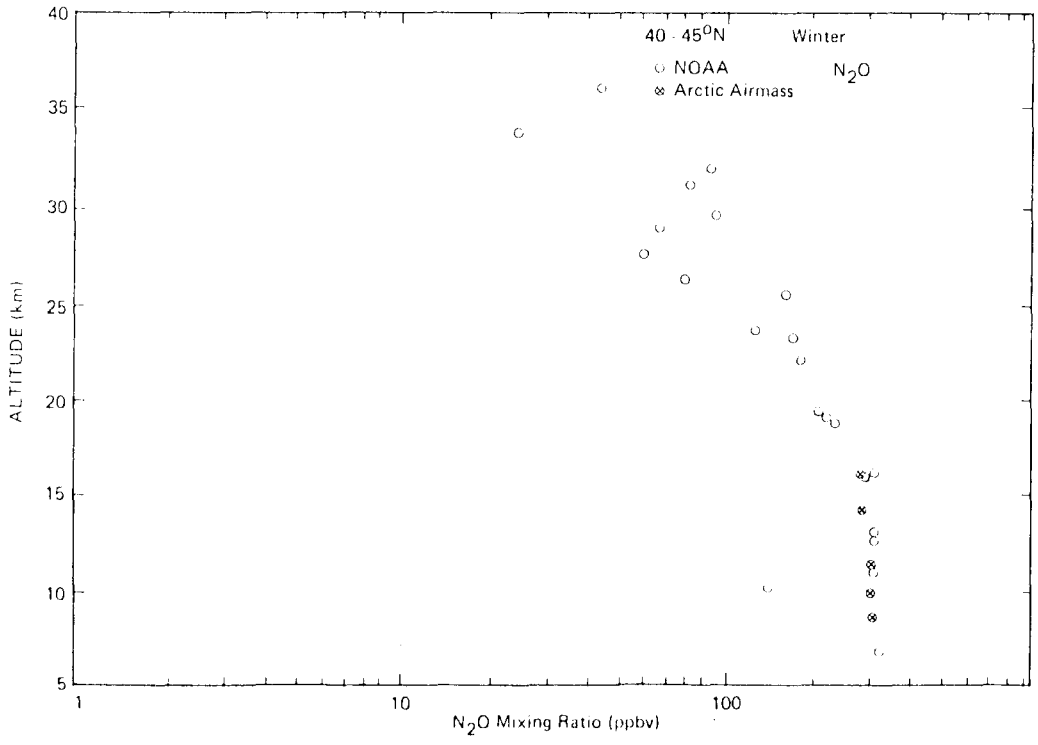

Figure 21-19. Midlatitude winter vertical profile of N_2O.

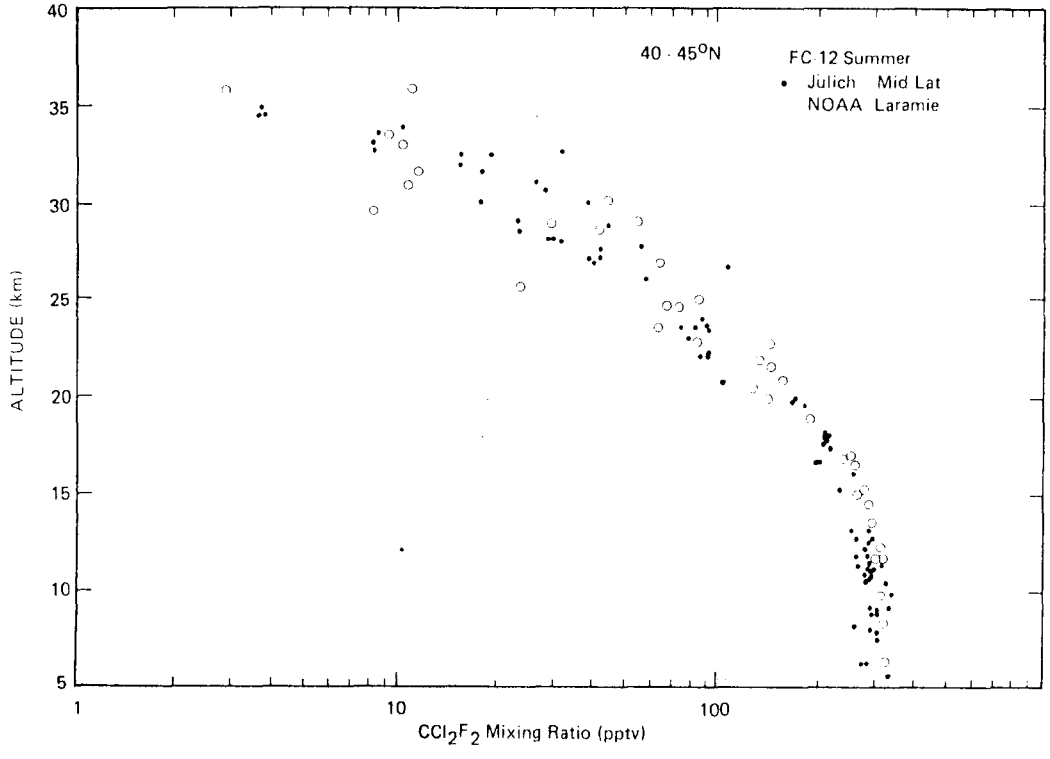

Figure 21-20. Midlatitude summer vertical profile of CCl_2F_2 (FC-12).

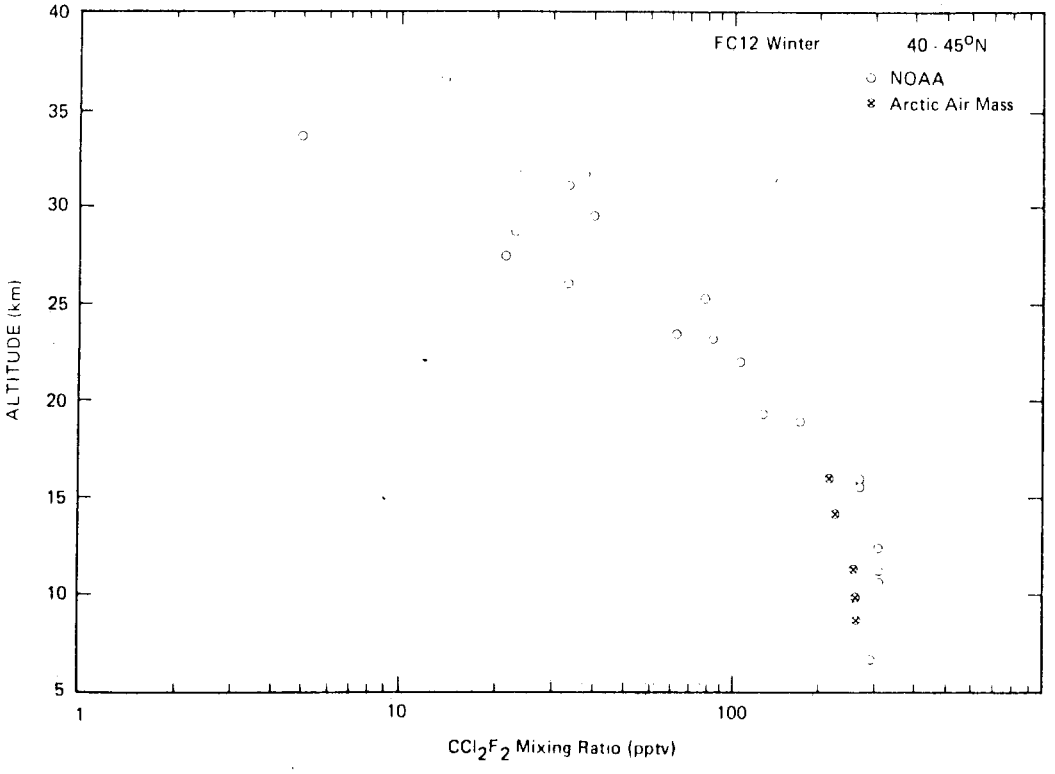

Figure 21-21. Midlatitude winter vertical profile of CCl_2F_2 (FC-12).

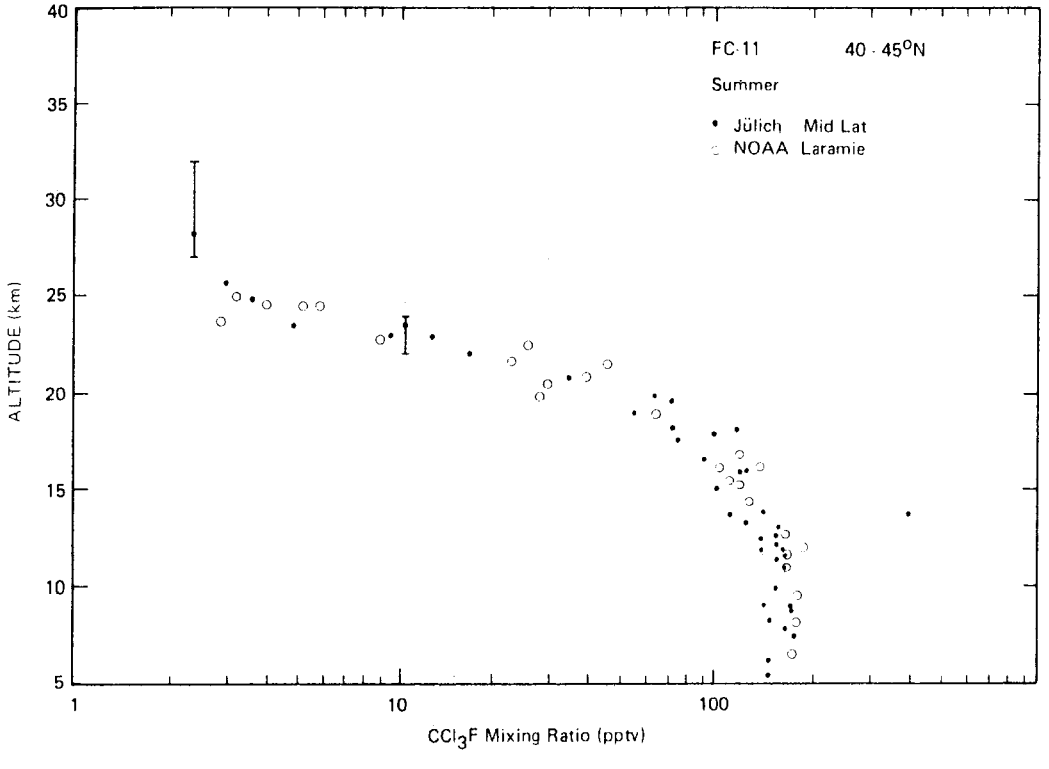

Figure 21-22. Midlatitude summer vertical profile CCl_3F (FC-11).

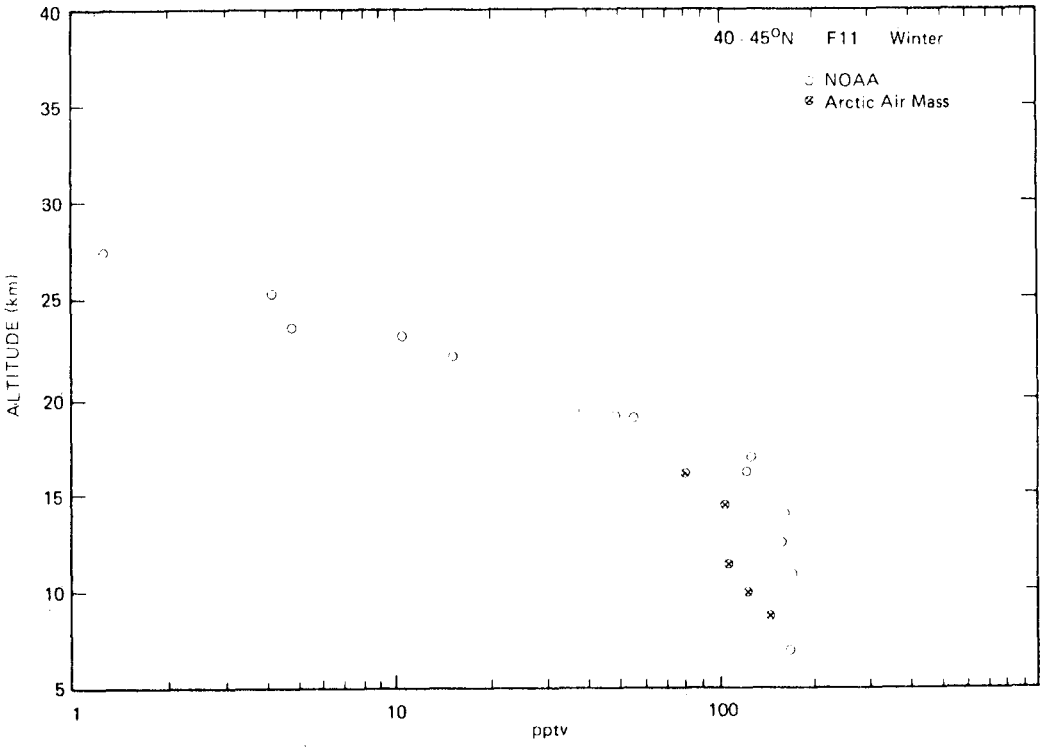

Figure 21-23. Midlatitude winter vertical profile of CCl_3F (FC-11).

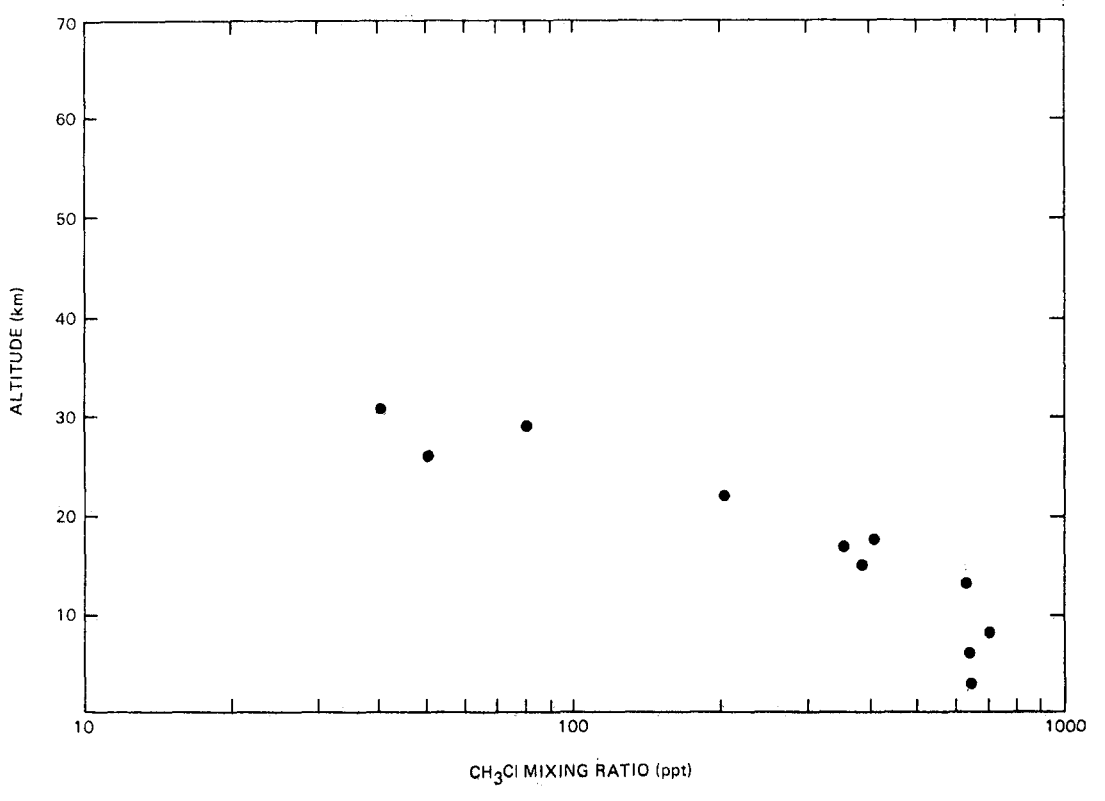

Figure 21-24. Vertical profile of CH_3Cl at 44° northern latitude. The data were measured by GC-FID and GC-MS [Penkett et al., 1979] from samples collected cryogenically during a joint balloon program [Fabian et al., 1979].

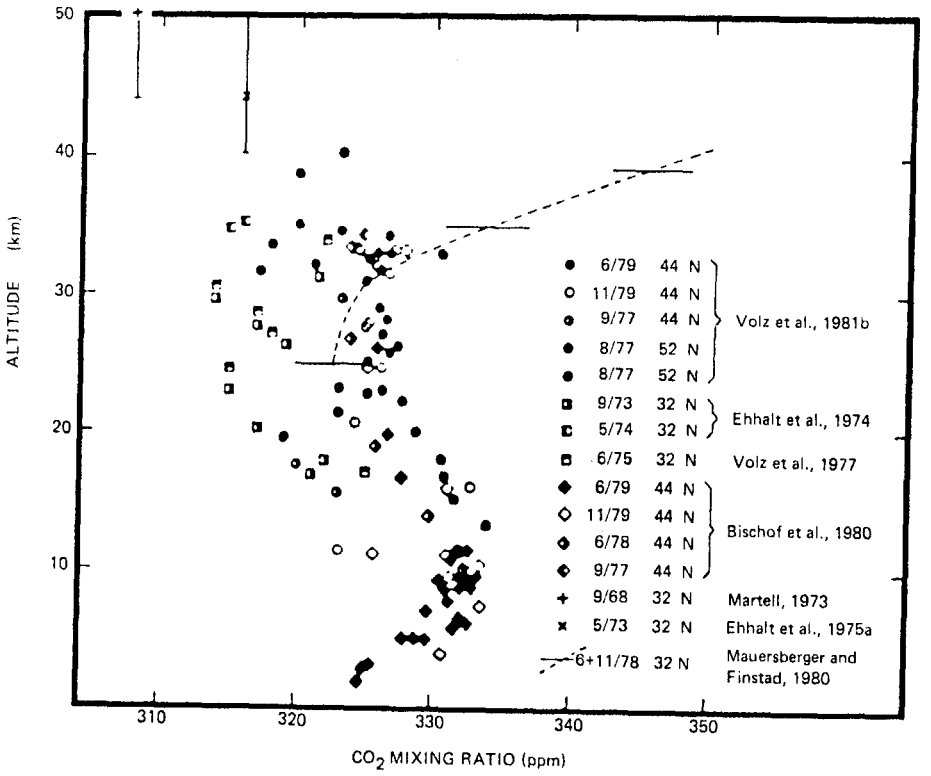

Figure 21-25. Vertical profiles of CO_2 at midlatitudes. Some of the scatter is due to the observed secular increase of CO_2 in the stratosphere [Volz et al., 1981] during the time the different profiles were measured.

the vertical profile of CO between the tropopause and 50 km. The combined data in Figure 21-26 suggest a decrease of CO across the tropopause and in the lower stratosphere up to 20 km. Above this altitude the CO mixing ratio is constant, at 10 ppb, up to 30 km. It then increases to 40 ppb around 40 to 50 km altitude. More reliable measurements of CO in the middle and upper stratosphere are required to establish the vertical profile.

21.2.3 Hydrogen-Containing Species

21.2.3.1 Molecular Hydrogen (H_2). Recent stratospheric measurements of H_2 are summarized in Figure 21-27. The profiles obtained at three latitudes show little vertical and latitudinal variation.

The data at 40 to 60°N show a clear decrease with altitude, from 0.55 ppm at the tropopause to 0.45 ppm at 35 km altitude [Ehhalt, 1978; Fabian et al., 1979]. A similar trend although with a much larger uncertainty can be deduced from the data at 60°N. No significant trend is found for the data at 32°N over Palestine, Texas. It should be noted that the absolute calibration of the NCAR data is about 10% lower than that of the KFA. It has been shown by Ehhalt and Tonnissen [1980] in a qualitative way that elevated levels of stratospheric H_2 are associated with, and probably caused by, increased concentrations of CH_4.

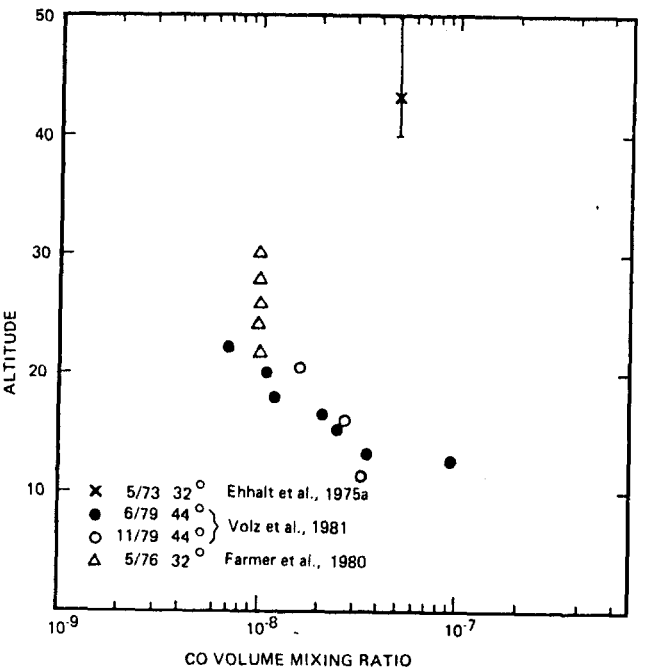

Figure 21-26. Vertical profile of CO at midlatitudes.

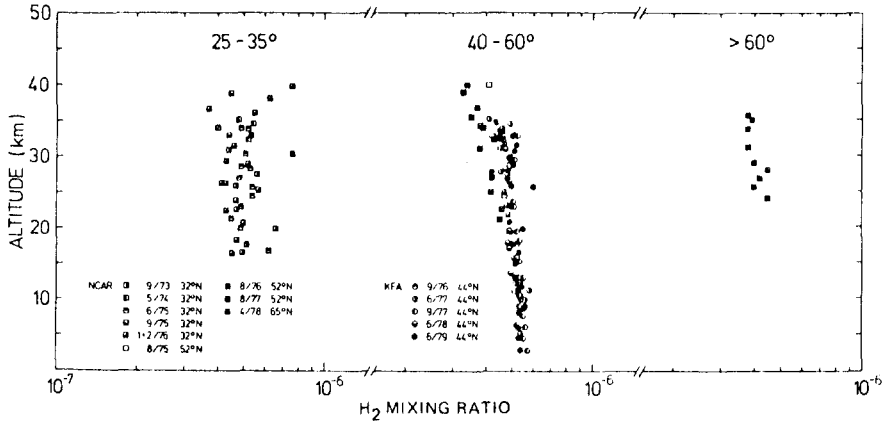

Figure 21-27. Vertical profiles of H_2 at different latitudes. The NCAR data are published by Pollock et al. [1980] and Ehhalt et al. [1975a,b] by the KFA data by Volz et al. [1981] and Fabian et al. [1979, 1981].

21.2.3.2 Methane (CH_4). Vertical profiles of CH_4 have been measured since 1965. Most of the sampling flights were performed at 32°N, 44°N, and 52°N. Only data from two flights exist for latitudes >60° (NAS) and only one profile for the tropics. Measurements were performed either by gas chromatography on grab samples and cryogenic samples collected *in situ* during balloon and aircraft flights or by using long path infrared absorption from balloons. In Figure 21-28 the results are plotted separately in four latitude bands. All NCAR measurements made prior to 1974 were multiplied by a factor of 1.2 [Heidt and Ehhalt, 1980].

At first glance, only the tropical profile deviates significantly from the others, showing a much weaker gradient in the stratosphere. This behavior, which is also confirmed by the profiles of other long-lived trace gases such as N_2O and FC-12, signifies a considerably stronger upward transport in the tropics than in mid-latitudes. A closer investigation shows some minor but still significant differences among the midlatitude profiles. The average profile at 32°N shows only a very weak gradient between 20 and 30 km, and on several occasions, profiles with a well-mixed layer in this altitude range were observed. This behavior can be explained by the stratospheric branch of the tropical Hadley circulation displacing air from the tropical mid-stratosphere with a weak CH_4 gradient into the lower stratosphere at 30°N, [Ehhalt and Tonnissen, 1980]. On some occasions, layers of almost constant mixing ratio were also observed at 44°N. In addition, from the individual profiles collected at 44°N, there is a slight hint of a seasonal variation of the stratospheric CH_4 concentration, especially above 25 km, where the average profile shows a relatively large variability compared to lower altitudes. At higher latitudes, the data though sparse indicate a more or less linear decrease of the CH_4 mixing ratio with altitude above the tropopause.

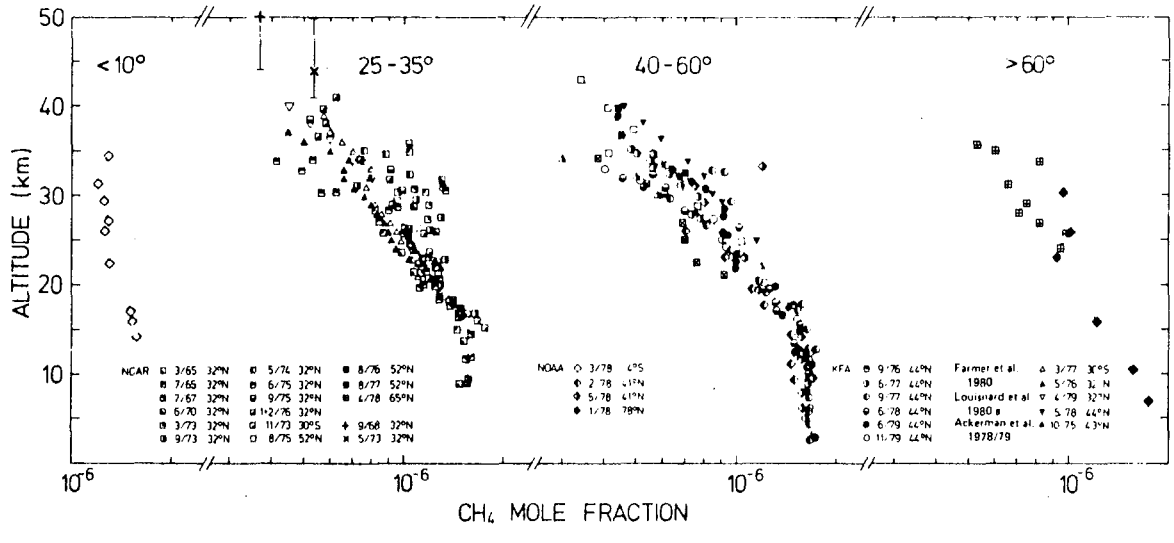

Figure 21-28. Vertical profiles of CH_4 at different latitudes. The NCAR data by Pollock et al. [1980], Ehhalt and Heidt [1973a, b], Ehhalt et al. [1974, 1975a,b]; the NOAA data by Bush et al. [1978]; and the KFA data by Volz et al. [1981], Fabian et al. [1979, 1981]. The NCAR data prior to 1975 were corrected by a factor of 1.2 [Heidt and Ehhalt, 1980].

21.2.3.3 Ethane, Propane, and Acetylene (C_2H_6, C_3H_8, and C_2H_2). Only three of the hydrocarbons present in the troposphere have been observed in the stratosphere; ethane, C_2H_6, propane, C_3H_8, and acetylene, C_2H_2. The tropospheric background mixing ratios of these species are quite low; around 1 to 2 ppb for C_2H_6 and up to several hundred ppt for C_3H_8. In addition, they show a strong latitudinal gradient with even lower values at the equator. The C_2H_6 mixing ratio at the equator is lower by about a factor of five; C_3H_8 and C_2H_2 decrease by a factor of ten [Rudolph et al., 1979; Singh et al., 1979; Harrison et al., 1979; Cronn and Robinson, 1979]. Because of their low tropospheric concentrations the fluxes of these gases into the stratosphere are small and their impact on the stratospheric carbon and hydrogen budgets is negligible. Singh and Hanst [1981] have proposed that oxidation products of ethane and propane are important carriers of reactive nitrogen.

C_2H_6 and C_3H_8 react rapidly with atomic chlorine, Cl, and can decrease the Cl concentration significantly in the lower stratosphere [Aiken and Maier, 1978; Rudolph et al., 1981]. Measured profiles of C_2H_6 have been used to deduce the vertical profile of Cl atoms in the lower stratosphere, where direct observation of Cl atoms is not yet feasible [Rudolph et al., 1981].

The measured vertical profiles of C_2H_6, C_2H_2, C_3H_8 are shown in Figures 21-29 through 21-32. All of these gases exhibit a strong decrease in the mixing ratio with altitude. The measured profiles of C_2H_2 and C_3H_8 agree reasonably well with those predicted from a one-dimensional steady-state model. In contrast C_2H_6, which is destroyed by reaction with Cl, decreases less steeply than predicted. This has been interpreted to indicate substantially lower Cl-atom concentrations in the lower stratosphere than predicted by models [Rudolph et al., 1981].

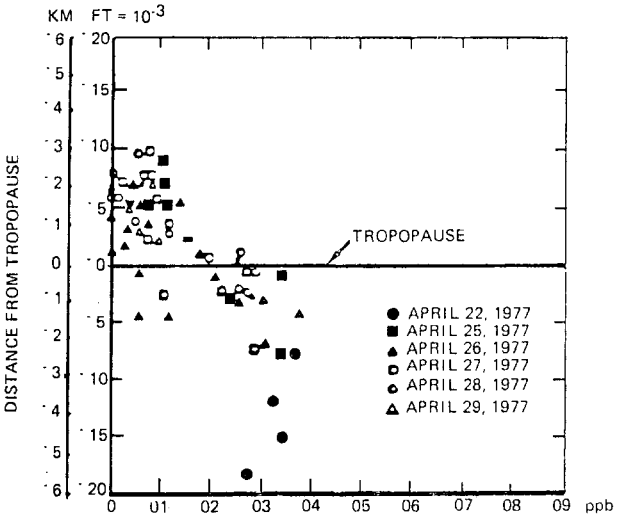

Figure 21-30. Distribution of acetylene relative to tropopause height. The latitude range of the samples from the first flight were 36 to 47°N and 36 to 38°N for the remaining flights.

21.2.4 Stratospheric Water Vapor (H_2O)

Ellsaesser et al. [1980] discussed the knowledge of the physical and chemical properties of stratospheric H_2O in 1979. In that work, a compilation of measured profiles was given in graphical form and a number of conclusions were drawn. In general, the basic Brewer theory of tropical "freeze drying" within the rising equatorial branch of the Hadley

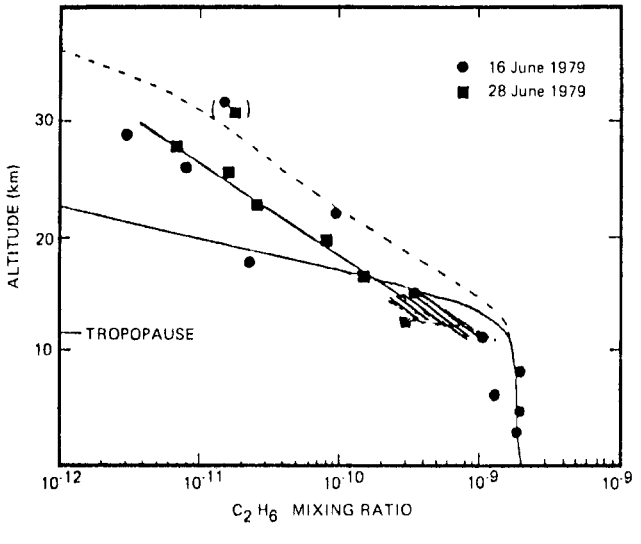

Figure 21-29. Vertical profiles of the C_2H_6 mixing ratio in the stratosphere over Southern France 44° N latitude [Rudolph et al., 1981]. The stippled area shows the range of data by Cronn and Robinson [1979] over San Francisco Bay area (37°N) in April 1977.

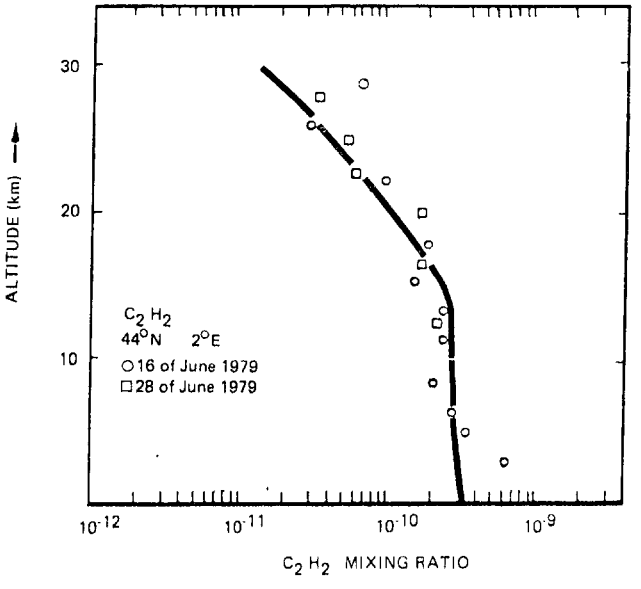

Figure 21-31. Vertical profiles of the C_2H_2 mixing ratio in the stratosphere over Southern France, 44°N latitude [Rudolph et al., 1981].

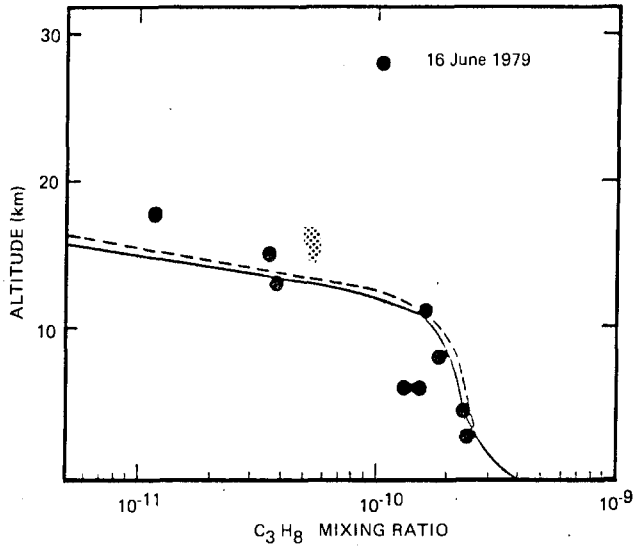

Figure 21-32. Vertical profiles of the C_3H_8 mixing ratio in the stratosphere over Southern France, 44°N latitude [Rudolph et al., 1981].

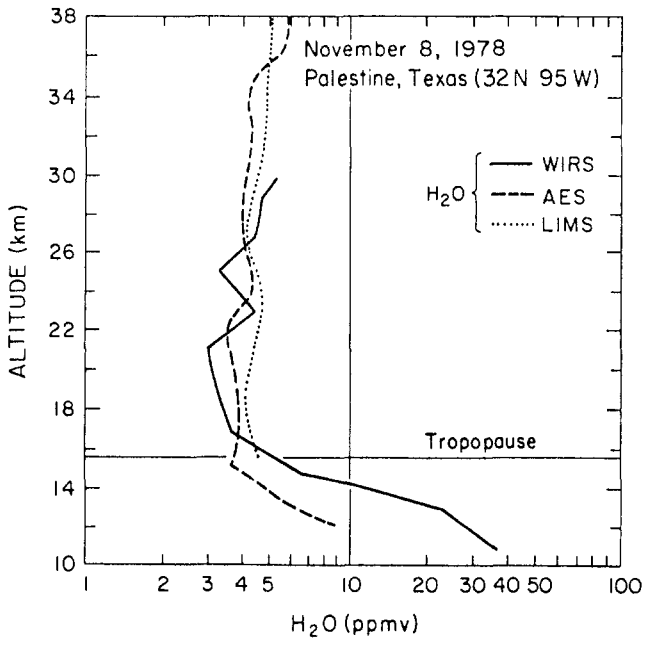

Figure 21-33. Measurements of H_2O mixing ratio over Palestine, Texas on 8 Nov 1978 by two balloon-borne *in situ* instruments (WIRS and AES) compared to the LIMS profile retrieved with the operational algorithm [Gille and Russell, personal communication].

cell was thought to be valid. However, a number of questions remained.

- Are there significant long-period trends in lower stratospheric mixing ratio, suggesting changes in circulation of tropical tropopause temperatures?
- Is the decrease in mixing ratio with height just above the tropical tropopause as identified by Kley et al. [1979] during their only tropical sounding a regular feature of the stratosphere?
- Are there latitudinal gradients of the mixing ratio? If so, are they poleward-directed or equator-directed?
- Are there increases in mixing ratio with height? If so, can the increase be fully accounted for by CH_4 oxidation?

21.2.4.1 Satellite Measurements. Water vapor profiles have been obtained by the LIMS instrument, extending from the tropopause up to ~50 km, for a number of specific occasions, and generally show a fairly gradual increase of mixing ratio with height over this range. An example of this data is compared in Figure 21-33 with profiles obtained simultaneously by two balloon-borne instruments: an infrared radiometer from the Atmospheric Environment Service (labelled AES), and the WIRS instrument of the National Physical Laboratory. The data agree closely giving encouragement that at least in the lower stratosphere, the LIMS data appears to agree well with independent observations.

21.2.4.2 Other Measurements. The observations shown in Figure 21-34 show an increase in H_2O mixing ratio between the tropopause, or in some cases a somewhat higher level, and 30 or 40 km altitude. The satellite observations seem to indicate a marked peak in the H_2O mixing ratio at the 55 to 60 km level. However, Rogers et al. [1977] and Waters et al. [1980] have reported constant mixing ratios, centered around 4 ppmv at these altitudes. Since there are no theoretical arguments for large mixing ratios peaking around 55 to 60 km, confirming measurements are needed before those results can be considered real.

A new *in situ* device, developed by Kley and his as-

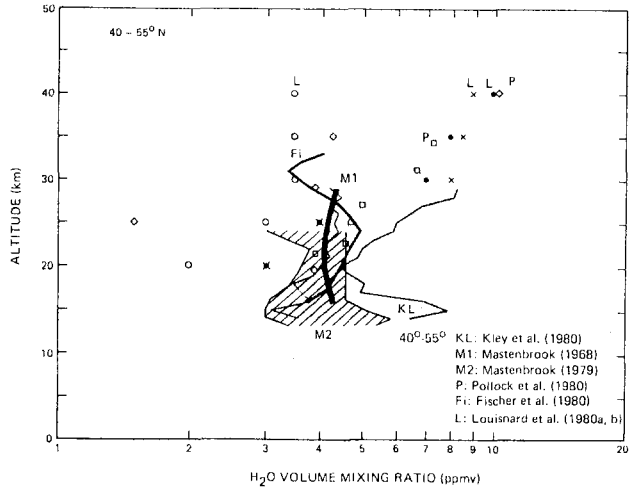

Figure 21-34. Altitude profile of H_2O between 40 and 55°N latitude. If more than one flight was made by a certain group, the banded area represents the range of their measurement.

sociates [Kley et al., 1979; Kley and McFarland, 1980] has now evolved as a powerful technique. These authors have built a sensitive instrument with a fast response time for balloons and aircraft which can resolve tens of meters in the vertical. Measurements of H_2O and temperature in mid-latitudes (Wyoming) generally show undersaturation in the upper troposphere although on one flight in Brazil [Kley et al., 1979] saturation was observed at the tropical tropopause. The results of the Brazil flight are shown in Figure 21-35. However, previous observations by Dobson and coworkers [Brewer, 1949; Dobson et al., 1946] over southern England (~52°N) have shown cases of both saturation *and* undersaturation below the tropopause. Saturation would indicate a contradiction to the Brewer model. Even supersaturation has been observed [Dobson et al., 1946; Kley et al., 1980]. It was pointed out by Kley et al. [1979] that tropical stratospheric air has a minimum mixing ratio at

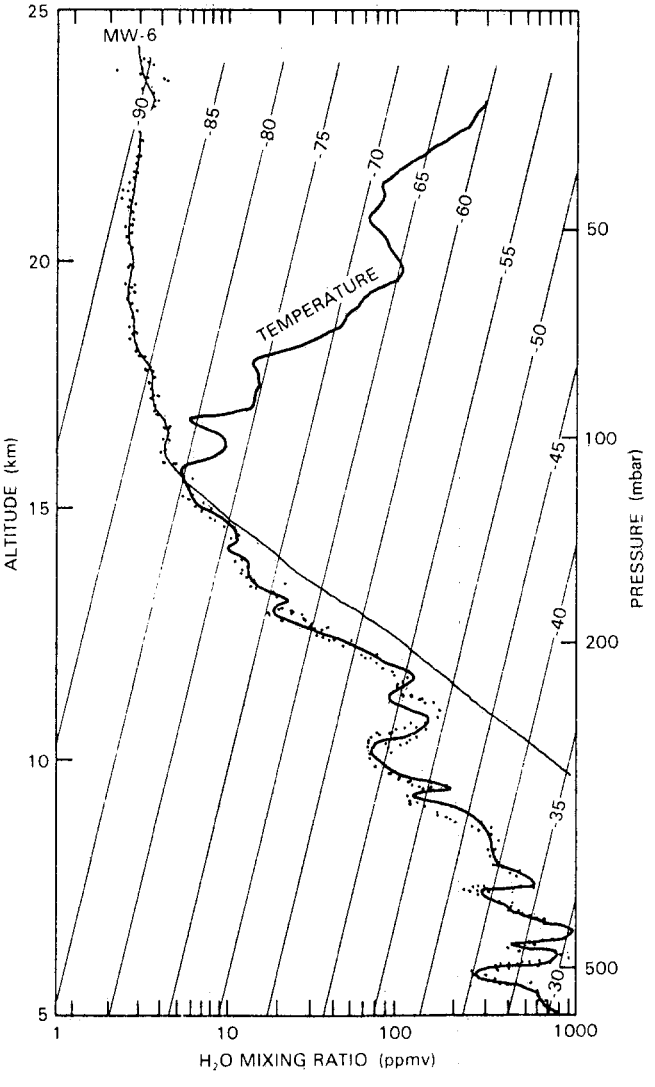

Figure 21-35. The water vapor mixing ratio measured over Quixeramobim, Brazil on 27 Sept 1978 [Kley et al., 1979].

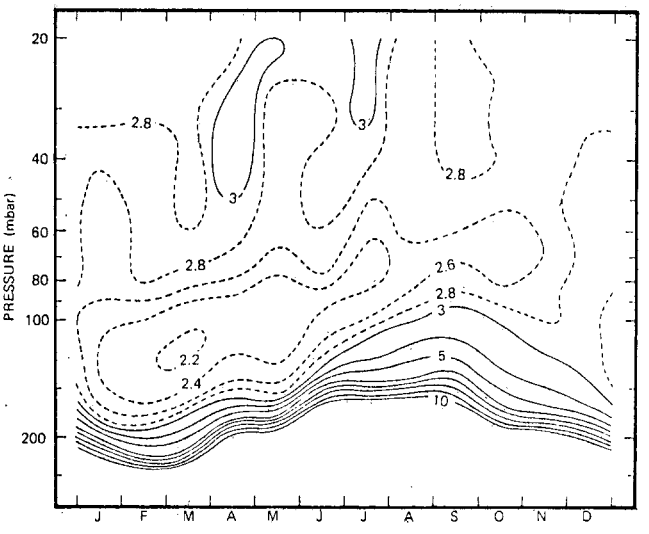

Figure 21-36. The mean annual variation of stratospheric water vapor at Washington, D.C., based on 12 years of data by Mastenbrook and Daniels [1980].

about 60 mb or 19 km (see Figure 21-35). This is well above the tropopause. Robinson [1980] has found more examples from literature studies. These observations indicate that the simple Brewer mechanism needs to be refined.

Another set of water vapor data are the frost point measurements of Mastenbrook that are being continued by NOAA. In a recent paper [Mastenbrook and Daniels, 1980] data from four flights over Washington, D.C. during the early part of 1979 are reported. A map of annual variations of stratospheric H_2O over Washington, D.C., based on 12 years of data, is presented here in Figure 21-36.

The composite water vapor profile of Figure 21-36 is recommended for chemical modeling purposes in the lower stratosphere at mid-latitudes ($z < 20$ km). Mastenbrook's instrument tends to produce altitude independent mixing ratios whereas Kley's instrument normally gives a moderate increase of 1 to 3 ppmv between tropopause and 32 km at mid-latitudes. For the equatorial lower stratosphere it is suggested that Figure 21-35 be used. This profile is similar to earlier ones by Mastenbrook [1968] but shows the hygropause clearly. It should be noted that it is the minimum in water vapor some 3 km above *tropical* tropopause that was referred to as hygropause by Kley et al. [1979].

21.2.5 Odd Oxygen

The principal oxygen radicals are $O(^3P)$, $O(^1D)$, $O_2(^1\delta)$, $O_2(^1\Sigma)$, O_2 (other excited states) and O_3. While it is feasible in this section to critically analyze all of the available data on the first five species, a thorough discussion of O_3 is obviously of such magnitude that it warrants special treatment (see Section 21.1). Atomic oxygen in the ^1D level is of critical importance for establishing the oxidation rate of source molecules which enter the stratosphere such as CH_4,

N_2O etc., but there currently are no observations of (O^1D) in the stratosphere. The electronically excited states, $O_2(^1\delta)$ and $O_2(^1\Sigma)$, have been observed but the data base is small. The remaining electronically excited states of O_2 ($A^3\Sigma_u^+$, $C^3\delta^u$, $C\Sigma_u^-$) have not been observed.

21.2.5.1 Atomic Oxygen ($O(^3P)$). There are six observations of $O(^3P)$ in the stratosphere, all obtained using a parachute-borne, *in situ* atomic resonance fluorescence instrument, the results of which are shown in Figure 21-37. Experimental accuracy is ±30% and experimental precision ±10% for each measurement [Anderson, 1975].

Several points are apparent from Figure 21-37. First, there is both local structure within and absolute displacement among observed distributions which exceed respectively the precision and accuracy of the measurements. It should also be noted that the local structure does not appear consistently. For example the profiles observed on October 25, 1977 and December 2, 1977 display a small degree of local structure, typically less than ±20% variation over an interval of ±1 km above approximately 34 km. Below that altitude significantly greater local structure is apparent, though seldom more than ±50%. On the other hand, the remaining four observations exhibit at least one example of major (factor of two) variation over ±2 km interval with an increasing structural development below the 33 to 35 km interval.

21.2.6 Odd Nitrogen

21.2.6.1 Nitric Oxide (NO) NO has been the most extensively studied stratospheric odd-nitrogen species. The last decade has seen numerous measurement programs apply a variety of experimental techniques at many different altitudes, locations, and seasons. Thus, the problem in establishing a picture of our best current experimental understanding of stratospheric NO is not a scarcity of data, but rather of making a proper assessment and selection of the data.

Altitude Profile

There have been a large number of measurements by many different groups of the NO mixing ratio as a function of altitude. The techniques employed in these measurements fall into two classes: *in situ* and remote. While the long-path, vertical-column measurements from the latter technique have provided some of the best information regarding the seasonal and latitudinal variations for NO, the determination of a detailed height profile from long-path data involves deconvolution at solar zenith angles near 90° in order to obtain the maximum number of absorbing molecules along the sight path. The rapid $NO \rightarrow NO_2$ and $NO_2 \rightarrow NO$ conversions at sunset or sunrise complicate the comparison of these data with model predictions.

As a consequence, *in situ* measurements are used here to establish the NO height profile. A limited number of

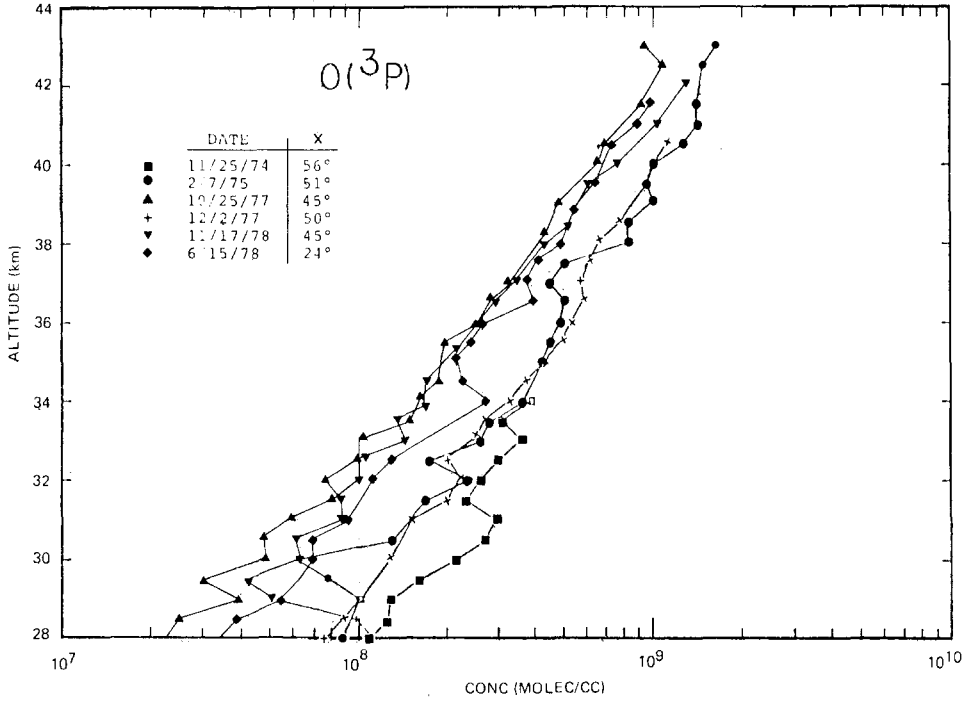

Figure 21-37. Observed concentration of $O(^3P)$ between 28 and 43 km in the stratosphere. All determined *in situ* using atomic resonance fluorescence.

midday long-path measurements are also included. The result is a more nearly homogeneous, relatively high sun profile that should afford a better defined comparison between observations and theory. The exclusion of the results of the remote techniques does not unduly restrict the size of the data set on which the present height profiles can be based, since there are a sizable number of *in situ* measurements made by several groups, using a variety of techniques: chemiluminescence deployed with balloons [Ridley and Howlett, 1974; Drummond et al., 1977], aircraft [Loewenstein et al., 1975], and rockets [Mason and Horvath, 1976]; photoionization mass spectrometer [Aikin and Maier, 1978], spin-flip laser absorption [Patel et al., 1974]. A balloon-borne pressure-modulated radiometer [Chaloner et al., 1978] has been used to obtain midday long-path information.

Assuming instrumental reproducibility, the variations in the results from a series of flights employing the same instrument are the best indicator of natural seasonal and geographic trends, since it is likely that differences between the results of different research groups and/or instrument packages can be dominated by unknown systematic instrumental discrepancies. Consequently, the approach used is (a) to examine separately the data of each group that has accrued sizeable sets for possible seasonal and geographic effects, and (b) then to combine the data of all of the groups into an appropriate profile.

Figure 21-38 shows the balloon-borne measurements of Ridley and coworkers [Roy et al., 1980; Ridley and Schiff, 1981; Ridley and Hastie, 1981] made in October, 1977 and thereafter. All six of these flights were made with a chemiluminescence instrument that incorporated an improved inlet and in-flight calibration procedure [Ridley and Schiff, 1981]. The internal consistency of the data set in Figure 21-38 strongly suggests that a sizable part of the much larger variation that this group observed earlier from flight-to-flight was instrumental. For example, the nearly coincident, half-filled symbols represent data gathered from three flights at the same place and season (32°N, fall), but in two different years. In addition, the data taken on two flights at the corresponding Southern Hemispheric latitude, but different equivalent season (SH, summer), are only slightly lower than the NH results. Lastly, measurements from the summer flight at 51°N lie wholly within the 32° data set. Since the differences between the results of the flights are very nearly equal to the variations within any one of the flights, these data present no evidence of systematic patterns over the given parameter ranges: summer and fall, 50° to 30°N and 30°S, solar zenith angle 37 to 75°. Therefore, they present no reason not to take a factor-of-three-wide band of NO mixing ratios as representative for these parameter ranges and for the indicated altitudes.

Figure 21-39 shows the rocket-borne chemiluminescence measurements made by Horvath and Mason over a

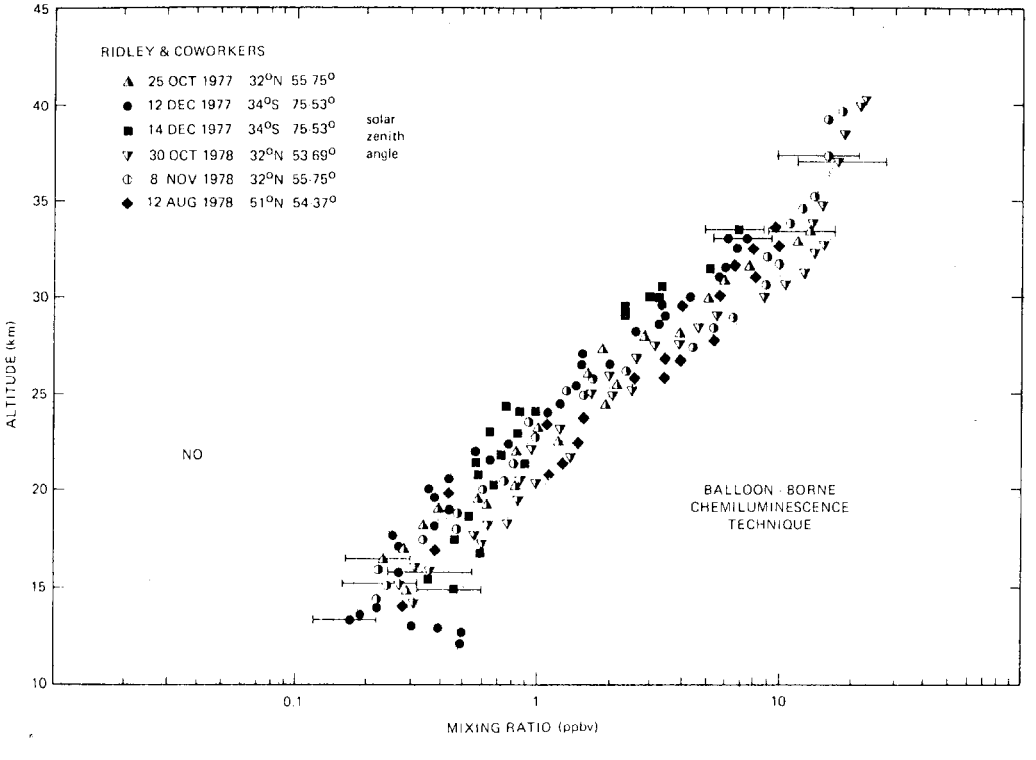

Figure 21-38. *In situ* NO mixing ratio measurements of Ridley and coworkers. All of the flights were made with instrumentation that incorporated a new inlet and flight calibration procedures.

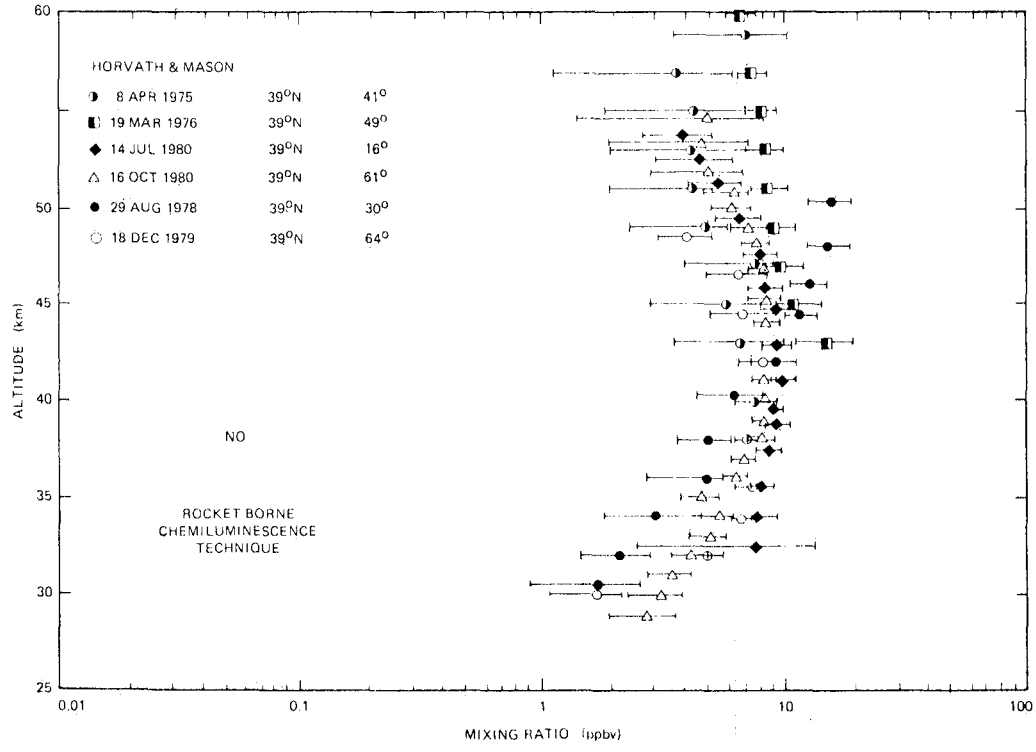

Figure 21-39. *In situ* NO mixing ratio measurements of Horvath and Mason. The 1980 measurements were made on parachute descent.

five-year period at one location, 39°N, and four seasons, [Mason and Horvath, 1976; Horvath and Mason, 1978; Horvath, personal communication]. There is good agreement within the data set. The later measurements (1980 and 1981) have better precision because they were taken on parachute descent, rather than rocket ascent. No clear seasonal trend emerges from this data set. The data set's homogeneity does, however, establish a factor-of-three band of NO mixing ratios at these altitudes, which are generally higher than those reached by Ridley and coworkers.

The measurement bands corresponding to the two extensive NO mixing ratio data sets are reproduced in Figure 21-40. The width of the indicated ranges includes essentially all of the individual measurements and their estimated uncertainties. The results of four other measurement series are shown. The first is that of Loewenstein and coworkers, whose chemiluminescence instrument has been flown extensively at two altitudes aboard U-2 aircraft [Loewenstein and Savage, 1975; Loewenstein et al., 1975, 1977, 1978a, b]. The rectangles in Figure 21-40 represent the range of NO mixing ratios found in spring, summer, and fall and over latitudes from 5° to 50°N. Measurements were also made in winter at mid-latitudes and above 50°N. A pronounced winter variation was found and is discussed in detail below. The winter variation is excluded from the data in Figure 21-40. The second measurement series represented in Figure 21-40 is a short one, namely, two flights by Patel and coworkers, who used a spin-flip Raman laser to detect NO in absorption in a multipass cell [Patel et al., 1974; Burkhardt et al., 1975]. Although only two flights were performed, the results, taken in the fall of 1973 and the spring of 1974, are in remarkably good agreement for several hours at float altitude. A single data point, representing the noontime mean, is given in Figure 21-40.

As Figure 21-40 shows, the data sets are in good agreement. Even though there are some discrepancies, there is nevertheless substantial overlap. There are, of course, some *in situ* and remote measurements that have been excluded from this comparison and that conflict with the data in Figure 21-40. It is worth stressing here that these exclusions were based on the reasons given above and not on the fact that they conflict. Furthermore, some of the excluded measurements agree with those in Figure 21-40.

Diurnal Variation

Observations have confirmed all of the major NO diurnal variations expected from the stratospheric odd-nitrogen chemistry: essentially no NO at night, a rapid increase at sunrise, a slow increase during the daytime, and a rapid decrease at sunset. All of these features have been observed in detail with both *in situ* and remote techniques.

The most extensive set of observations are from the *in situ* studies of Ridley and coworkers, who used their balloon-borne chemiluminescence instrument. Figures 21-41 and 21-42 show sunrise and sunset data, respectively. The sunrise 1975 flight employed two separate chemiluminescence instruments [Ridley et al., 1977], neither of which had the improved inlet calibration procedures adopted in 1977 [Ridley and Schiff, 1981]. Although it might be for-

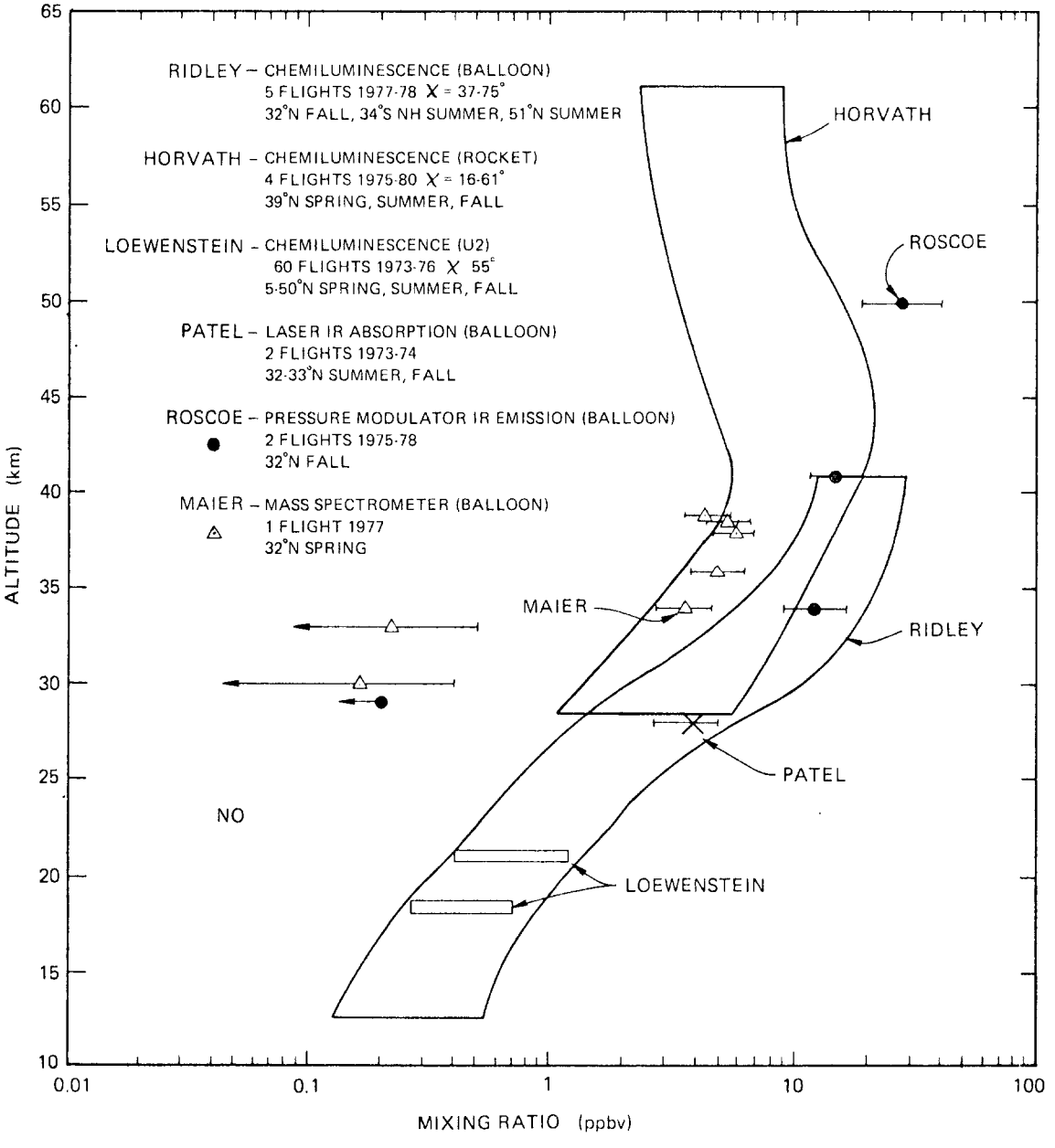

Figure 21-40. *In situ* NO mixing ratio measurements of several series of flight yielding self-consistent results.

tuitous, the NO mixing ratios are, however, in accord with those from their later flights (see Figure 21-38). Figure 21-42 shows this group's sunset measurements [Ridley and Schiff, 1981]. Both sets of data reveal these rapidly changing events in remarkable detail and Figure 21-41 clearly shows a slow NO increase during the daytime.

Seasonal Variation

The variation of NO with season necessarily requires an extensive measurement program. Fortunately, several such studies have been conducted with different techniques. The various results are in reasonable harmony.

The most extensive of such investigations are those of Loewenstein and coworkers using a U-2 chemiluminescence instrument. The studies have revealed two major seasonal effects. The first of these stems from a 4-year flight series at 21.3 km during all months of the year. The results are shown in Figure 21-43 [Loewenstein et al., 1977]. A rather sharp winter minimum and a broader summer maximum is apparent. The ratio of the maximum and minimum concentrations is about six. The reproducibility of the pattern over 4 years makes it difficult to doubt its reality. Furthermore, the same trend, although defined by less data, has been found at 18.3 km.

The second striking seasonal variation discovered by Loewenstein and coworkers is shown in Figure 21-44. The data are from several summer and fall flights at 18 km

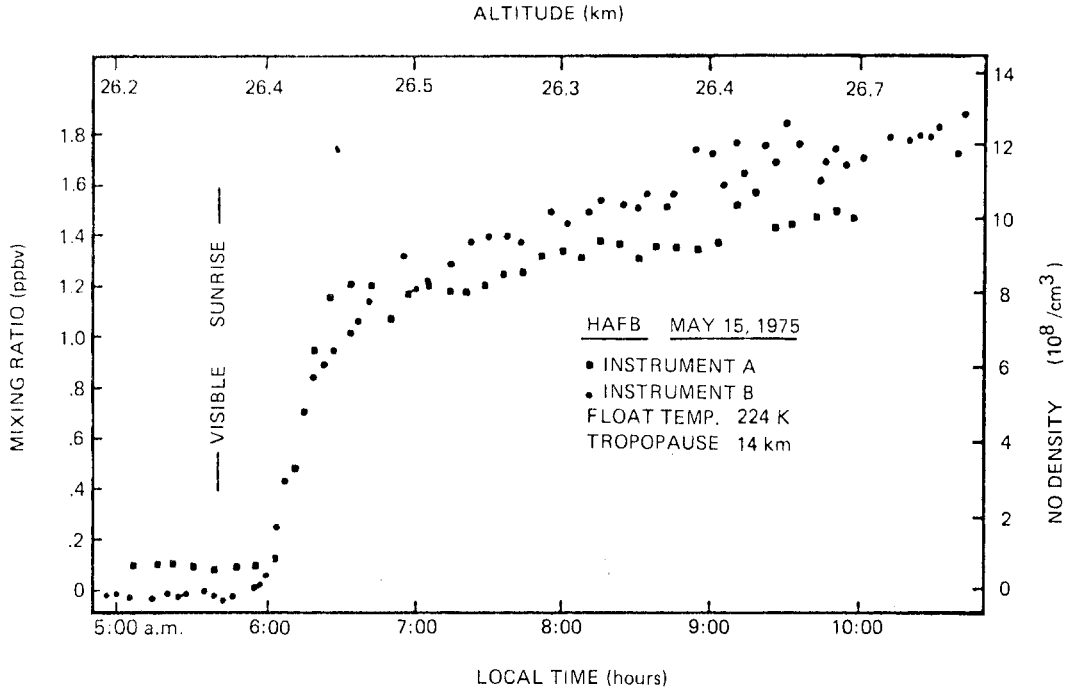

Figure 21-41. The sunrise *in situ* NO measurements of Ridley et al. [1977] obtained using two chemiluminescence instruments simultaneously flown on 15 May 1979 near 33°N, 106°W.

altitude and from 5°N to 80°N latitude. North of about 50° or 60°, the NO concentration exhibits a marked seasonal variation; the summer values are an order of magnitude larger than the fall values. There were no winter or spring high-latitude flights, so only a summer-fall comparison is possible. The fall high-latitude values are nearly zero; therefore, the winter values cannot be much lower. At 21 km, the high-latitude data are sparse; hence, the spring-fall difference seen at 18 km could not be investigated.

Latitudinal Variations

Between 5°N and about 50°N, there is substantial evidence that the latitudinal variation of NO is not large. Figure 21-47 shows the north-south variation for summer at 18 and 21 km altitude measured by Loewenstein et al. [1978a]. These data are typical of those obtained from their other north-south transects. The largest 5°N-to-50°N difference is about 2.5, the values increasing in a northern direction.

21.2.6.2 Nitrogen Dioxide (NO_2). Several extensive flight and ground-based measurement programs have established a better picture of stratospheric NO_2 in recent years. NO_2 is a rather variable constituent, both in time and in location, and some of its now recognized variations, such as the winter minimum at high latitudes, are an unanswered challenge to theory.

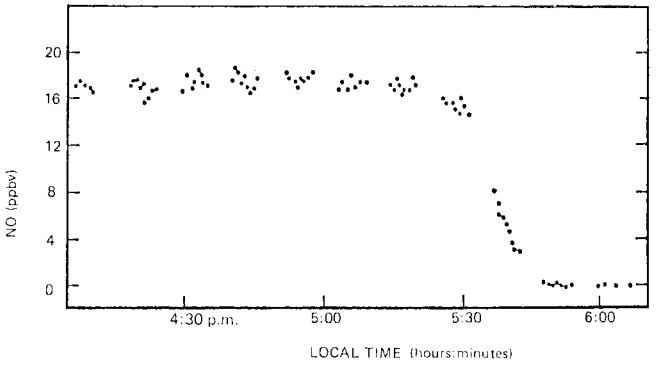

Figure 21-42. The sunset *in situ* measurements of Ridley and Schiff [1981] obtained with a chemiluminescence instrument flown on 8 Nov 1978 near 32°N, 96°W.

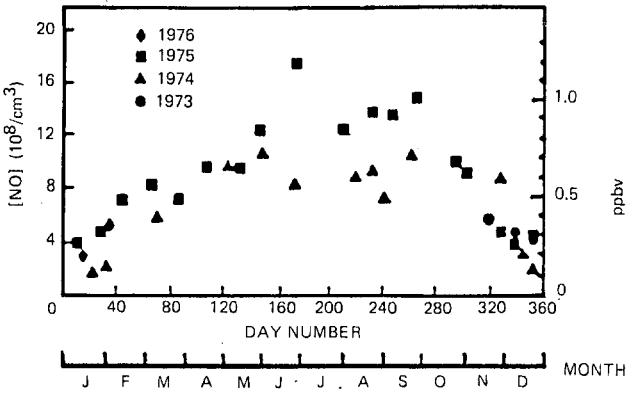

Figure 21-43. Nitric oxide seasonal data (122°W, 40°N) summary at 21.3 km. The in situ NO measurements of Loewenstein et al. [1977] obtained with a chemiluminescence instrument.

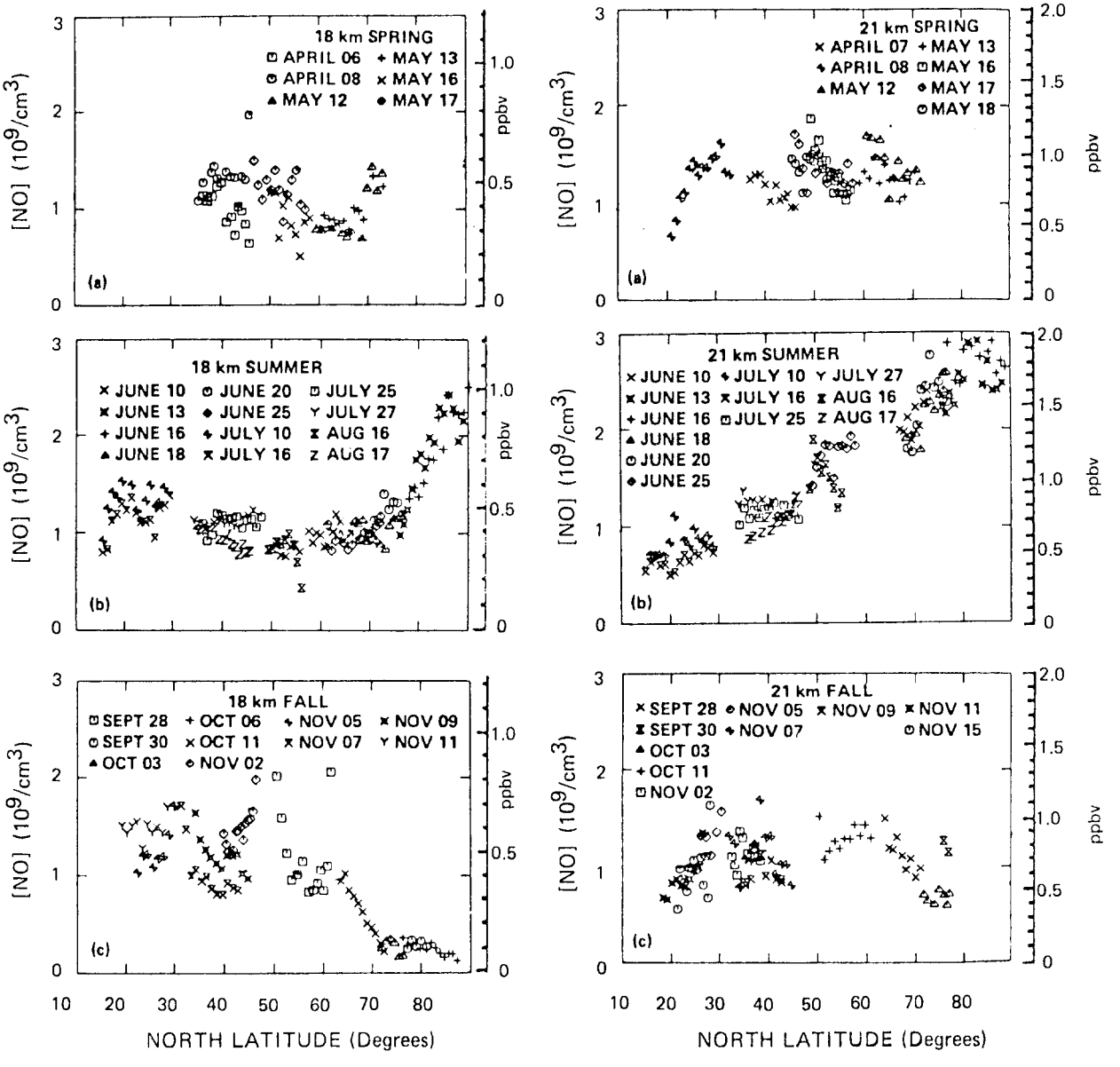

Figure 21-44. The *in situ* NO measurements of Loewenstein et al. [1978a] obtained with a chemiluminescence instrument in 1975 and April–May 1976.

Altitude Profile

There are virtually no *in situ* measurements of NO_2 in the stratosphere; hence, essentially all of the information about the NO_2 altitude profile has come from remote techniques. Most of these methods have required the long path associated with the rising or setting Sun, obtaining the vertical variation of the NO_2 mixing ratio by unfolding it from the change of the slant column density as a function of the viewing angle. Thus, the majority of the NO_2 altitude profile measurements are grouped into either sunrise or sunset profiles. The sunset mixing ratios of NO_2 are larger than those at sunrise, the increased NO_2 having been formed by the photolysis of N_2O_5. In addition to this sunrise/sunset difference, there are marked seasonal and latitudinal variations in the vertical column of NO_2. As noted in detail below, the NO_2 vertical-column values increase with increasing latitude and are larger in the summer than winter. Therefore, the large number of profile observations must be gathered into subgroups of certain times, places, and seasons, in order to have a well-defined, homogeneous profile. The largest of these is the subset of sunset profiles. This subset is examined here to see if they also show latitudinal or seasonal trends.

Figures 21-45, 21-46, and 21-47 are observed sunset profiles at approximately 32°, 48°, and 55°N, respectively. Each profile is made up of at least two flights. The error bars reflect the reported uncertainties.

Figure 21-45 contains the results of the extensive flight series of Murcray and coworkers, who employed infrared [Murcray et al., 1974; Blatherwick et al., 1980] and visible

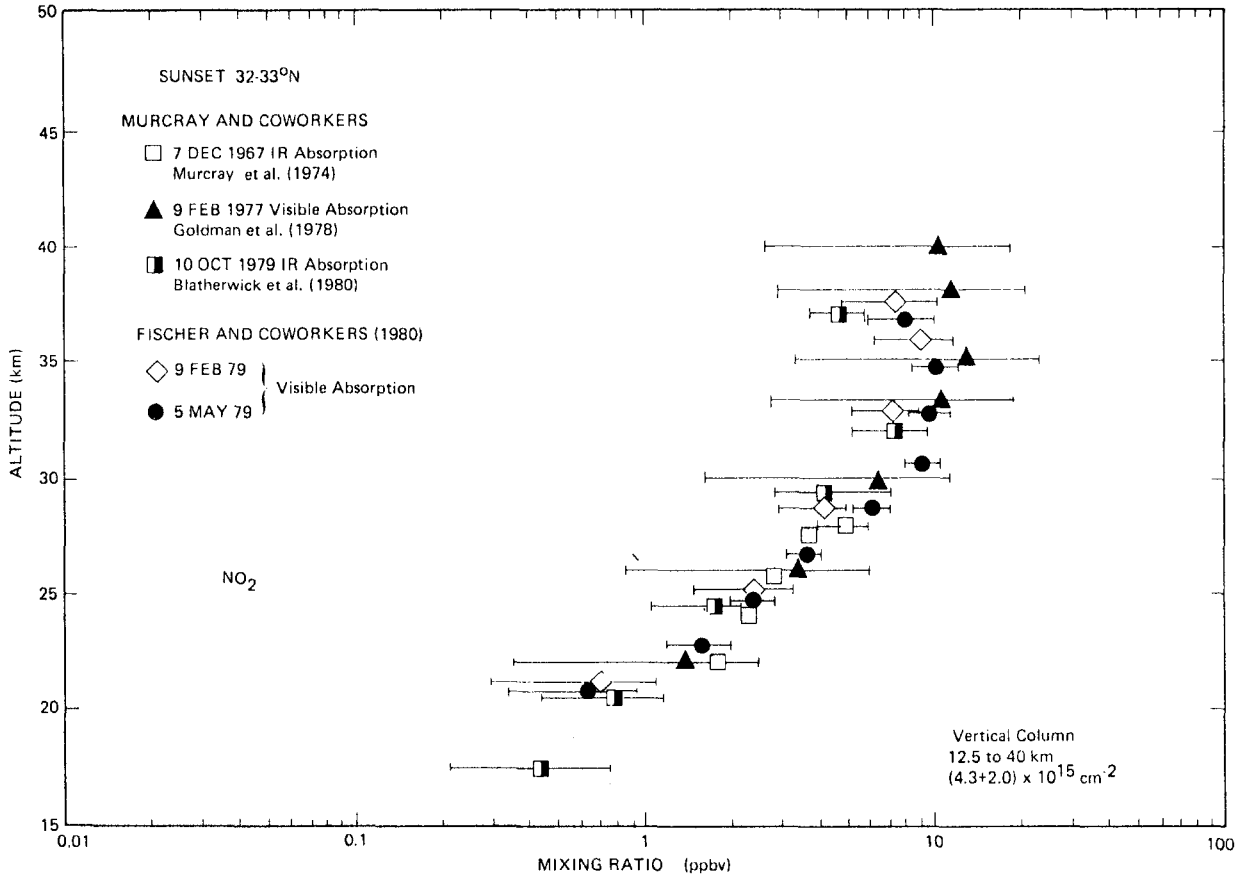

Figure 21-45. Remote measurements of the sunset altitude profile of NO_2 made at 32 to 33°N latitude.

[Goldan et al., 1978] absorption techniques from a balloon platform launched in the southern United States. Accompanying these data are the results of the two recent flights of Fischer and coworkers [personal communication, 1981]. The data set includes winter, spring, and fall flights, but there are no obvious seasonal differences between the profiles. This lack of variation is in accord with the vertical-column observations, which find little seasonal variation at latitudes below 35°N. However, the lack of a summer flight precludes the most sensitive test, namely, a summer/winter comparison.

Figure 21-46 gives the results of flights that were made in the early 1970s using infrared absorption on balloon [Ackerman and Muller, 1973; Ackerman et al., 1975] and aircraft [Fontanella et al., 1975] platforms in France. The 16×10^{-9} value of Rigaud et al. [1977] at 37 km in May of 1976 seemed too large to warrant inclusion. Three seasons are represented (winter is missing), but the small data set and the experimental uncertainties complicate the examination for seasonal trends.

Figure 21-47 shows the results from flights made over a 3-year period in Canada using visible absorption techniques [Kerr and McElroy, 1976; Evans et al., 1978]. Two sets of results are shown. The data of Evans et al. [1978] summarize the results of four flights. All five flights occurred in the summer.

The data in Figures 21-45, 21-46, and 21-47 are in good agreement within each latitude range. The high-latitude mixing ratios are up to a factor of two larger than the mid-latitude values in the range from 15 to 30 km, as a comparison of Figures 21-45 and 21-47 shows. Since the concentrations associated with such profiles reach a maximum value at about 25 km, these larger high-latitude values cause the associated vertical-column value to be larger. Although the uncertainties are relatively large, this 2.4×10^{15} cm^{-2} difference, which is a 50% increase corresponding to a 20° change in latitude in the summer, is in good agreement with the change that has been observed in vertical-column studies of the latitudinal dependence of NO_2 in the summer. Unfortunately, no one research group has data represented in two or more of Figures 21-45 through 21-47. Therefore, it remains possible that the agreement may be fortuitous, particularly since the 45° to 50°N vertical-column datum does not fit very well into the trend. It is nevertheless reassuring that the associated vertical-column values determined from these profiles agree fairly well with those directly measured.

Figure 21-48 contains the results of measurements that

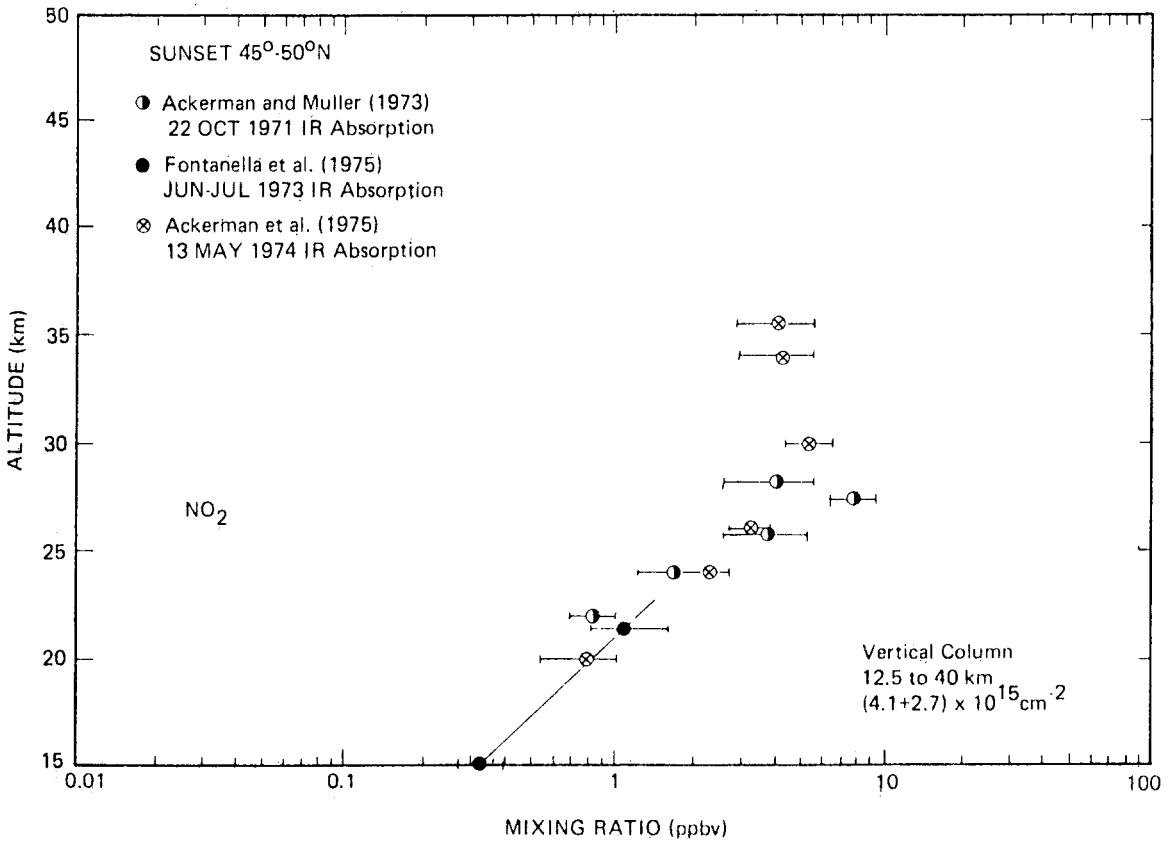

Figure 21-46. Remote measurements of the sunset altitude profile of NO_2 made at 45 to 50°N latitudes.

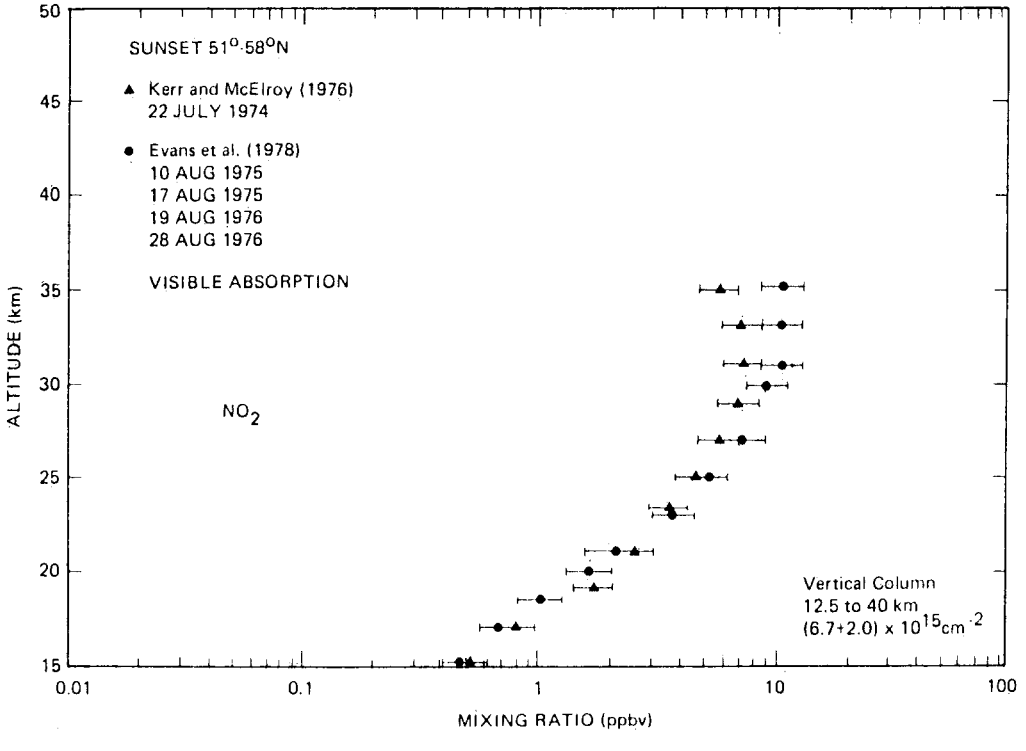

Figure 21-47. Remote measurements of the sunset altitude profile of NO_2 made at 51 to 58°N latitudes.

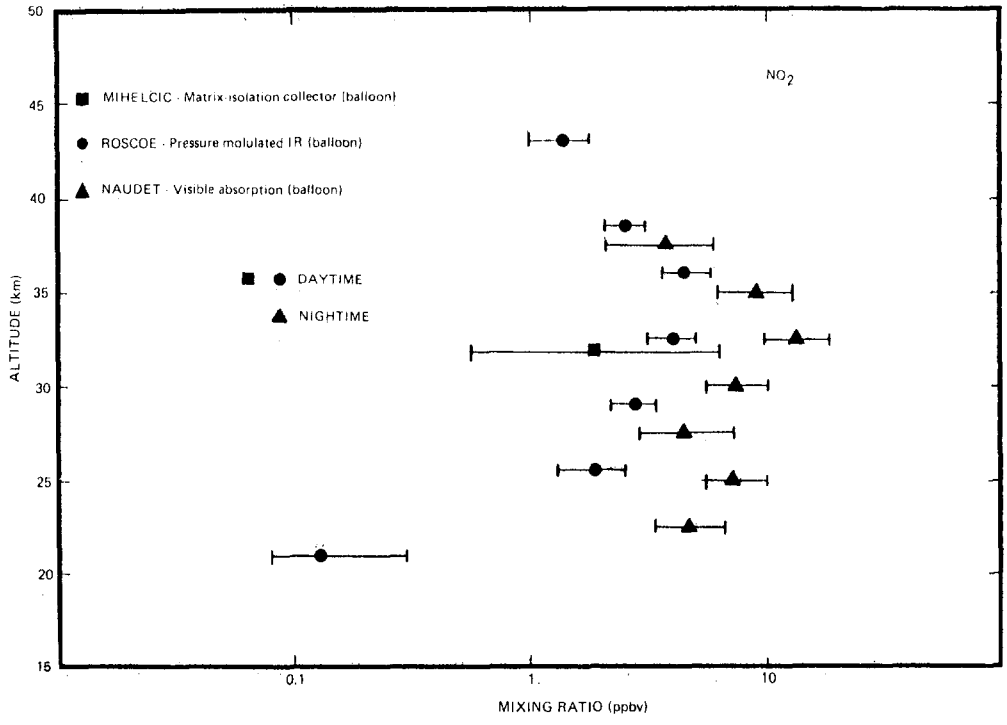

Figure 21-48. Results of full daytime and full nighttime measurements of NO_2. The data of Roscoe et al. [1981] (daytime) and Naudet et al. [1980] (nighttime) were obtained using long pathlength techniques, while the daytime data of Mihelcic et al. [1978] were collected *in situ*.

were made in full daytime and nighttime. The daytime studies are from the long-path pressure-modulated infrared radiometer of Roscoe et al. [1981] and the *in situ* matrix isolation collector of Mihelcic et al. [1978]. Earlier daytime long-path studies [Harries et al., 1976; Drummond and Jarnot, 1978] had considerably less precision and are not included here. The nighttime study is the long-path absorption investigation of Naudet et al. [1980] who used a star as light source.

Diurnal Variations

Both vertical-profile and vertical-column measurements have defined the diurnal variation of NO_2. Figure 21-49 shows the morning-evening difference reported by Evans et al. [1978], who averaged the results of four flights. The decrease from evening to morning is about a factor of two, which agrees with vertical-column measurements. Figure 21-50 shows the results of Mankin and coworkers [Coffey et al., 1981], who used infrared absorption spectroscopy

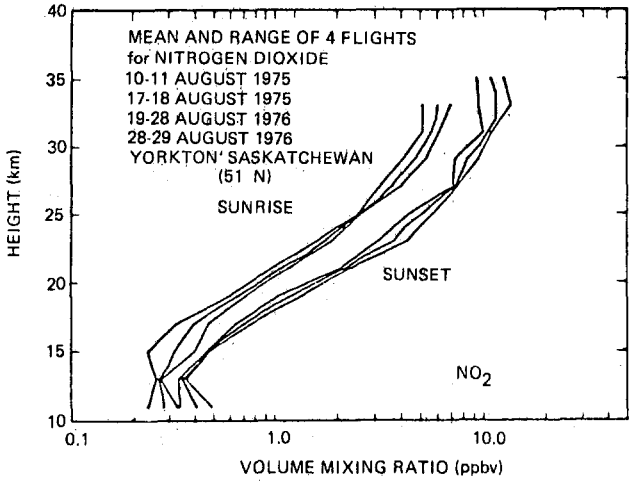

Figure 21-49. The sunrise and sunset altitude profiles of NO_2 reported by Evans et al. [1978] from the Canadian stratoprobe flight series. The upper and lower limits indicate the maximum observed deviations from the mean. The measurements were made using a balloon-borne visible absorption apparatus.

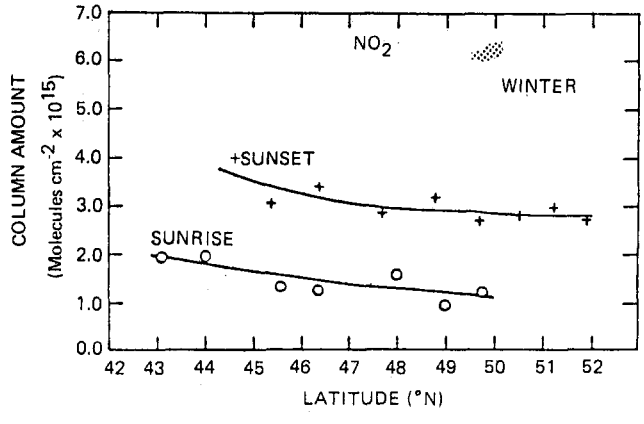

Figure 21-50. Sunrise and sunset vertical-column measurements of Mankin and coworkers, who used an infrared absorption apparatus on an aircraft platform [Coffey et al., 1981].

aboard an aircraft. Noxon's ground-based absorption spectroscopic technique [Noxon et al., 1979; Noxon, 1980] shows a factor of two larger NO_2 vertical column density at night when compared to daytime values, which is consistent with the above studies. Girard et al. [1978/1979], using similar techniques, did not initially find a sunrise-sunset difference; however, recent, more precise measurements (Girard, personal communication) have found this difference.

Seasonal Variations

The seasonal variations of NO_2 are best illustrated by the extensive ground-based measurements of Noxon [1979]. Figure 21-51 shows the results of 4 years of vertical-column measurements at various northern latitudes. The winter minimum and summer maximum is extremely regular and the ratio is as large as a factor of five at the higher latitude. Girard et al. [1978/79] report the same seasonal trend, but it is less well defined in their smaller data set. Other vertical column measurements have also been less extensive and some unusually large values have been reported [Pommereau and Hauchecorne, 1979].

21.2.6.3 Nitric Acid (HNO_3). HNO_3 has been studied with a variety of *in situ* and remote techniques. The main features of the height profile have been established and much of the latitudinal variation is now well established. The current status is summarized in the section below and the details are contained in the remaining sections.

Altitude Profile

The altitude profile of nitric acid in the stratosphere has been established experimentally by *in situ* and remote techniques at Northern Hemispheric midlatitudes and is shown in Figure 21-52.

Two *in situ* methods are represented. The first is that of Lazrus and Gandrud [1974], who used a filter collection technique on balloon and aircraft platforms. The second *in situ* method is the rocket-borne ion-sampling technique of Arnold and coworkers [1980], with which the HNO_3 mixing ratio is deduced from the observed ion concentrations and the ion chemistry leading to their formation from the ambient HNO_3.

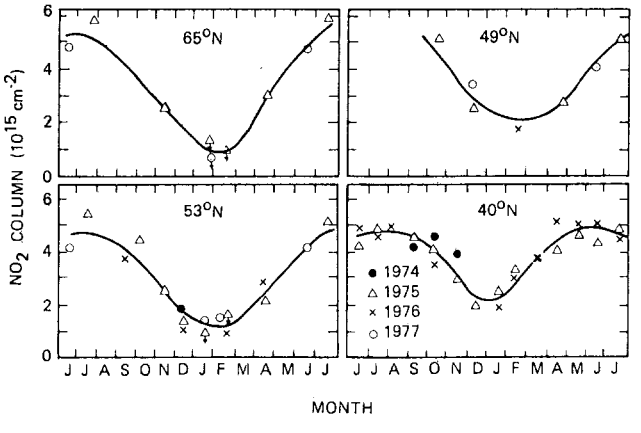

Figure 21-51. Seasonal variation of late-afternoon NO_2 at four latitudes, as given by the ground-based visible absorption spectroscopic measurements by Noxon [1979]. The abundance should be multiplied by 1.25 [Noxon, 1980].

The remote measurements have employed the long path associated with the rising or setting sun. Since HNO_3 has a long lifetime, the time of the day at which the measurement was made is not as critical a parameter as it is for NO and NO_2. Thus, both *in situ* and remote measurements can be meaningfully intercompared in Figure 21-52. Both infrared emission [Evans et al., 1978; Harries et al., 1976; Murcray, personal communication, 1980] and absorption [Fontanella et al, 1975] have been used. The data of Evans et al. [1978] represent the mean of the results of four flights. All of the data in Figure 21-52 are in good agreement, with the exception of the lower-altitude results of Lazrus and Gandrud [1974] which tend to be lower than the other measurements.

There is no obvious seasonal trend in these profile data. Lazrus and Gandrud [1974] reported that their winter and spring measurements showed higher HNO_3 concentrations than did their summer and fall measurements, but the data were too sparse to be able to make a more positive statement. The vertical column density associated with these profile measurements in Figure 21-52 is $(8.6 \pm 4.0) \times 10^{15}$ cm^{-2}, which is in fair agreement with the vertical-column measurements discussed below.

Diurnal Variation

No change in the HNO_3 abundance as a function of the time of the day has been observed.

Seasonal Variation

At latitudes less than about 40°N, there is no strong evidence to support a large seasonal variation. The vertical-column measurements of Mankin and coworkers, who used an aircraft-borne infrared absorption instrument [Coffey et al., 1981], found essentially no summer-to-winter change, as Figure 21-53 shows. Lippens and Muller [1980] found the slightly higher value $(1.8 \pm 0.4) \times 10^{16}$ cm^{-2} at 40°N in April.

Latitudinal Variation

The latitudinal variation of the vertical column of HNO_3 is well documented [Murcray et al., 1975, Coffey et al., 1981]. There is a strong increase in the vertical-column density with increasing latitude, both in the Northern and Southern Hemispheres. Figure 21-54 shows the data of Murcray et al. [1975]. Above about 50 to 60°N latitude, there appears to be a pronounced seasonal variation. At these high latitudes, the winter HNO_3 concentration is high (see Figure 21-53) and in the early summer, it seems to be much lower, as the data of Murcray et al. [1978] in Figure 21-55 show.

21.2.6.4 Nitrogen Trioxide (NO_3). A single height profile is available for nighttime NO_3 [Naudet et al., 1981]. The measurements were made at 43°N in September from a balloon. They are based on absorption in the visible region using Venus as the light source. The derived profile and stated uncertainties are shown in Figure 21-56.

The corresponding column abundance between 20 and

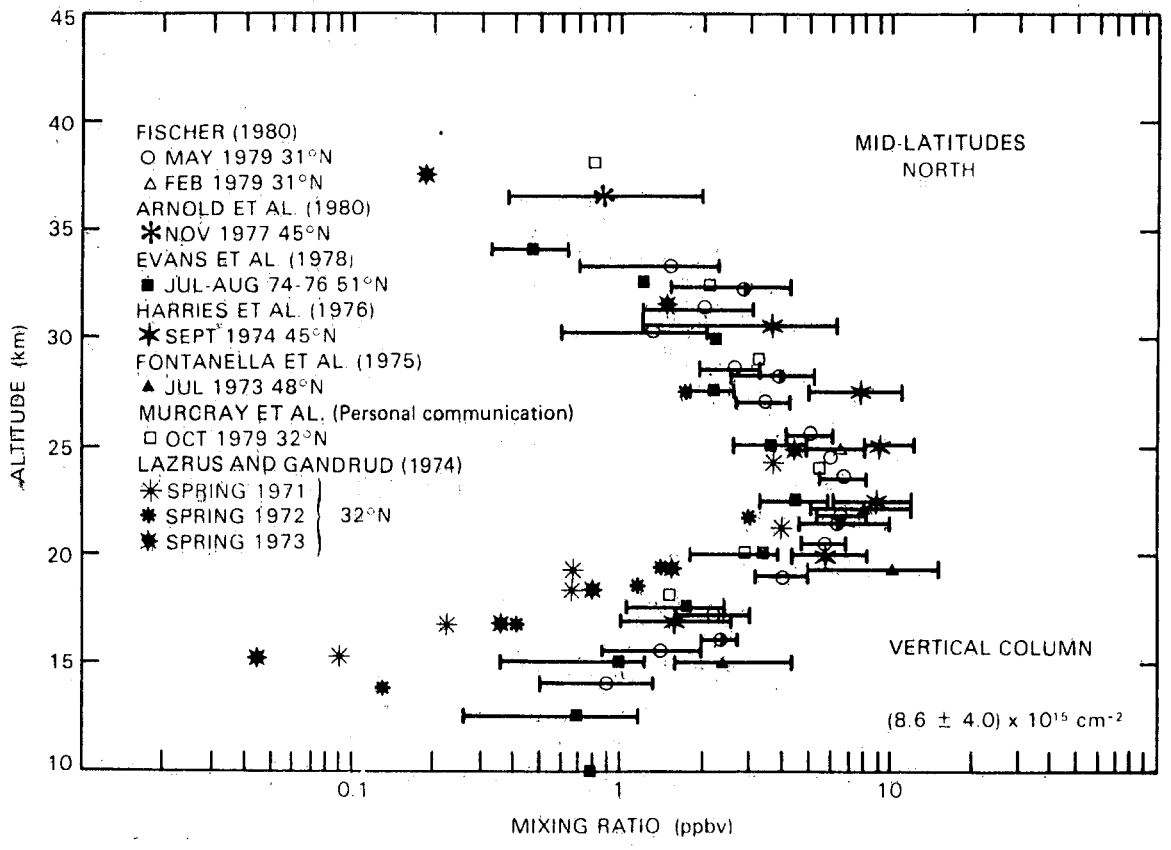

Figure 21-52. *In situ* and remote measurements of the HNO_3 mixing ratio at northern midlatitudes.

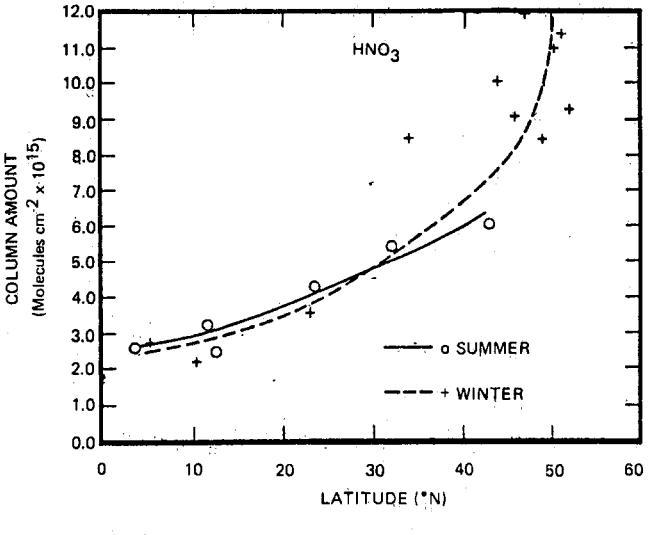

Figure 21-53. Evidence for the lack of seasonal variation in the vertical column density of HNO_3 at latitudes less than 40° as measured by Coffey et al. [1981] using infrared absorption.

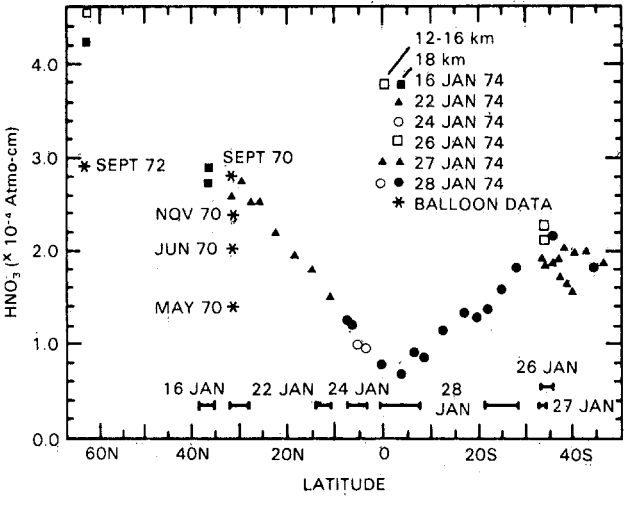

Figure 21-54. The latitudinal variation in the vertical column density of HNO_3, as measured by Murcray et al. [1975] using infrared emission (1 atm cm = 2.7×10^{19} molecules/cm^2).

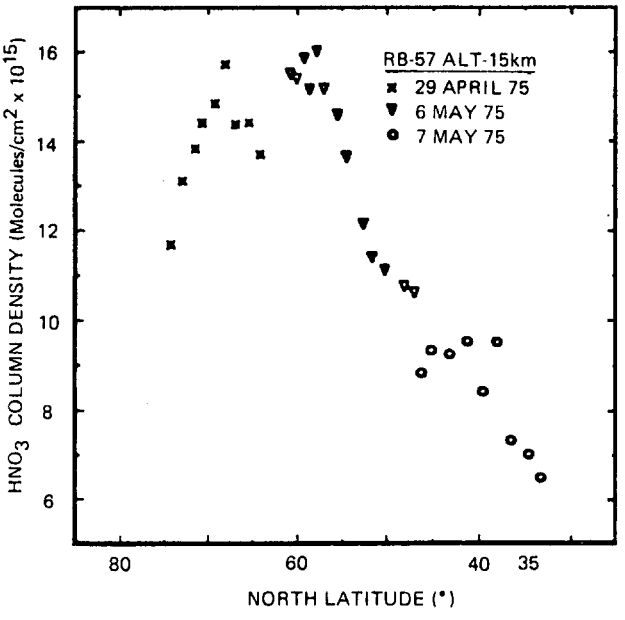

Figure 21-55. The decline of the HNO_3 vertical column density at high latitudes in the spring north of 70° as seen by Murcray et al., [1978] using infrared emission.

39 km is (3.5 ± 1.2) × 10^{13} cm^{-2}. This appears to be consistent with Noxon's estimate of about 10^{14} cm^{-2} in the spring and an upper limit of 4 × 10^{13} cm^{-2} in the summer.

21.2.6.5 Nitrogen Pentoxide (N_2O_5). There have been no new measurements of N_2O_5. This situation remains as reported in NASA RP 1049: A tentative detection of 2 ppbv at 30 km a few hours after sunrise by Evans et al. and an upper limit of 1.2 × 10^{15} cm^{-2} above 18 km in February by Murcray.

21.2.6.6 Peroxynitric Acid (HO_2NO_2). Despite the recent interest in this species no detection of its presence has been reported. The upper limit remains at 0.4 ppbv as reported in NASA RP 1049.

21.2.7 Odd Hydrogen

21.2.7.1 Hydroxyl Radical (HO). Hydroxyl has been observed in the stratosphere by four independent techniques:

- Solar flux induced resonance fluorescence observed by a rocket-borne spectrophotometer [Anderson, 1971a; Anderson, 1971b] which provides a local concentration measurement by determining the change in total column emission rate as a function of altitude.

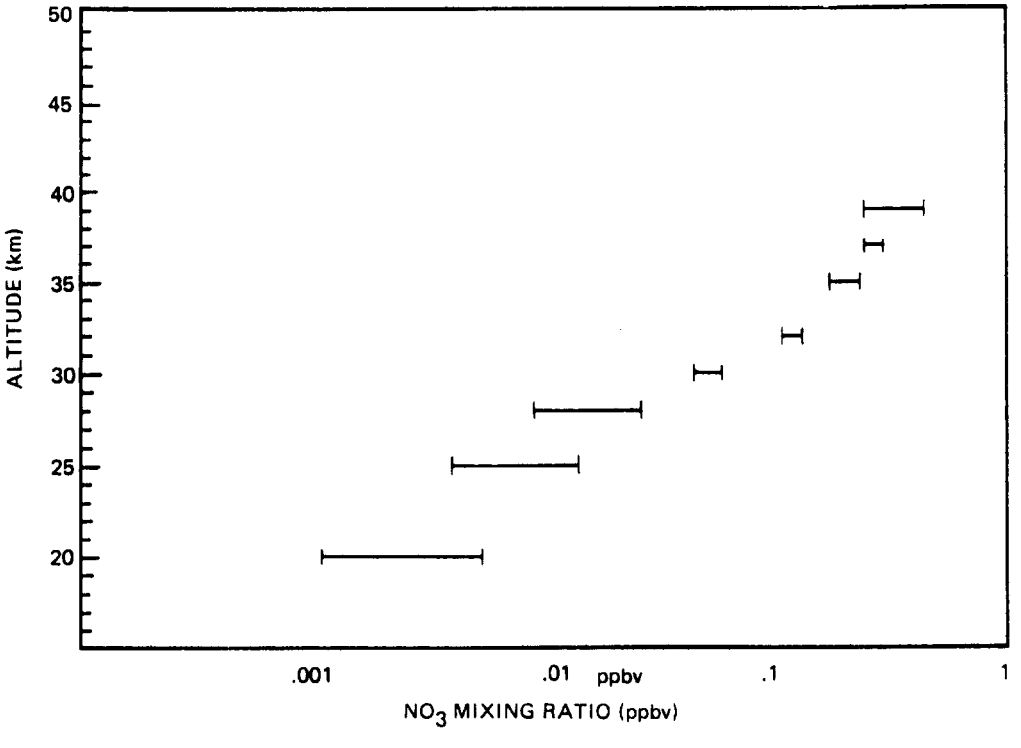

Figure 21-56. Vertical nighttime profile of NO_3 [Naudet et al., 1981] measured using visible absorption with Venus as a light source.

- Balloon-borne *in situ* molecular resonance fluorescence using a plasma discharge resonance lamp to induce fluorescence. The fluorescence chamber is lowered through the stratosphere on a parachute to control the altitude and velocity of the probe [Anderson, 1976; Anderson, 1980].
- Ground-based high resolution solar absorption by a PEPSIOS (Poly-Etalon Pressure Scanned Interferometer) instrument which resolves a single rotational line in the (O-O) band of HO at 309 nm. The total column density of terrestrial HO between the instrument and the sun is observed, dominated by the altitude interval 25 to 65 km [Burnett 1976, 1977; Burnett and Burnett, 1981].
- Balloon-borne laser induced detection and ranging (LIDAR) in which a pulsed laser system coupled to a telescope is used to observe the backscattered fluorescence from HO. The laser is tuned to the 1-0 band of the A-X transition at 282 nm and the fluorescence at 309 nm (the 0-0 band) is observed as a function of time following the laser pulse [Heaps and McGee, 1982].

Data from the upper stratosphere rocket data from Anderson [1975] and the stratosphere balloon data using *in situ* resonance fluorescence [Anderson, 1980] and LIDAR [Heaps and McGee, 1982] are used to form a composite HO profile (Figure 21-57) with an upper limit of the mean tropospheric HO concentration taken from the methyl chloroform lifetime studies and tropospheric laser experiments.

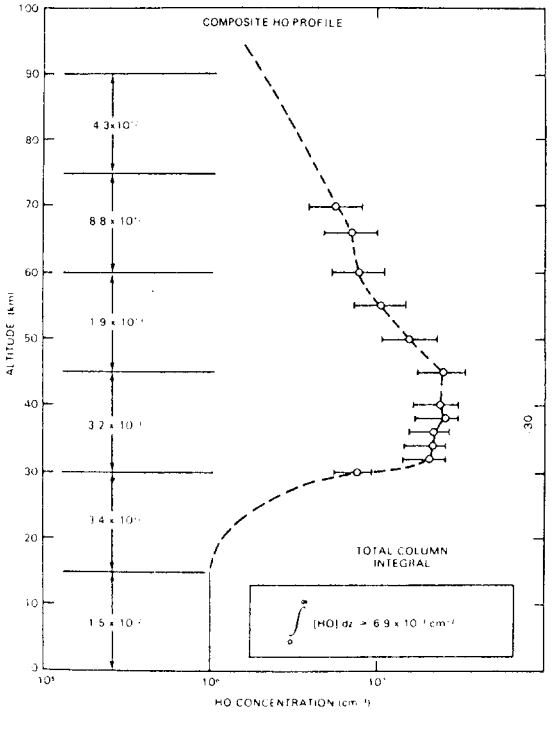

Figure 21-57. A composite HO profile based on the rocket and balloon data. The tropospheric concentration is estimated from methyl chloroform studies and the tropospheric laser experiments.

In summary, an analysis of balloon and rocket data of HO in the stratosphere and ground-based total column observations leads to the following conclusions:

1. There is substantial agreement among the three techniques; the *in situ* data provides a consistent picture of the altitude dependence of HO between 30 and 70 km implying a peak concentration at 40 km of 2.4×10^7 cm^{-3} and a total column density at midday of 6.9×10^{13} cm^{-2}. The midday total column abundance determined from the ground is 5.7×10^{13} cm^{-2}.
2. There is a systematic increase of approximately 1×10^{13} cm^{-2} per year between December 1976 and December 1979 and a suggestion of a yearly spring maximum and fall minimum. The spring to fall decrease is approximately 30%.

21.2.7.2 Hydroperoxyl Radical (HO_2). A total of four HO_2 observations have appeared in the literature, one by the matrix isolation technique and three by the resonance fluorescence method. Those observations are summarized in Figure 21-58. There is significant scatter evident in those observations which should not be attributed to atmospheric variability until:

- The signal-to-noise ratio of the observations is improved;
- Simultaneous observations of photochemically related species such as HO or H_2O demonstrates a correlation in concentration fluctuations.

21.2.7.3 Atomic Hydrogen (H). There are no reported observations of atomic hydrogen in the stratosphere either direct or indirect, nor have any upper limits been reported.

21.2.7.4 Hydrogen Peroxide (H_2O_2). The only reported observation of H_2O_2 is the tentative result reported by Waters et al. [1981] using the Balloon-Borne Microwave Limb Sounder (BMLS) to observe the purely rotational emission of H_2O_2 at 204 GHz. All aspects of the experimental hardware and uncertainties analysis are identical to that discussed in the BMLS section of the CIO discussion.

21.2.8. Odd Chlorine

21.2.8.1 Chlorine Oxide (CO).

Seasonal Variation

Although there is an indication of some seasonal dependence in CIO, the data base is clearly inadequate to draw any clear conclusions. This question should be addressed both by an improvement in the accuracy and precision of the balloon-borne methods and by the more extensive deployment of ground-based methods. Only when those are done in concert will an adequate definition of this important point emerge.

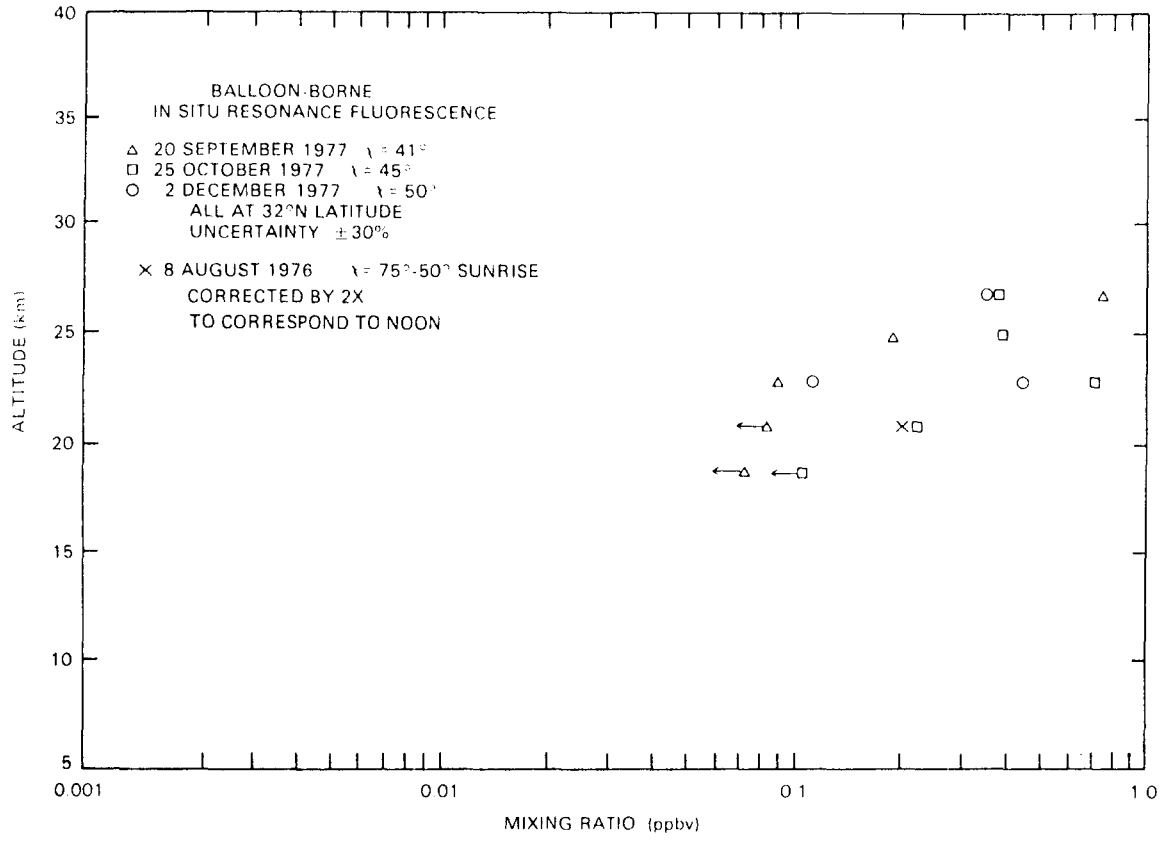

Figure 21-58. Vertical profiles of HO_2 from balloon-borne resonance fluorescence measurements [Anderson et al., 1981].

Latitude Variation

There is virtually no information on the critical question of latitude variation. The balloon-borne observations are all carried out at 32°N and the ground based data at 42°N. As will be noted in the subsequent sections, if the steep gradient in ClO below the peak is characteristic of both mid- and low-latitude conditions, the interpretation of chlorine induced depletion will be significantly simpler.

21.2.8.2 Hydrogen Chloride (HCl). HCl in the stratosphere has been observed by three different remote sensing techniques and one *in situ* method. Most of the presently available data on the vertical profile of concentration come from balloon-borne observations made at ~32°N latitude (Texas and New Mexico); there are, in addition, single profiles taken at 30°S (Australia) and 65°N latitude (Alaska). The profile measurements cover the altitude range from 14 to 40 km, and are supplemented by values for the total column abundance in the upper stratosphere. There is insufficient data from which to discern any seasonal variability, and the location of the altitude of peak relative abundance is not clearly established. The available data cover the period from 1975 to 1980.

Altitude Profile

Balloon-borne near-infrared absorption spectroscopy has been used to obtain vertical profiles covering the 14 to 40 km altitude range (Figure 21-59). Several groups of investigators have made measurements by this method, and obtained results which are in fairly good agreement. In addition there have been observations made by pressure-modulation radiometry, by emission spectroscopy and by absorption spectroscopy from the ground (Figure 21-60).

Seasonal Variation

Since many of the IR absorption measurements of HCl were made at the same latitude (32° and 33°N), it might be expected that any seasonal trend would be seen in this subset of the data. The results, however, do not show any variation greater than the quoted uncertainties associated with each measurement. (It should be mentioned also that the same conclusion regarding the absence of a seasonal variation was reached by Lazrus et al. [1977] from the base-impregnated filter measurements of total acidic chloride vapor.) With the currently improved precision of the remote spectroscopic instrumentation, profiles with associated uncertainties of perhaps less than 10% can be anticipated for the near future; thus, more sensitive tests of the seasonal variability of HCl could be made, provided sufficiently frequent observational opportunities are available.

21.2.8.3 Chlorine Nitrate ($ClONO_2$). The only specific detection claimed for $ClONO_2$ to date is that of Murcray et al. [1979] by IR absorption. The accuracy of the result is

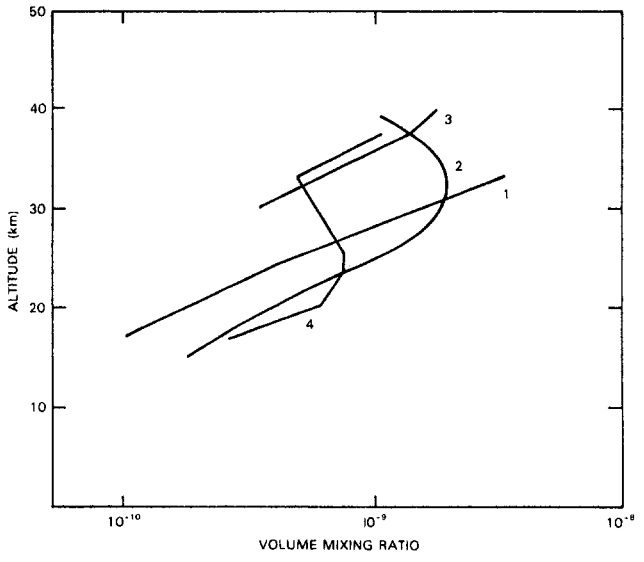

Figure 21-59. HCl measurements by (1) ground-based spectroscopy (June 79 profile), (2) pressure modulator radiometry, (3) far IR emission, and (4) *in situ* filter collection.

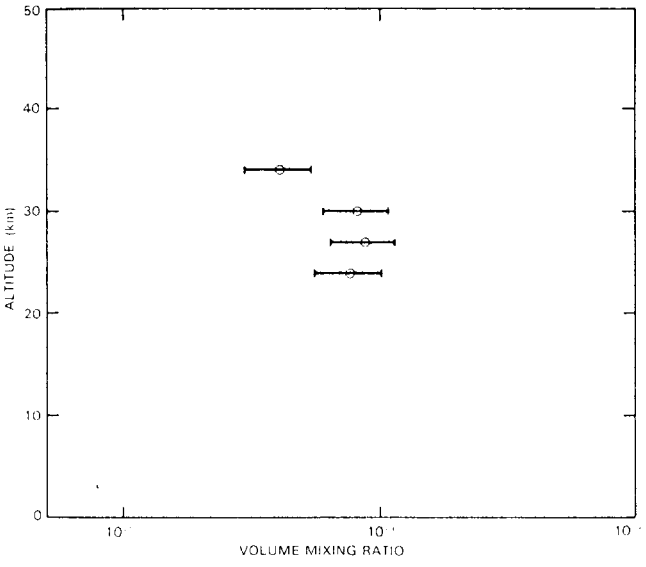

Figure 21-61. Distribution of $ClONO_2$ [Murcray et al., 1980].

affected both by modeling assumptions and by uncertainties in the intrinsic spectroscopic parameters involved in the analysis of the data (see below). The *in situ* sampling method, collection on base impregnated filters [Lazrus et al., 1977], is sensitive to all acidic chloride (see HCI) so that its results can only be used to provide an upper limit estimate for $ClONO_2$. Since the filter data are not compatible with the IR data for HCI, they cannot aid in evaluating the available remote sensing data for $ClONO_2$.

The published values from Murcray's observations, an October 1978 balloon flight (see Figure 21-61), differ from the preliminary values given in NASA RP 1049. The measurements were made by the limb absorption method, that is, by observing the sun through the atmosphere at sunrise or sunset from a stratospheric balloon platform. The strong infrared absorption by $ClONO_2$ at 1292 cm^{-1} was used by Murcray and his coworkers in their analysis; this band coincides in the stratospheric spectrum with strong absorptions by the natural gases, N_2O, CH_4, and H_2O. As the absorptions due to these constituents increase (i.e., at the lower tangents heights of observation), the superimposed $ClONO_2$ absorption is completely masked. However, even at the higher altitudes, where the $ClONO_2$ absorption might be discernible against the spectral background, the maximum expected effect does not exceed 5% or 6% depression of the HCI continuum. Thus the quantitative analysis is dependent both on the spectral model and on the quality of the experimental data. With these considerations in mind, the published data may at best indicate a possible specific identification of $ClONO_2$: the deduction of a profile of concentration with associated experimental errors of $\pm 25\%$ does not seem justified. An upper limit concentration of 10^{-9} by volume, between 25 and 35 km altitude is consistent with the observational data.

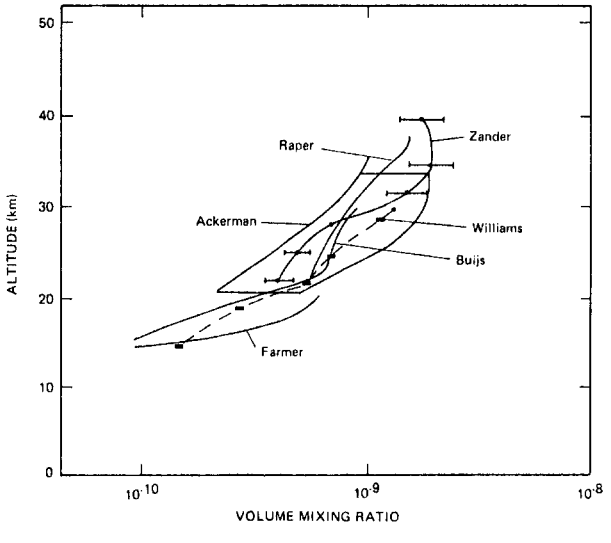

Figure 21-60. HCl distribution from balloon-borne IR absorption spectroscopy.

21.2.9 Other Halogens

21.2.9.1 Hydrogen Fluoride (HF). Stratospheric HF has been measured by several different groups using both remote sensing and *in situ* techniques. The measurements for the most part have been made at different locations and seasons and do not include a sub-set of observations similar to those for HCI from which a most probable profile can be derived. The measurements that have been made to date are summarized in Figure 21-62.

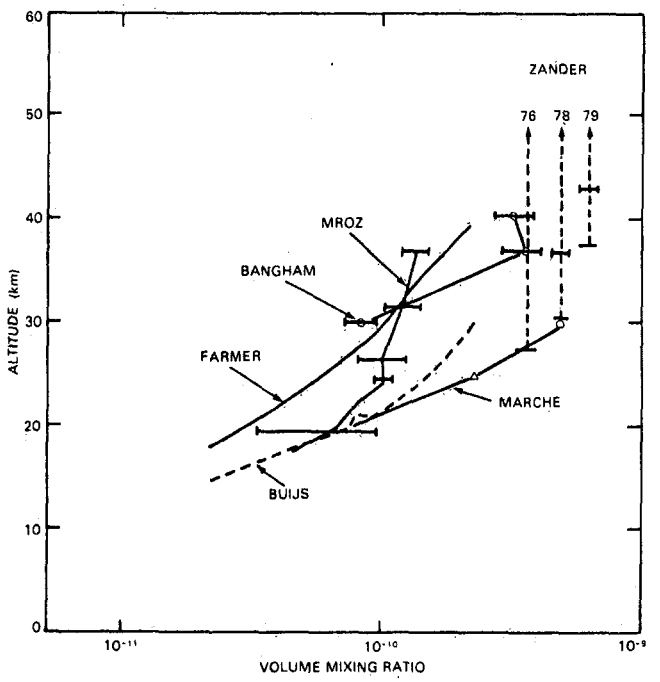

Figure 21-62. Stratospheric HF profile measurements.

21.3 MESOSPHERE

Within the mesosphere, the concentration of many of the minor species can vary by orders of magnitude during a diurnal cycle. The photochemical time constants are so short that extreme gradients are found when temporal variations are studied. However, it is still instructive to consider a case such as Figure 21-63a to indicate the approximate concentrations under a particular set of conditions. Here the results from a time dependent one-dimensional dynamic model are shown based on the work of Keneshea et al. [1979] for the case of midlatitude noontime conditions. There are additional minor species which are not shown in Figure 21-63a; however, these are of particular aeronomic interest. The time constants of some of the middle atmosphere minor species which are controlled by chemical lifetime and transport are shown in Figure 21-63b from a model by Allen et al. [1981]. Part of the discussion of the mesospheric composition will necessarily overlap into the region of lower thermosphere because of the important span between 90 and 120 km where the atmosphere departs from its mixed state to begin diffusive separation. Our understanding of this

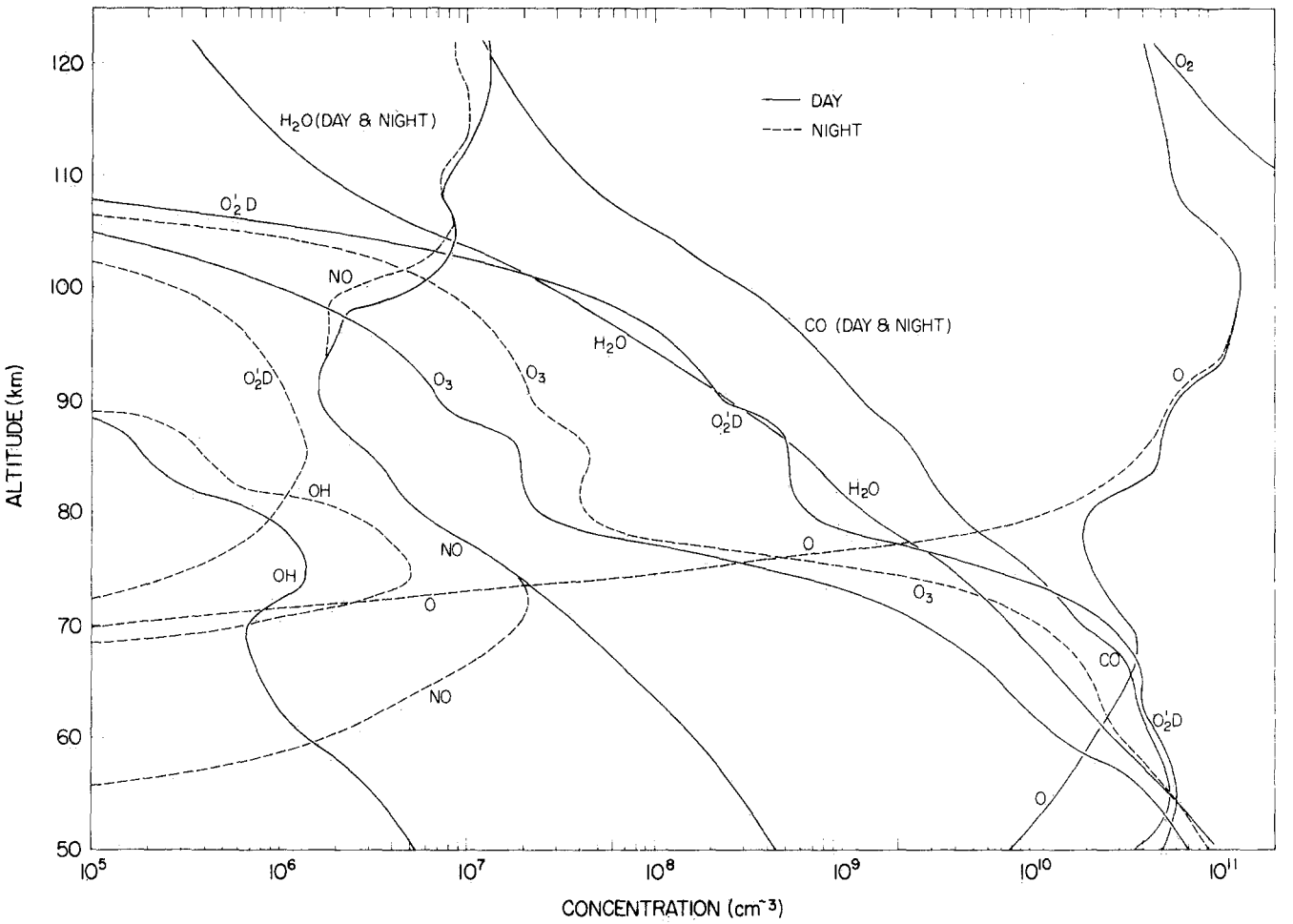

Figure 21-63a. Vertical profiles of neutral minor constituents for noontime conditions at 45°N latitude from time dependent model calculations [Keneshea et al., 1979] (Reprinted with permission from Pergamon Press Ltd. © 1979.)

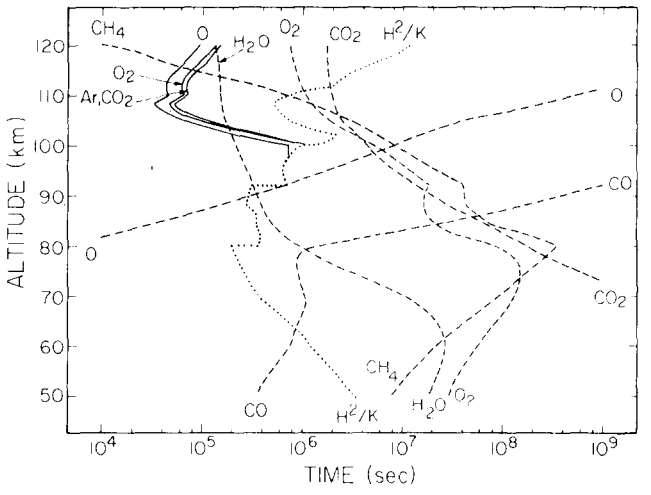

Figure 21-63b. A comparison of the chemical lifetimes (dashed line) of middle atmosphere species and the time scales for transport due to eddy diffusion (dotted line) and molecular diffusion (solid line) [Allen et al., 1981].

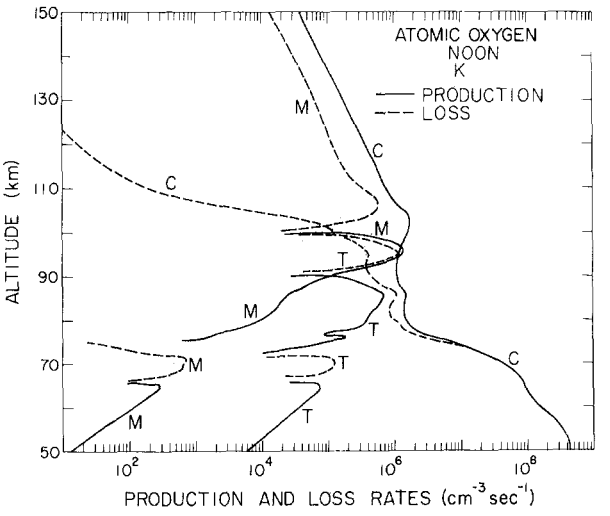

Figure 21-64a. Comparison of the production (———) and loss terms (– – – –) for atomic oxygen at noon. The curves are labeled to represent the contributions of chemistry, C, the amplitude of the molecular flux gradient, M, and the amplitude of the turbulent flux gradient, T [Keneshea et al., 1979]. (Reprinted with permission from Pergamon Press Ltd. © 1979.)

region has progressed significantly during the last 10 years because of the development of more advanced instruments for rocket investigations [von Zahn, 1973]. For convenience, the discussion will be divided into the following catagories: the oxygen constituents (O, O_3), the carbon-oxygen constituents (CO_2, CO), the hydrogen-oxygen constituents (H_2O, OH, HO_2, H_2O_2), the nitrogen-oxygen constituents (NO, NO_2, N_2O), the excited state species ($O_2[^1\Delta_g]$, $N[^2D]$), the meteoric/dust, constituents, and the inert gases (He, Ne, Ar, Kr, Xe). The acids, halogens and chlorine compounds and other trace species have been discussed in the section on the stratospheric species and these are less important in our current understanding of the mesosphere.

21.3.1 The Oxygen Constituents

The atomic oxygen, which results primarily from the dissociation of molecular oxygen in the Schumann-Runge bands, is an important minor species in the mesosphere and becomes the major atmospheric species in the thermosphere for altitudes between 160 and 700 km. The atomic oxygen in the mesosphere is strongly controlled by transport. Eddy diffusion mixes the oxygen atoms to lower altitudes where they are lost by three-body reactions to form ozone in the lower mesosphere.

Figures 21-64a and 21-64b show the results of the one-dimensional time-dependent calculations for atomic oxygen at noon and at midnight. The curves show the production and loss associated with the chemistry, molecular transport and turbulent transport of the atomic oxygen. In Figure 21-65 the midlatitude diurnal variation of atomic oxygen is shown. At altitudes below 80 km, the very pronounced local time dependence is observed. The variation observed is due to the chemistry changes with the assumed constant diffusion profiles. The measurement of atomic oxygen in the mesosphere requires use of rather complicated techniques because of its highly reactive properties and the influence of the measuring instrument in the relatively high pressure of the mesosphere. Mass spectrometers in this region must be cryo-pumped to reduce the gas collisions within the analysing field. The techniques which have been used include mass spectrometers [Philbrick et al., 1973; Offermann and

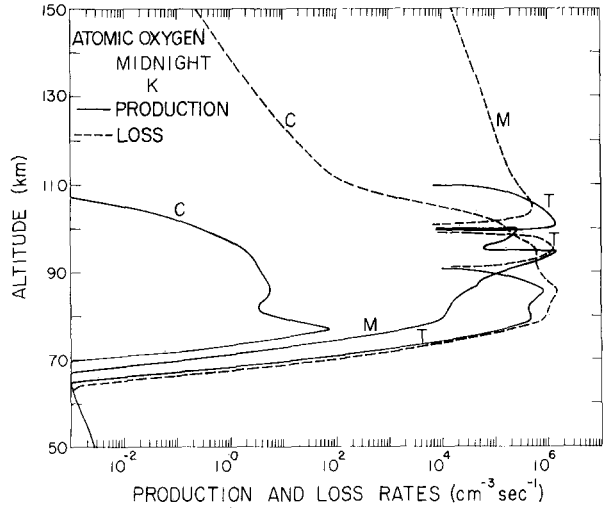

Figure 21-64b. Comparison of the production and loss terms in the chemical model for atomic oxygen at midnight. The labels are the same as in (a) [Keneshea et al., 1979]. (Reprinted with permission from Pergamon Press Ltd. © 1979.)

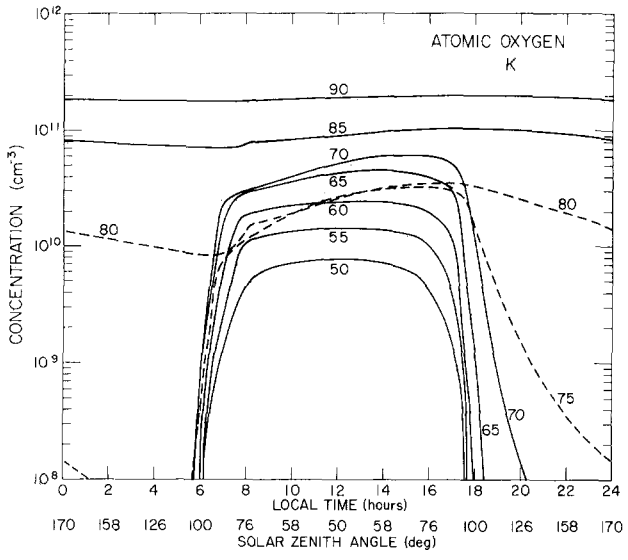

Figure 21-65. Diurnal variation of atomic oxygen between 50 and 90 km from model calculations [Keneshea et al., 1979] (Reprinted with permission from Pergamon Press Ltd. © 1979.).

Grossmann, 1973; Arnold and Krankowsky, 1977], photometers for 5577 Å emission [Dandekar, 1972; Offermann and Drescher, 1973], silver film oxidation [Henderson, 1971], resonance fluorescence [Dickinson et al., 1974; Howlett et al., 1980], NO chemiluminescence [Golomb and Good, 1972], atomic absorption [Dickinson et al., 1974], and from hydroxyl airglow [Good, 1976]. A study of the existing data by Offermann et al. [1981] has shown a strong correlation of the atomic oxygen column density between 80 and 120 km with the measured peak density. This correlation (see Figure 21-66) is quite good considering the large variability which is observed in the individual profiles shown in Figure 21-67. The oxygen profile is strongly affected by the transport properties at a given time. The fact that a large amplitude variation that may be expected due to eddy diffusion was shown in the study of Keneshea and Zimmerman [1970]. Offermann et al. [1981] also pointed out the anti-correlation of the argon and atomic oxygen behavior which is expected with changes in the eddy diffusion. Most of the measure-

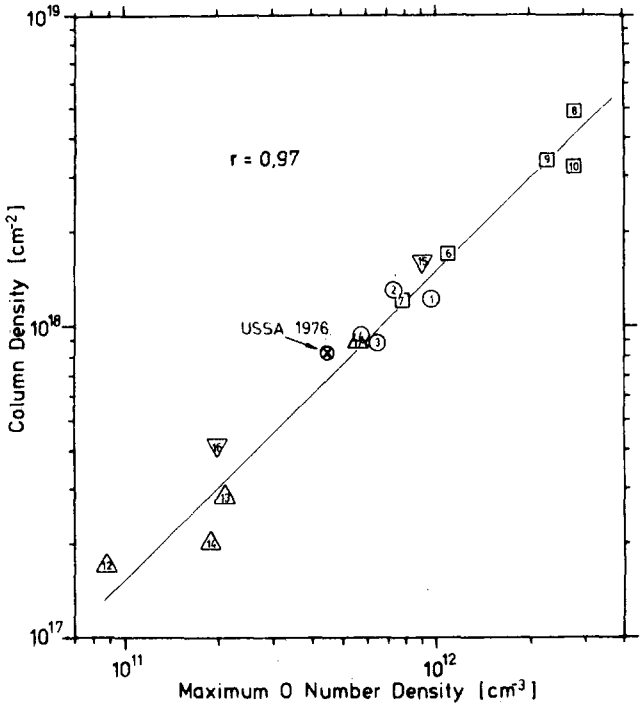

Figure 21-66. Atomic oxygen layer peak density vs O layer content. Layer content is represented by the column density up to 110 km. Different measuring techniques of 16 rocket flights are indicated by different symbols. Model values from USSA 1976 are given for comparison and the straight line is at 45°. Identification numbers in symbols are described in original text [Offermann et al., 1981] (Reprinted with permission from Pergamon Press Ltd. © 1981.).

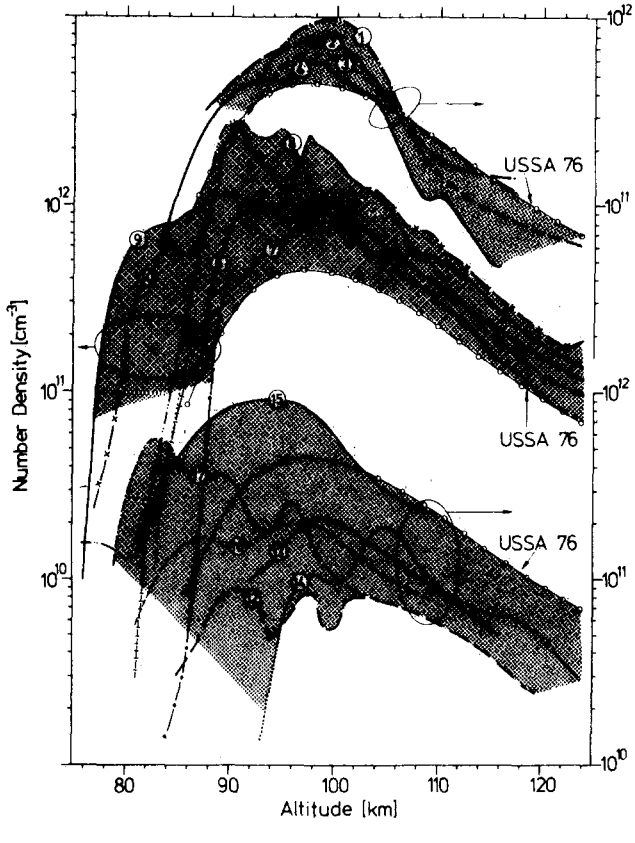

Figure 21-67. Atomic oxygen number density profiles as obtained from 16 *in situ* measurements. Results from 3 different measuring techniques are grouped together (shaded areas) and refer to 3 different density scales. USSA 1976 model profile is given for comparison with each of the 3 groups. Profile identification numbers are given in original text [Offermann et al., 1981] (Reprinted with permission from Pergamon Press Ltd. © 1981.).

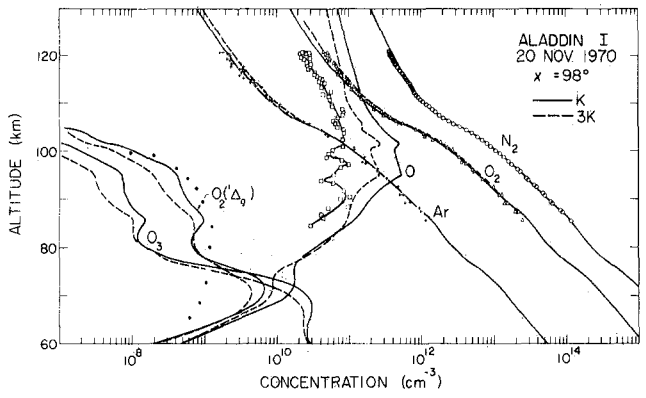

Figure 21-68. Comparison of computed species profiles for turbulent diffusivities K and 3 K (solid dashed curves) with measured profiles for O (squares), O_2 (triangle), N_2 (circles), Ar (crosses), and $O_2(^1\Delta_g)$ (dots) for the ALADDIN I program [Keneshea et al., 1979]. (Reprinted with permission from Pergamon Press Ltd. © 1979.)

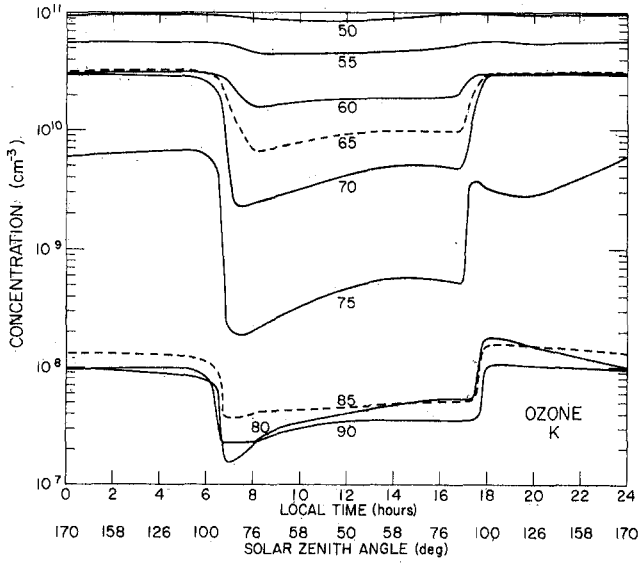

Figure 21-70. The model calculation of the diurnal variation of the O_3 [Keneshea et al., 1979]. (Reprinted with permission from Pergamon Press Ltd. © 1979.)

ments of atomic oxygen show the irregular structure in the altitude region between 90 and 110 km due to the turbulent layers in that region. The calculations of atomic oxygen in a time-dependent transport model also show irregularities in this region where the eddy diffusion profile is irregular. An example of this structure is observed in the measurement and model calculations for the ALADDIN I experiment shown in Figure 21-68. The series of ALADDIN (*A*tmospheric *L*ayering *A*nd *D*ensity *D*istribution of *I*ons and *N*eutrals) experiments and models have provided some of the most important foundation for our current understanding of the middle atmosphere properties and therefore several of those results are used for illustration.

Model calculations for the ozone production and loss for midnight at midlatitudes is shown in Figure 21-69. The diurnal variation of the O_3 is shown in Figure 21-70. The measurements of ozone have been refined and both *in situ* and remote sensing techniques have provided accurate results in the stratosphere. However, there are relatively few measurements of the ozone in the mesosphere. A comparison of photometer measurements and model calculations is shown in Figure 21-71.

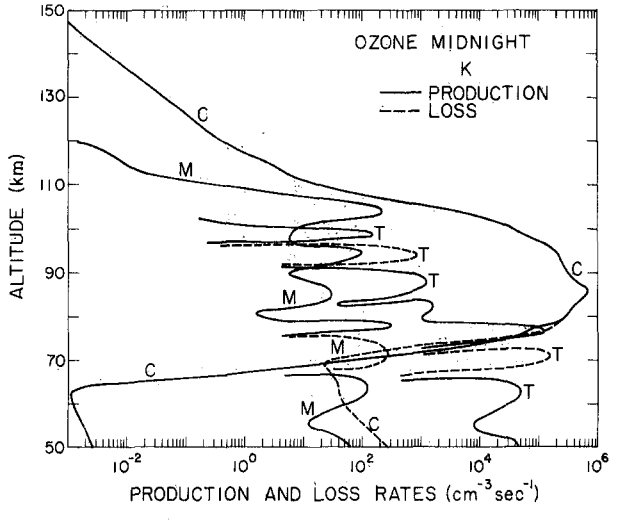

Figure 21-69. Model calculations for the ozone production and loss for midnight at midlatitudes. The label C represents chemistry effects, M represents molecular transport, and T represents turbulent transport [Keneshea et al., 1979]. (Reprinted with permission from Pergamon Press Ltd. © 1979.)

21.3.2 Carbon-Oxygen Constituents

The atmospheric carbon dioxide, CO_2, and its dissociative product, CO, are very important species for the role they contribute to the radiation balance and thermal structure of the middle atmosphere. The CO_2 molecules are also important in some of the chemical reactions for formation of the negative ion species of the D region. In Figure 21-72, the results of a calculation by Hays and Olivero [1970] are shown for the CO_2 dissociation and transport by eddy diffusion. The various curves represent two extremes for the recombination and a range of eddy diffusion values. The fact that the CO_2 remains near ground level mixing ratio values for altitudes up to the turbopause has been substantiated by measurements shown in Figure 21-73. Trinks and Fricke [1978] pointed out that in addition to solar dissociation, the CO_2 concentration at higher altitudes is also con-

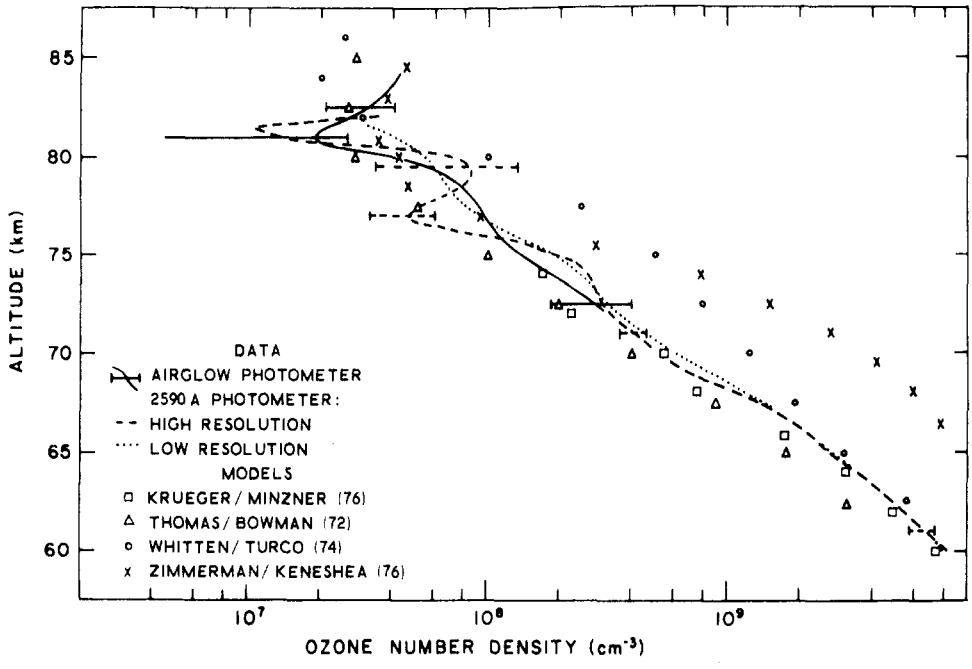

Figure 21-71. Comparison of photometer measurements and model calculations of ozone [Weeks et al., 1978].

trolled by loss from an ion molecule reaction with O^+. The calculations of the CO_2 and CO behavior in the mesosphere and thermosphere require solution of the time-dependent transport equations with appropriate considerations of the photodissociation, diffusion transport and loss by the ion molecule reaction. The CO_2 emission in the 15 μm and 4.3 μm bands has also been measured by rocket-borne IR spectrometers, Stair et al. [1975]. The measured IR signal results from a combination of the contributions of the CO_2 concentration and the temperature.

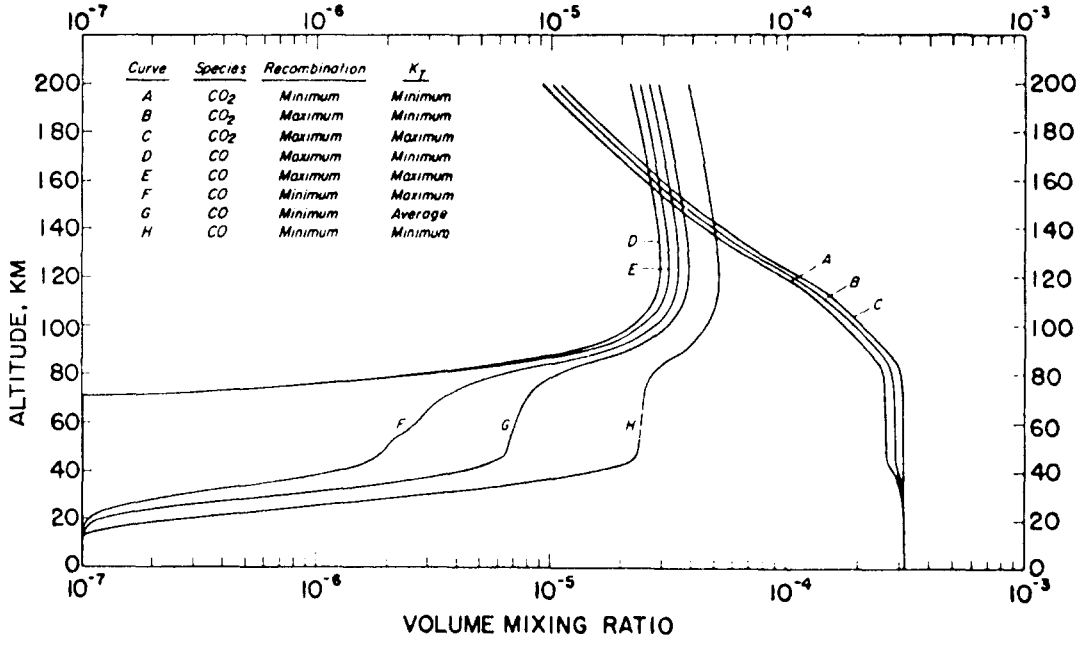

Figure 21-72. Calculated profiles of the volume mixing ratios of CO_2 and CO [Hays and Olivero, 1970]. (Reprinted with permission from Pergamon Press Ltd. © 1970.)

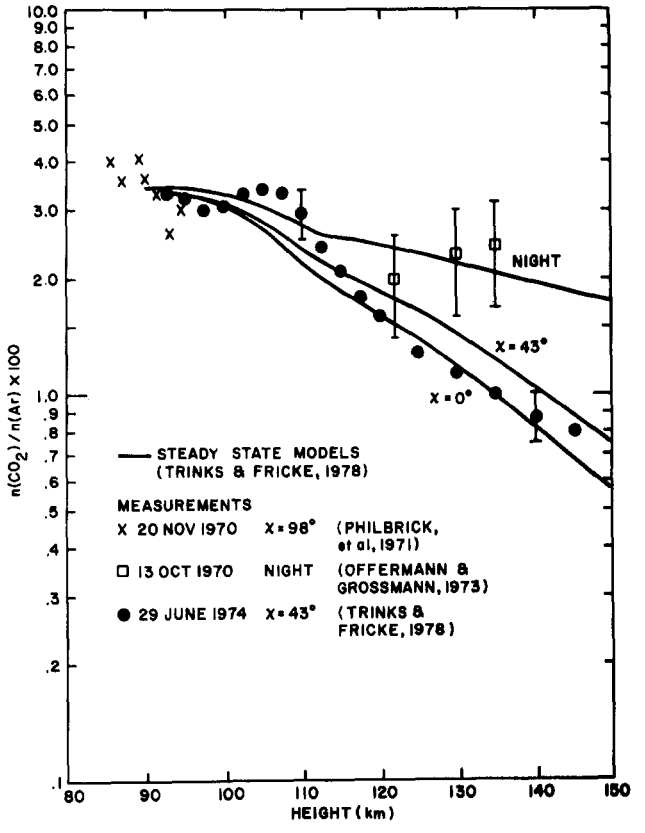

Figure 21-73. Calculated and measured $n(CO_2)/n(Ar)$ ratio for three zenith angles. Data are from the sources indicated. Day-night differences are expected due to solar dissociation of CO_2 and due to an ion chemistry reaction with O^+.

21.3.3 Hydrogen-Oxygen Constituents

The hydrogen constituents are important in many of the chemical processes in the middle atmosphere. Figure 21-74 provides an overview of the important photochemistry and transport involving the hydrogen constituents. The H_2O concentration leads to the formation of H and OH which in turn react with O, O_2, and O_3 as indicated in Figure 21-75. The oxygen chemistry in the mesosphere is strongly tied to the hydrogen concentration through reactions with OH and H_2O. In Figure 21-76 the differences between the steady state photochemical calculations and the time dependent calculations for O, H_2O, and H are shown for noon midlatitude conditions. This example, from the Keneshea et al. [1979] model, emphasizes the importance of the time-dependent calculations for the mesospheric processes. The H_2O in the mesosphere participates in another important process, the formation of the water cluster ions which are the dominant positive and negative ion species of the lower D region. The model calculations of the diurnal variations of OH and H are shown in Figures 21-77 and 21-78. The question of the mixing ratio of the H_2O which is appropriate to various mesosphere conditions is yet to be answered. One of the ways of inferring the possible concentrations of H_2O, as well as certain other minor species, is from the ion composition in the D region when the temperature is known and the laboratory measured rate constants are used, Ramseyer et al. [1983], Kopp and Philbrick [1983]. The H_2O reactions in the mesosphere are not as simple as would be inferred in Figure 21-75, but in fact include several of the other minor species as indicated in Figure 21-79.

21.3.4 The Nitrogen-oxygen Constituents

The nitric oxide concentration in the mesosphere is primarily responsible for the formation of the D-region. This results from solar Lyman- α radiation ionization at low altitudes within a window of the O_2 absorption. The NO production rate increases dramatically during periods of particle ionization. Figure 21-80 shows the nitric oxide production rate associated with some particle events. The model calculations of Brasseur [1984] for the verticle flux of nitric oxide in the mesosphere are shown in Figure 21-81. Figure 21-82 shows the meridional distribution of nitric oxide which is consistent with the vertical flux shown in Figure 21-81

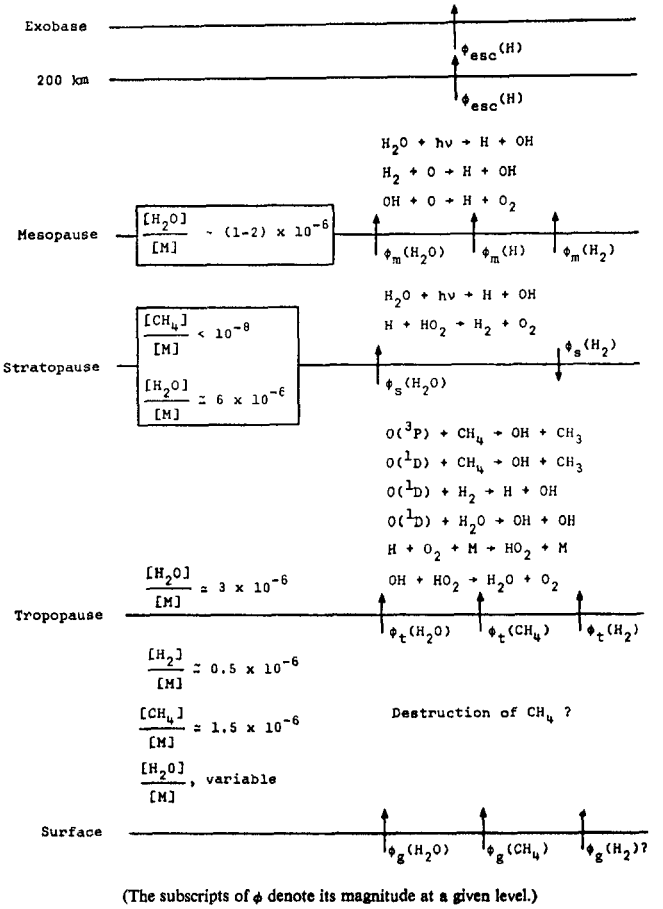

Figure 21-74. Photochemistry and transport of hydrogen constituents [after Strobel, 1972].

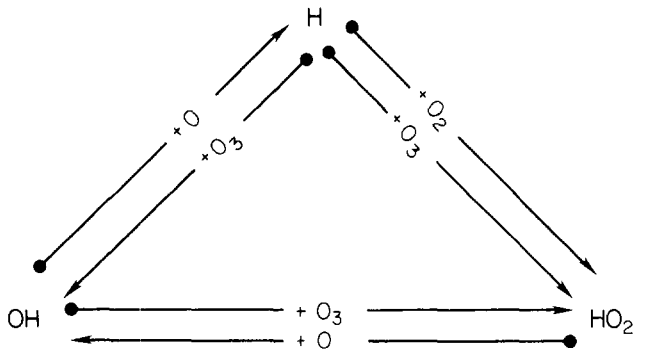

Figure 21-75. Principal reactions in which H, OH, and HO_2 are involved with O and O_3 [after Strobel, 1972].

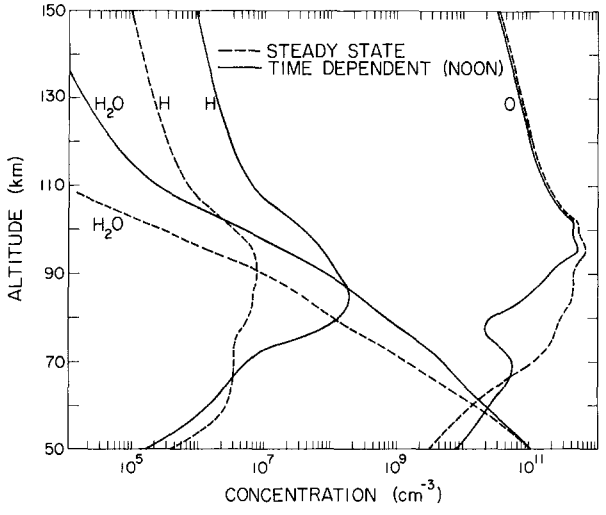

Figure 21-76. Hydroxyl radical variation from the time dependent model [Keneshea et al., 1979]. (Reprinted with permission from Pergamon Press Ltd. © 1979.)

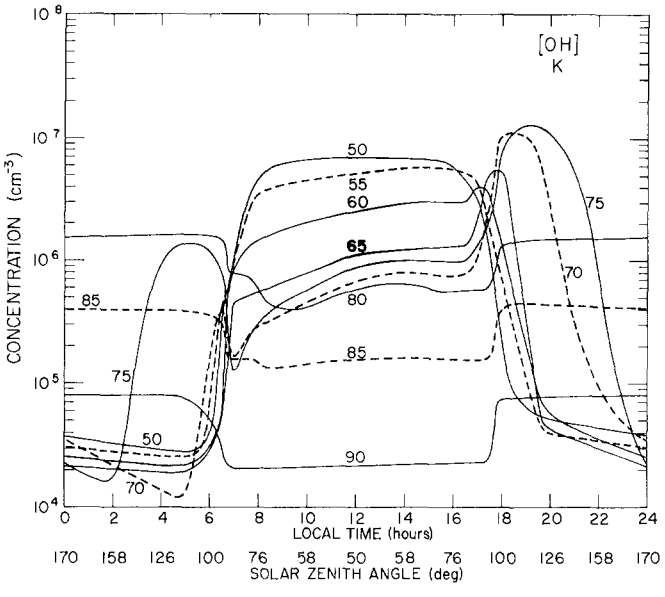

Figure 21-77. The steady-state profiles (dashed curves) and the noontime profiles (solid curves) taken from the last solution day of the time-dependent calculations for the species O, H, and H_2O [Keneshea et al., 1979]. (Reprinted with permission from Pergamon Press Ltd. © 1979.)

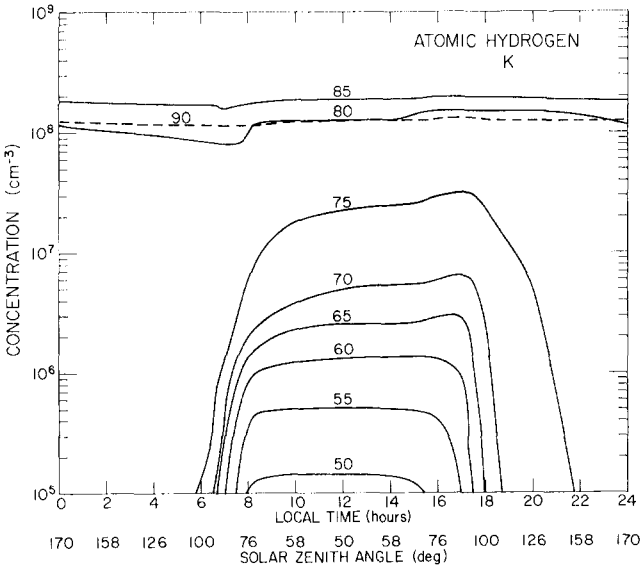

Figure 21-78. Atomic hydrogen variation from the time-dependent model [Keneshea et al., 1979]. (Reprinted with permission from Pergamon Press Ltd. © 1979.)

(based on Ebel [1980]). The meridional distribution of NO shown in Figure 21-83 is in better agreement with the measurements of NO profiles and results from a better choice of the eddy diffusion coefficient. The result emphasizes again the important role of the dynamics in the mesosphere. In Figure 21-84, the steady-state concentrations of ON (mean odd nitrogen - all nitrogen other than N_2), $N(^4S)$, and the fractional abundance of NO relative to odd nitrogen. The important reactions in the odd nitrogen constituents in the atmosphere are shown in Figure 21-85.

21.3.5 Meteoric and Dust Constituents

The resonance fluorescence dayglow emission of several of the meteoric debris species, such as sodium and lithium,

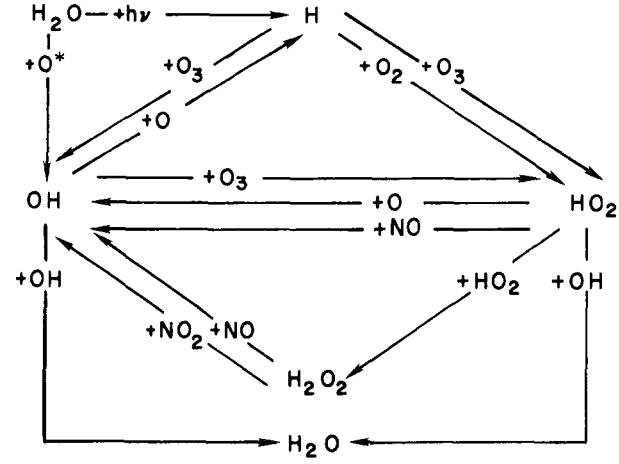

Figure 21-79. Fundamental H_2O reaction diagram [after Strobel, 1972].

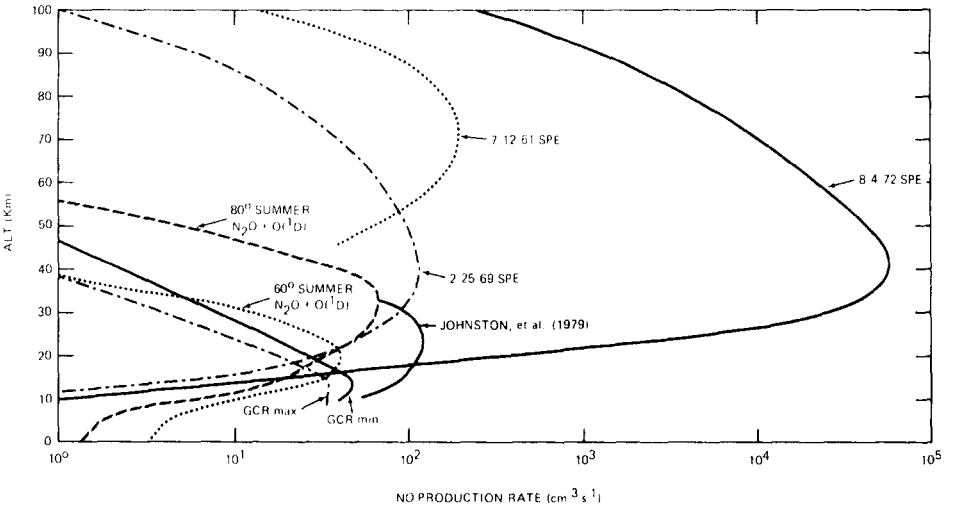

Figure 21-80. Instantaneous nitric oxide production rates for Galactic Cosmic Ray (GCR) (at solar maximum and minimum), Solar Proton Events (SPE) (July 12, 1961, February 25, 1969, August 4, 1971), and oxidation of nitrous oxide (60° summer, 80° summer, and Johnston et al. [1979] at 60° summer [Jackman et al., 1980]).

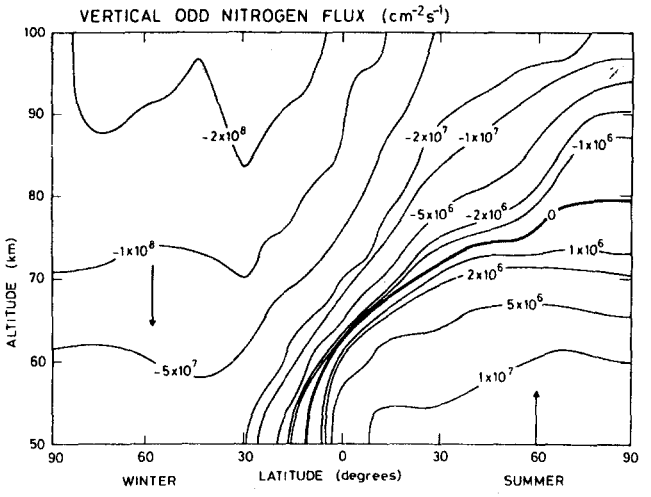

Figure 21-81. Meridional distribution of the vertical flux of nitric oxide based upon the exhange coefffficients suggested by Ebel, 1980 [Brasseur, 1984].

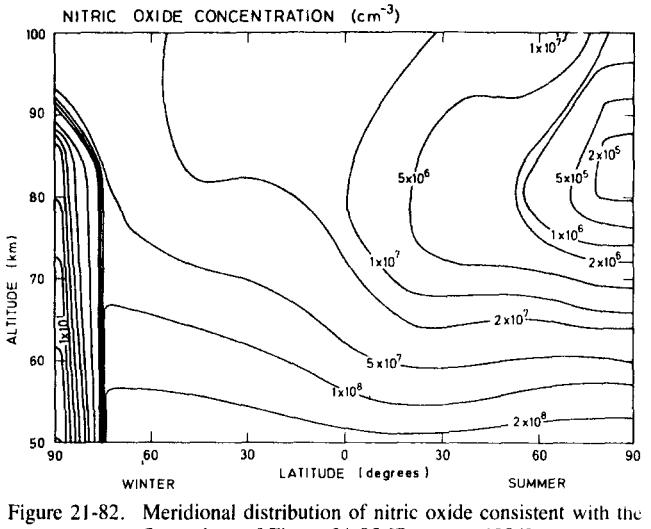

Figure 21-82. Meridional distribution of nitric oxide consistent with the flux values of Figure 21-85 [Brasseur, 1984].

has been monitored for many years. The ions of iron, magnesium, aluminum, calcium, etc. have been often measured and found to represent an almost continual input of the meteoric species to the upper atmosphere. Sodium and other species have been measured by LIDAR techniques by groups in France [Megie et al., 1978] and the U.S. [Richter et al., 1981]. The results of the sodium calculations from a model by Kirchoff et al. [1981] are shown in Figure 21-86. The meteoric and volcanic dust injected into the atmosphere is important in several areas. The dust can serve as a nucleation

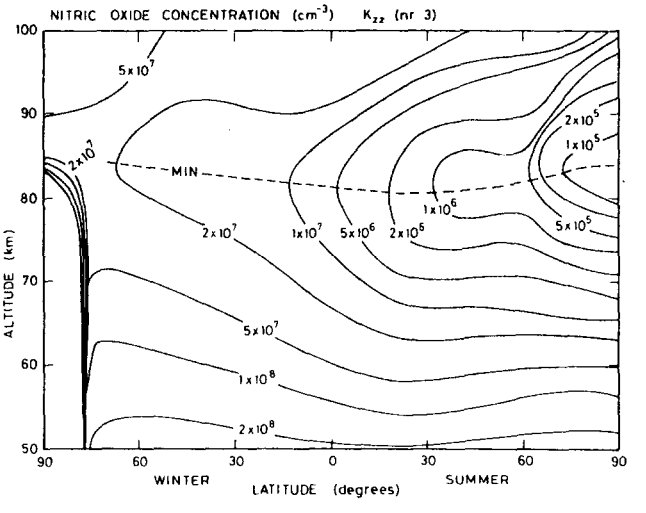

Figure 21-83. Improved model calculation for the nitric oxide meridional distribution by better choice of the dynamical properties in the calculation [Brasseur, 1984].

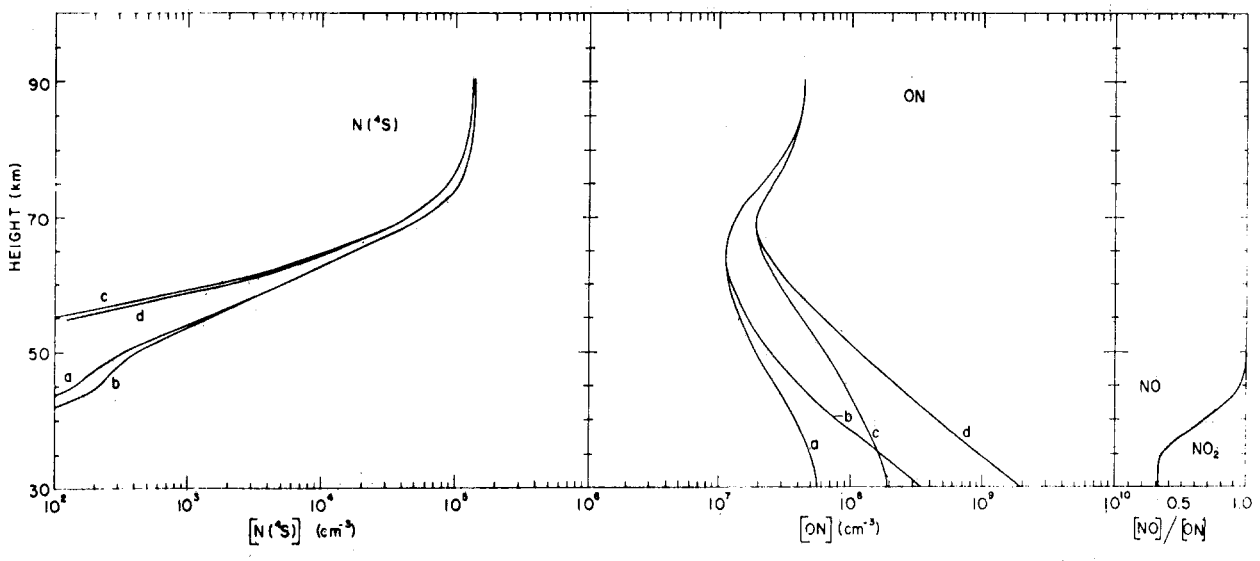

Figure 21-84. Density profiles for N(⁴S) and odd nitrogen and relative daytime concentrations of NO and NO_2 for various models. Curve *a*, large NO dissociation rate and $\partial[NO]/\partial z$ = O at lower boundary; curve *b*, same as curve *a* but $\phi(ON)$ = O at lower boundary; curve *c*, same as curve *a* but small NO dissociation rate; and curve *d*, small NO dissociation rate and $\phi(ON)$ = O at lower boundary [after Strobel, 1971].

Level	Sources	Exchange Reactions	Sinks
Exobase			
THERMOSPHERE	$O^+(^4S) + N_2 \rightarrow NO^+ + N(^4S)$ $N_2^+ + O \rightarrow NO^+ + N(^4S \text{ or } ^2D)$ $N_2^+ + e \rightarrow 2N(^4S \text{ or } ^2D)$ $e(\text{fast}) + N_2 \rightarrow 2N(^4S \text{ or } ^2D)$ $N_2 + h\nu(\lambda\lambda 800\text{-}1000\text{Å}) \rightarrow 2N(^4S \text{ or } ^2D)$	$NO^+ + e \rightarrow N(^4S \text{ or } ^2D) + O$ $N(^4S) + O_2 \rightarrow NO + O$ $O_2^+ + N(^4S) \rightarrow NO^+ + O$ $N(^2D) + O_2 \rightarrow NO + O$ $N(^2D) + O \rightarrow N(^4S) + O$ $e + N(^2D) \rightarrow e + N(^4S)$ $O_2^+ + NO \rightarrow NO^+ + O_2$	$N(^4S) + NO \rightarrow N_2 + O$ $N(^2D) + NO \rightarrow N_2 + O$ $\downarrow \phi_1(NO) \sim 2.5 \times 10^8 cm^{-2} sec^{-1}$
Mesopause			
	$\downarrow \phi_1(NO) \sim 2.5 \times 10^8 cm^{-2} sec^{-1}$		
Mesosphere and Upper Stratosphere	$N_2 + h\nu(\lambda\lambda 1100\text{-}1250\text{Å}) \rightarrow 2N(^4S)$	$NO + h\nu(\lambda\lambda 1750\text{-}1910\text{Å}) \rightarrow N(^4S) + O$ $NO + h\nu(\lambda 1216\text{Å}) \rightarrow NO^+ + e$ $NO^+ + e \rightarrow N(^4S \text{ or } ^2D) + O$ $N(^4S) + O_3 \rightarrow NO + O_2$ $N(^4S) + OH \rightarrow NO + H$ $N(^4S) + O_2(^1\Delta) \rightarrow NO + O$ $N(^2D) + O_2 \rightarrow NO + O$ $O_3 + NO \rightarrow NO_2 + O_2$ $NO_2 + h\nu(\lambda < 3975\text{Å}) \rightarrow NO + O$ $+ h\nu(\lambda < 2750\text{Å}) \rightarrow N(^4S) + O_2$ $O + NO_2 \rightarrow NO + O_2$ $N(^4S) + NO_2 \rightarrow 2NO$	$N(^4S) + NO \rightarrow N_2 + O$ $N(^4S) + NO_2 \rightarrow N_2 + O_2$ $\rightarrow N_2 + 2O$ $\rightarrow N_2O + O$ $\downarrow \phi_2(NO + NO_2) < 10^7 cm^{-2} sec^{-1}$
Middle Stratosphere			
	$\downarrow \phi_2(NO + NO_2) < 10^7 cm^{-2} sec^{-1}$		
Lower Stratosphere and Troposphere	$O(^1D) + N_2O \rightarrow 2NO$ $N_2O + h\nu(\lambda < 2500\text{Å}) \rightarrow N(^4S) + NO$	$O_3 + NO \rightarrow NO_2 + O_2$ $NO, NO_2 \rightarrow HNO_2, HNO_3, NO_3, N_2O_5$	$N(^4S) + NO \rightarrow N_2 + O$ $N(^4S) + NO_2 \rightarrow$ see above removal of HNO_2 and HNO_3 by precipitation processes
	Air pollution		$\downarrow \phi(HNO_2 + HNO_3) = ??$
Ground			

Figure 21-85. Sources, sinks, and exchange reactions of odd nitrogen [after Strobel, 1971].

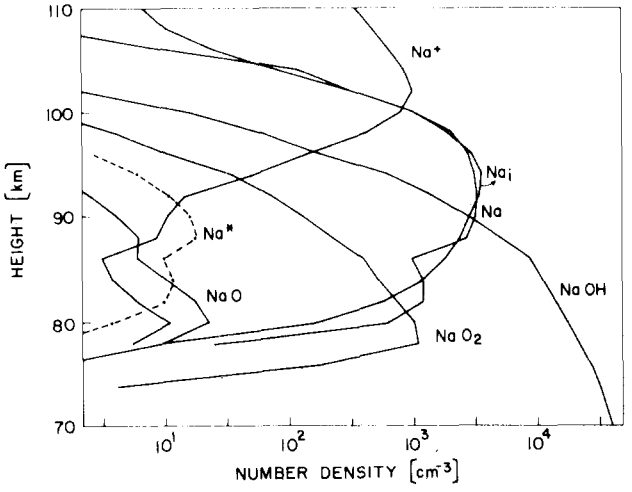

Figure 21-86. Calculated flux model sodium density profile. The production of excited sodium in units of cm^{-3} s^{-1} is designated by Na*, and Na_i is the average measured profile shown for comparison [Kirchhoff et al., 1981].

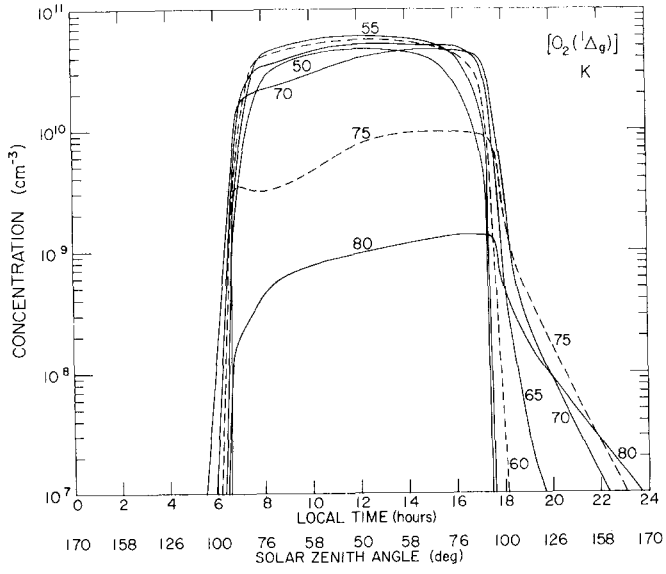

Figure 21-88. $O_2(^1\Delta_g)$ time dependence calculated from one-dimensional model [Keneshea et al., 1979]. (Reprinted with permission from Pergamon Press Ltd. © 1979.)

center for partical growth, possibly important in development of noctilucent clouds, or may be the source for species which can have significantly longer lifetimes, such as the meteoric ion lifetimes which are important in the formation of sporadic E layers.

21.3.6 The Inert Gases

The nobel gases provide the opportunity of studying the effects of transport without the complications of the chemical processes which also affect most species. The region near 100 km is of particular interest because of the turbopause or cessation of mixing of the species. This region is particularly important when attempting to model the thermosphere because of the effect on the distribution of the species. Figure 21-87 shows a summary of the published Ar/N_2 ratios in this region. The structure in the profiles indicates that the transition to molecular diffusion is not smooth, but is rather complicated by a region of alternating laminar and turbulent layers with rather strong peaks in the eddy diffusion. Argon is probably the most important of the inert species because it provides a good tracer for the transition from mixed to diffusive regions. It is also the "thermometer" in determining the temperature structure in the lower thermosphere.

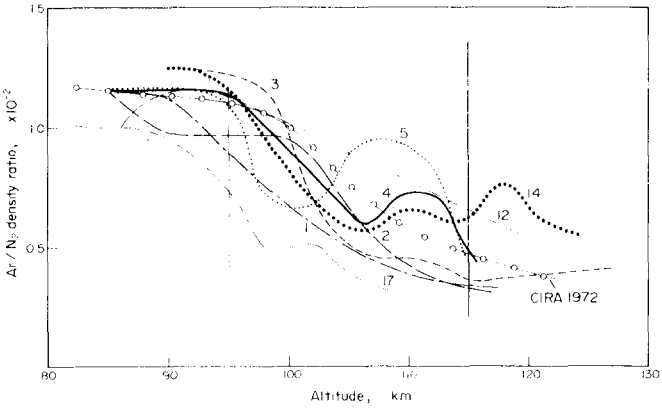

Figure 21-87. Number density ratios of argon and nitrogen vs altitude. CIRA 1972 Mean Reference Atmosphere profile is given for comparison. Profile identification numbers are given in original text [Offermann, 1981]. (Reprinted with permission from Pergamon Press Ltd. © 1981.)

21.3.7 Excited Species

Several species in excited states deserve special consideration because of the pronounced effect that they have in the mesospheric chemistry. Two of the most interesting are $O_2(^1\Delta_g)$ and $N(^2D)$. The $O_2(^1\Delta_g)$ provides an important source of ionization in the D region because of its higher energy state. In Figure 21-88 the model calculations of the temporal variation of the $O_2(^1\Delta_g)$ are shown. Figure 21-89 shows a comparison of several rocket flight measurements with model calculations of the $O_2(^1\Delta g)$. Measurements of the near-IR emission associated with this species are useful to infer some properties of the mesospheric chemistry because it is involved in the O and O_3 reaction schemes.

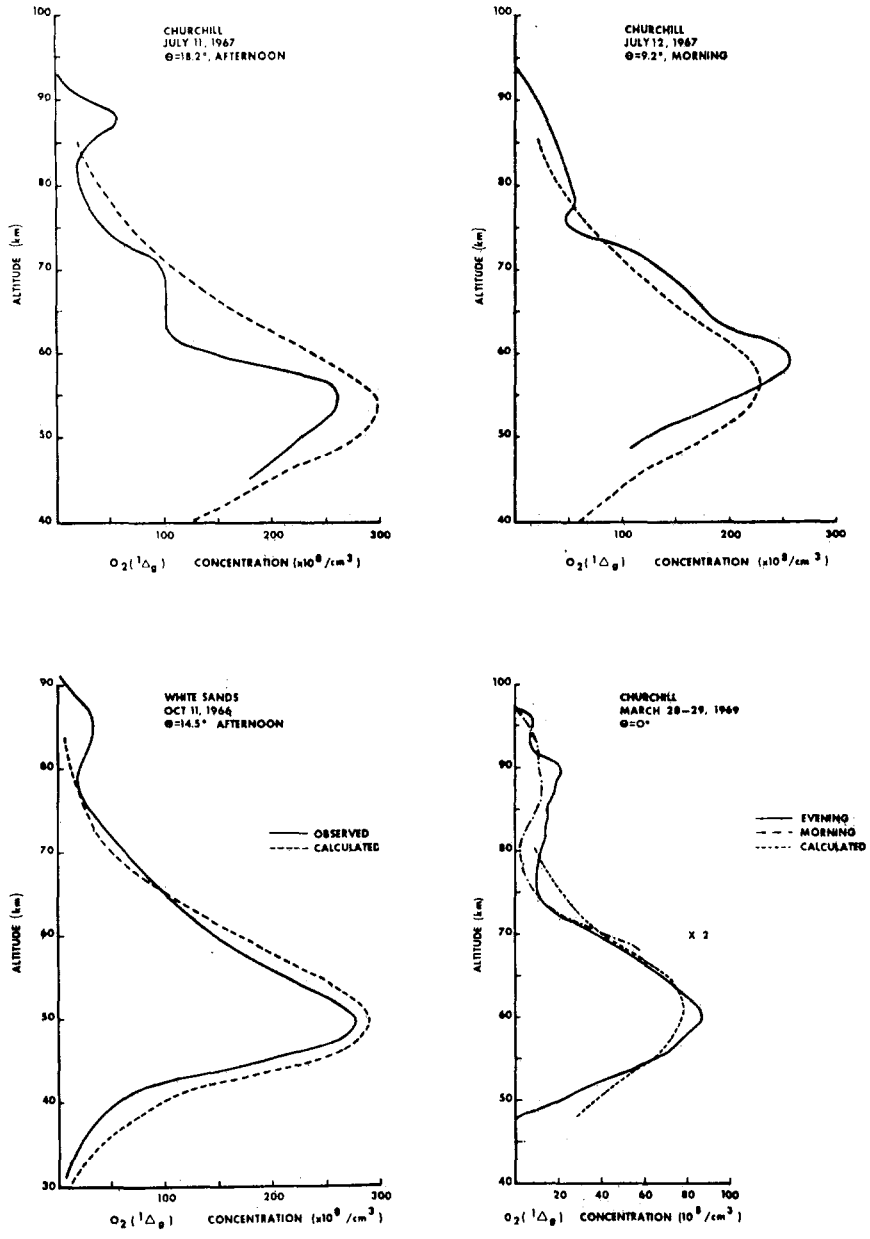

Figure 21-89. Comparison of calculated with observed altitude profiles of $[O_2(^1\Delta)]$ [after Evans and Llewellyn, 1970].

21.4 IONIZED CONSTITUENTS

21.4.1 Overview

The ionosphere is created mainly by the absorption of solar ultraviolet and x ray radiation in the earth's upper atmosphere. Hence, the initial ions are formed in some proportion to their respective neutral parent populations. The atmosphere is composed primarily of N_2 and O_2 below 100 km, the homosphere, where the atmospheric gases are generally well-mixed. Above this altitude, in the heterosphere, which virtually coincides with the thermosphere, atomic oxygen rapidly becomes a major constituent with increasing altitude and is the dominant species above about 170 km, depending upon thermospheric expansion due to solar activity. A fairly linear relationship exists, for example, between solar radiation monitored at 10.7 cm and thermospheric temperature [Nicolet, 1963].

The fact that the principal thermospheric species is atomic above a certain height has profound implications with respect to absolute electronic and ionic concentrations. The ionosphere is basically a weak, neutral plasma, that is, the total positive ion concentration equals the electron plus the

total negative ion concentration. (Negative ions are important only in the D region, below 90 km.) Ionization is depleted when oppositely charged particles recombine. However, the rate coefficient, $\sim 10^{-12}$ cm^3 s^{-1}, for (radiative) recombination between atomic positive ions and electrons, particularly $O^+ + e \rightarrow O + h\nu$ where $h\nu$ represents a photon, is five orders of magnitude slower than the (dissociative) recombination rates of common ionospheric molecular ions like O_2^+ and NO^+. These vastly different loss rates are the main reason that the maximum electron (or total positive ion) concentration of the F region, approximately 10^6 cm^{-3}, nominally occurs near 300 km, even though the maximum photoionization rate is near 150 km, the base of the F region. This region contains the overwhelming bulk of the total ionospheric charged particle content. This peak altitude is a function of latitude, solar activity, plus chemical and transport loss processes. Above the peak of the F layer, ions are lost mainly by transport to lower altitudes. Below the F layer maximum, ionization is depleted largely by ion-molecule reactions between O^+ ions and O_2 and N_2 which create O_2^+ and NO^+ ions, respectively. These diatomic ions recombine rapidly with electrons.

The E region, nominally 90 to 150 km, is comprised mainly of O_2^+ and NO^+ ions. A majority of the initial ions created by the absorption of solar x rays and EUV radiation in this region are N_2^+ ions, which react rapidly with O_2 and O at these altitudes to form O_2^+ and NO^+ ions. Some O_2^+ ions are formed directly from the solar ionization of O_2. Depending upon the relative electron and NO concentrations, a signficant fraction of O_2^+ ions may undergo charge transfer with NO to form NO^+ ions. The E region frequently is enhanced by precipitating kilovolt electrons at high latitudes, an energy (and hence altitude) regime common to auroral ionization. The transport of ionization generally is unimportant in the E region where the lifetime of molecular ions is rather short, roughly $3 \times 10^6/[e]$ s, where [e] is the electron concentration in cm^{-3}. An important exception occurs when atomic (meteoric metal) ions are present and the wind fields are favorable with respect to the creation of a sporadic E layer, a thin layer (2 km) of ionization that can attain ionic (electronic) concentrations exceeding 10^6 cm^{-3} in contrast to typical daytime midlatitude concentrations of 1 to 2×10^5 cm^{-3}.

The smallest portion of the ionosphere is the D region, roughly 50 to 90 km. It contains less than 0.1% of the total ionospheric charged particle content. This region acts as the upper boundary of the earth-ionospheric wave-guide for LF and VLF electromagnetic radiation. In addition, HF and VHF electromagnetic waves may suffer attenuation since the electron-neutral collision frequency is greatest in this lowest portion of the ionosphere because of the high neutral concentrations. This attenuation is minimal for the normal quiet D region which has a daytime maximum electron concentration of about 10^3 cm^{-3} near 80 km. However, solar flares may produce greatly enhanced x ray radiation below 10 Å which can increase electron concentrations by 10 fold or more, creating an SID (sudden ionospheric disturbance) lasting 10 to 20 minutes. At higher latitudes, precipitating protons (sometimes accompanied by energetic electrons) associated with a solar proton event (SPE) produce an enhanced D region, which in the SPE case, spreads out over the entire polar cap and may last several days. An SPE may be intense enough to blackout HF transmissions and, therefore, is known also as a polar cap absorption (PCA) event.

The D region is the most complex part of the ionosphere from a chemical standpoint. Neutral concentrations are sufficiently great to permit three-body processes to be important. Complex hydrated ions are observed, mainly hydronium ions, $H_3O^+ \cdot (H_2O)_n$, even though the initial ion formed in the quiet D region is apparently NO^+ which arises from the ionization of a minor gas, nitric oxide, by the strong solar radiation line, HL$y\alpha$. For the disturbed D region, where the initial ions are formed roughly in proportion to their neutral concentrations, O_2^+ ions essentially are the only initial positive ions since N_2^+ ions very rapidly undergo charge transfer with O_2 at these altitudes. The effectiveness of three-body processes in the D region also allows for the formation of negative ions since the attachment rate of an electron to a molecule in a two-body collision is very slow. The negative species in the D region are mainly ionic below about 70 km by day and 80 km at night. Galactic particles maintain a constant ionization production rate of significance to the lower D region, < 65 km, and the stratosphere. A nominal midlatitude rate (cm^{-3} s^{-1}) is 10^{-17} times the total neutral concentration, [M], in cm^{-3}. The cosmic ionization rate varies with latitude, being a factor of 10 higher at the pole, and weakly, about a factor of two, with inverse solar activity [Swider, 1969]. Ionization of air (78% N_2, 21% O_2) by energetic particles leads to an ionic production rate relatively distributed [Swider, 1969] as 62 : 17 : 14 : 07 for $N_2^+ : O_2^+ : N^+ : O^+$ where the atomic ions originate from dissociative ionization.

At night, as already noted, galactic cosmic rays maintain a weak ionization in the low D region and stratosphere. Electrons have a feeble presence in the upper D region above about 80 km as a result of solar HL$y\alpha$ and HL$y\beta$ radiation which is transported to the nightside of the earth through scattering processes within the hydrogen geocorona. Ionization maintained by the absorption of this radiation is a maximum in the E region and prevents nighttime ionic concentrations from decreasing below about 10^3 cm^{-3}. Along the auroral oval, the nighttime (or daytime) E region can attain and even exceed normal midday, midlatitude, concentrations. The high latitude D region is also susceptible. Simple formulas are available to describe the total ion and electron profiles in the SPE-disturbed nighttime D region [Swider et al., 1971]. The electron concentration formula is

$$[e] = \left[\left(\frac{L(A)}{2\alpha_D}\right)^2 + \frac{q}{\alpha_D}\right]^{1/2} - \frac{L(A)}{2\alpha_D}$$

where $\alpha_D = 6 \times 10^{-7}$ cm^3 s^{-1}, q is the total ionization production rate and $L(A) = k_1 [O_2]^2 + k_2 [O_2] [N_2]$; the

bracketed terms refer to molecular concentrations in cm^{-3} and $k_1 = 1.4 \times 10^{-29}$ (300/T) exp (−600/T) $cm^6\ s^{-1}$ with $k_2 = 10^{-31}$ $cm^6\ s^{-1}$ [Phelps, 1969]. Weak x ray and UV stellar sources of ionization [Gough, 1975] also may contribute to the ionization of the nighttime E and D regions. But, for MF and HF transmissions these nighttime regions are practically nonexistent except at high latitudes when disturbed and whenever sporadic E layers are prominent.

The F layer decays slowly at night since O^+ ions cannot effectively recombine with electrons except through transport to altitudes below about 250 km where there is sufficient O_2 and N_2 to form O_2^+ and NO^+, respectively, which (dissociatively) recombine rapidly with electrons. This action can be virtually stopped in its entirety by horizontal winds, and especially at the equator, electromagnetic drift mechanisms which can elevate the entire layer [Rishbeth, 1968]. Little scattered solar radiation is present in the nighttime F layer save for some He lines.

21.4.2 Positive Ion Distributions

Figure 21-90 is a composite picture [Narcisi, 1973] of the E and F regions during solar minimum when the F layer maximum has a relatively low height, about 250 km. The data were taken from Hoffman et al. [1969] for altitudes above 250 km, from Holmes et al. [1965] for altitudes 250 to 115 km, and from Narcisi [1968] for altitudes below 115 km. Atomic oxygen ions clearly are the major ions in the F region. Molecular ions NO^+, O_2^+ and N_2^+ decline rapidly with increasing altitude in the lower F region because of their short lifetimes in the presence of large quantities of electrons and their decreasing production rate with altitude, either being formed directly by the ionization of the neutral gas (N_2^+, O_2^+) or partly (O_2^+) or completely (NO^+) from ion-molecule interactions. The ions N_2^+ and N^+ are depleted rapidly below 200 km because of fast reactions with O_2 (N^+, N_2^+) and O (N_2^+). The N^+ ion originates from the dissociative ionization of N_2 [Nicolet and Swider, 1963]. The H_2O^+ ions are contaminents arising from the process $O^+ + H_2O \rightarrow H_2O^+ + O$. Water outgasses profusely from rockets and satellites although the latter "dry out" after several days. In the upper F region, He^+ and H^+ ions are observed since He and H are present at great altitudes in the thermosphere. A few doubly charged ions are created by solar radiation and are observed in the high F region where low neutral concentrations prevent their immediate disappearance by means of ion-molecule reactions.

Typical nighttime E and F regions are shown in Figure 21-91 [Narcisi, 1973]. Data above 200 km were taken from Hoffman (1967); data from 220 to 140 km are from Holmes et al. [1965]; and results below 140 km are from Narcisi [1971] with dashed curves from Giraud et al. [1971]. Meteoric ions are omitted. The depth of the valley near 150 km is quite varible as are many of the features in the figure including the peak concentrations of the E and F layers. The O^+ ion remains the major F region ion. However, hydrogen ions are now more prominent. This feature arises roughly because of the absence of solar radiation and because the reaction $H^+ + O \leftrightarrows O^+ + H$ is virtually thermoneutral. Figures 21-90 and 21-91 represent midlatitude conditions. The equatorial situation is not too different, but the high-latitude ionosphere does have two striking features (see discussion by Narcisi [1973]): (1) a persistent light ion trough in H^+ and He^+ with the former ion's concentration declining by 1 to 2 orders of magnitude near ±60° geomagnetic latitude, and (2) a variable poleward peak of ionization. There are a number of other features such as a winter bulge in He^+.

The E region is the easiest portion of the ionosphere to

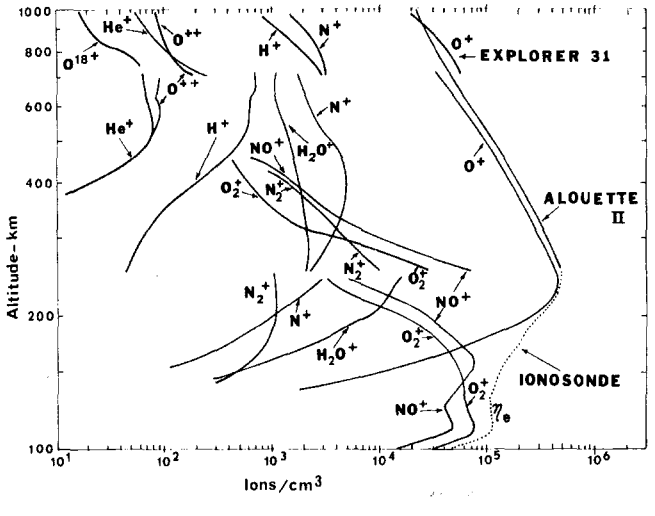

Figure 21-90. Ion composition of the midlatitude daytime ionosphere near solar minimum [Narcisi, 1973].

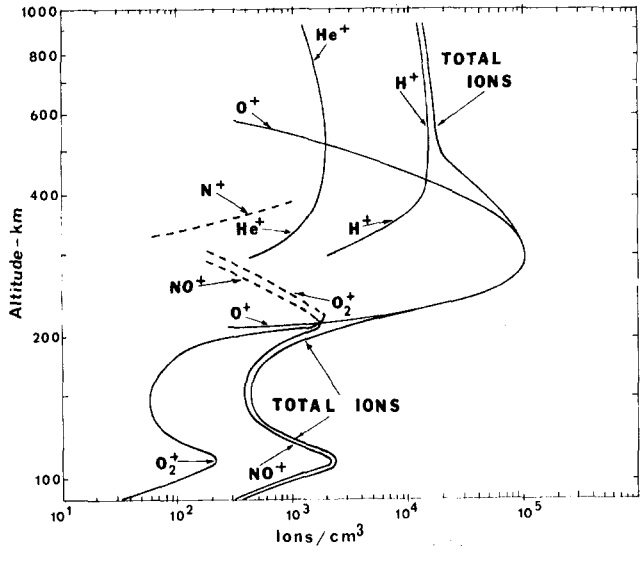

Figure 21-91. Ion composition of the midlatitude nighttime ionosphere [Narcisi, 1973].

assess since the transport of ionization is unimportant except for sporadic E layers and, perhaps at night, when charge concentrations are low (ion/electron lifetimes long). A model of the midlatitude E region [Keneshea et al., 1970] has been available for over a decade. In Figure 21-92, model electron concentrations are plotted for selected altitudes as a function of solar zenith angle, the angle between the sun and the local vertical coordinate. Since the calculations originally were performed to match twilight ionic composition data for Eglin AFB in Florida, the minimum solar zenith angle was about 22°. The accompanying figure (21-93) illustrates the ratio of the two major ions, NO^+ and O_2^+. The ratio is about unity for most altitudes in the daytime, but quite large at night. This behavior is dependent upon the quantity of nitric oxide present in the E region for the conversion of O_2^+ ions into NO^+ ions through charge exchange, $O_2^+ + NO \rightarrow NO^+ + O_2$. In the daytime, many of the O_2^+ ions recombine with electrons before charge transfer can occur. The much lower electron concentrations at night make the charge transfer process relatively more effective, and hence $[NO^+]/[O_2^+]$ greater. Strobel et al. [1974] calculated the nighttime E region using a more detailed picture of scattered HLyα and HLyβ as a function of solar position. However, the nighttime E region generally is quite variable because of electromagnetic drift, sporadic E layer formation, and, at the higher latitudes, electron precipitation, which apparently is a function of Kp, the geomagnetic planetary three-hour range index [Voss and Smith, 1980]. Figure 21-94 depicts a nighttime sporadic E layer having a peak electron concentration of 10^4 cm^{-3} near 90 km. The principal meteoric ions in the layer are Fe^+ (56 amu) and Mg^+ (24 amu) with lesser amounts of Ca^+ (40 amu) ions. The normal E region ions are O_2^+ (32 amu) and NO^+ (30 amu). The ion with mass 37 amu represents $H_3O^+ \cdot H_2O$, a D region ion. In general, intense sporadic E ($fE_s > 5$ MHz) is most likely during daytime midlatitude summer [Smith and Matsushita, 1962].

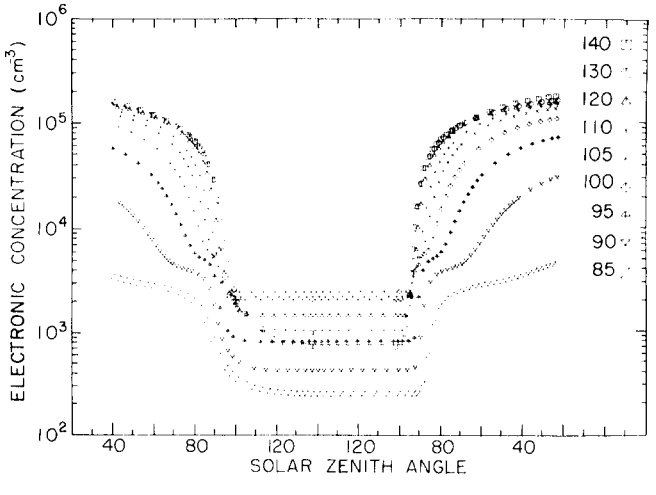

Figure 21-92. Diurnal model of quiet E region electron concentrations at altitudes from 85 to 140 km [Keneshea et al., 1970].

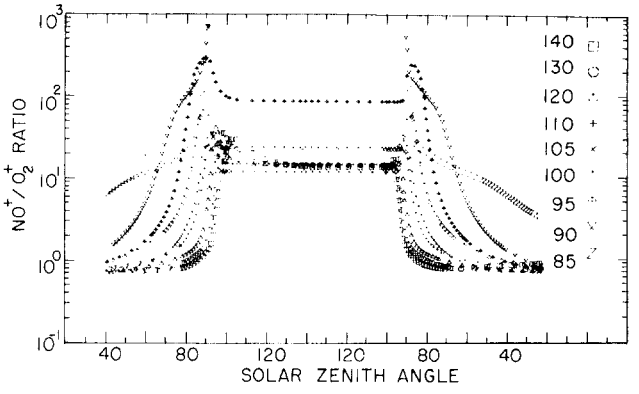

Figure 21-93. Dirunal model of quiet E region positive ion ratio $[NO^+/O_2^+]$ at altitudes from 85 to 140 km [Keneshea et al., 1970].

The importance of transport is evident in Figure 21-95 where an experimental sunset ion profile at a solar zenith angle of 99° and a theoretical profile excluding ion transport [Keneshea et al., 1970] is compared to a model including transport due to measured winds [Keneshea and MacLeod, 1970]. The disturbances apparent in Figures 21-94 and 21-95 should not detract from the fact that the Keneshea et al. [1970] model remains valid for the normal midlatitude E region since even recent measurements [Trost, 1979] are in good agreement with their model which is for moderate solar activity. Under auroral conditions, the $[NO^+]/[O_2^+]$ ratio tends to be higher than unity, the approximate midlatitide daytime value, as shown by a survey (Figure 21-96) of eight auroral flights by Swider and Narcisi [1977]. This higher ratio reflects a greater quantity of NO in the auroral or higher-latitude E region as compared with midlatitudes, particularly in the winter, when photodissociation of NO is minimal.

Narcisi and Bailey [1965] were the first to report that hydronium ions are the dominant positive ions of the D region. Figure 21-97 illustrates the difference between the E region where NO^+(30 amu) and O_2^+(32 amu) are dominant and the D region where $H_5O_2^+$ (37 amu), $H_7O_3^+$ (55 amu) and $H_9O_4^+$ (73 amu) are the principal ions. The ions labeled 24 amu and 56 amu represent meteoric Mg^+ and Fe^+ ions, respectively. Depending upon the temperature and $[H_2O]$, even heavier hydronium ions may be present in the D region like $H_{11}O_5^+$ and $H_{13}O_6^+$. Shock heating can lead to the observation of lighter species. Hydronium ions recombine with electrons at dissociative recombination rates 5 to 10 times greater [Biondi, 1973] than those for O_2^+ and NO^+ ions, respectively. Hence, the conversion of NO^+ and O_2^+ ions to hydronium ions provides for a lesser D region than would be present in the absence of this conversion. Under disturbed conditions, enhanced ion and electron concentrations tend to lower the crossover altitude between simple molecular ions ($NO^+ + O_2^+$) and hydronium ions, because dissociative recombination becomes more competitive with increased [e] as compared to ionic conversion

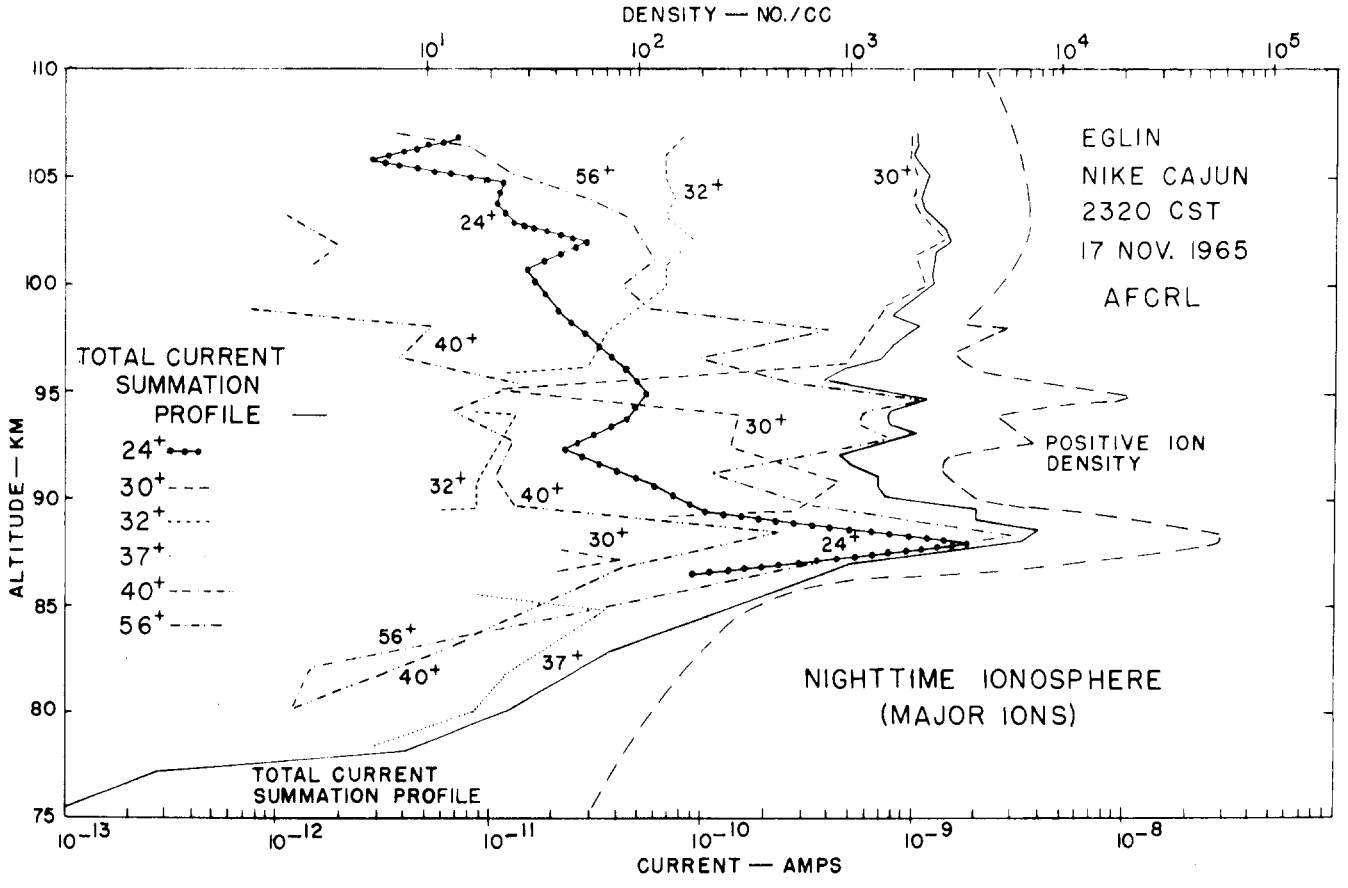

Figure 21-94. Ion composition of a nighttime sporadic E layer [Narcisi, 1969].

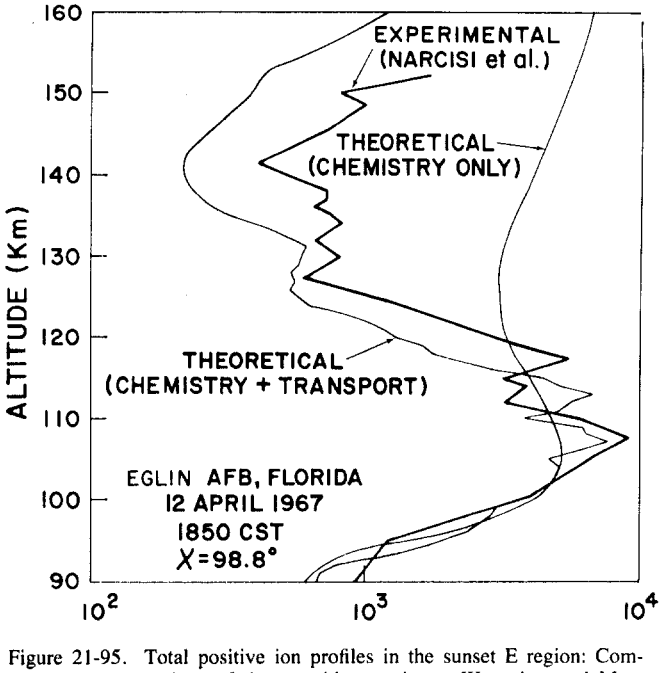

Figure 21-95. Total positive ion profiles in the sunset E region: Comparison of theory with experiment [Keneshea and MacLeod, 1970].

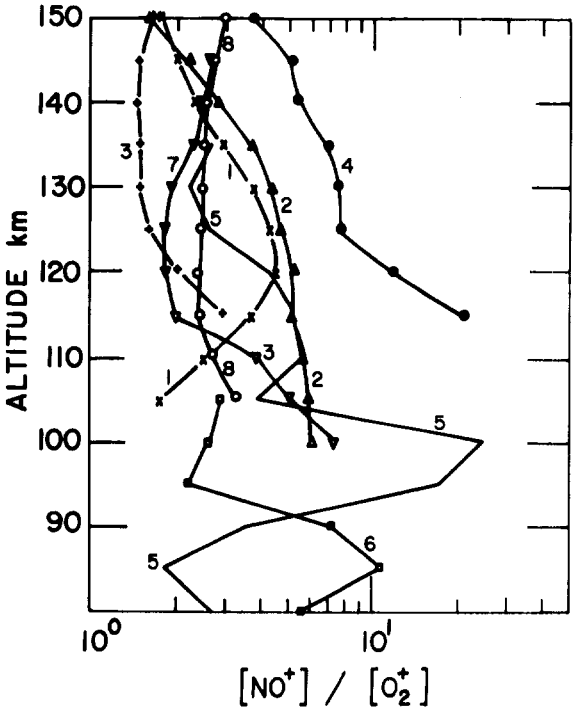

Figure 21-96. The positive ion ratios measured during eight known auroral E region rocket flights [Swider and Narcisi, 1977].

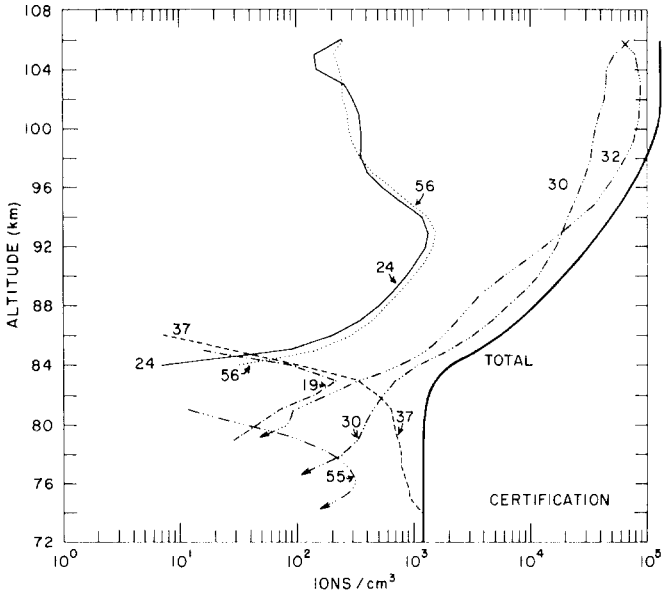

Figure 21-97. Positive ion distributions measured in the lower E and upper D regions at a 20° solar zenith angle [Narcisi et al., 1971].

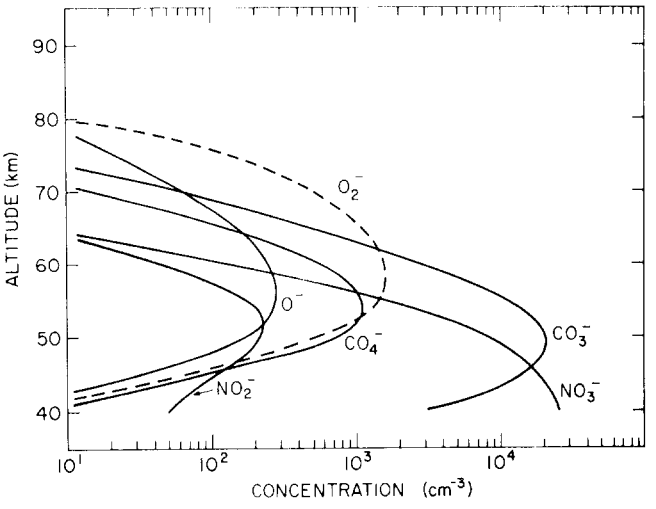

Figure 21-99. Theoretical negative ion profiles commensurate with Figure 21-100 [Swider et al., 1978].

processes which rely only upon the neutral concentrations. Figure 21-98 compares a theoretical model for the 3 November 1969 SPE (PCA) with the measured electron concentrations and is a good example of hydronium ion distributions in a disturbed D region. Similar behavior should occur for an SID. Below about 60 km, the hydronium ions in the figure appear to be in thermodynamic equilibrium and only a knowledge of the water vapor concentration (about 6 ppmv), the temperature and the thermodynamic parameters [Kebarle et al., 1967] are needed in order to derive the relative hydronium ion composition. Since electron concentrations are lower in the quiet D region, thermodynamic equilibrium may be appropriate up to 70 km or even higher. However, in the atmosphere, processes involving CO_2 may aid the formation of heavier hydronium ions. Hence, the thermodynamic expression of Kebarle et al. [1967] should be used with caution.

The quiet D region positive ion composition differs little at night from day except that the concentrations are less at night. As might be expected, the crossover between simple ions ($NO^+ + O_2^+$) and hydronium ions rises—from about 82 km by day to 86 km at night [Narcisi, 1973]. The positive ion distributions of the daytime D region have been modelled extensively by Reid [1977].

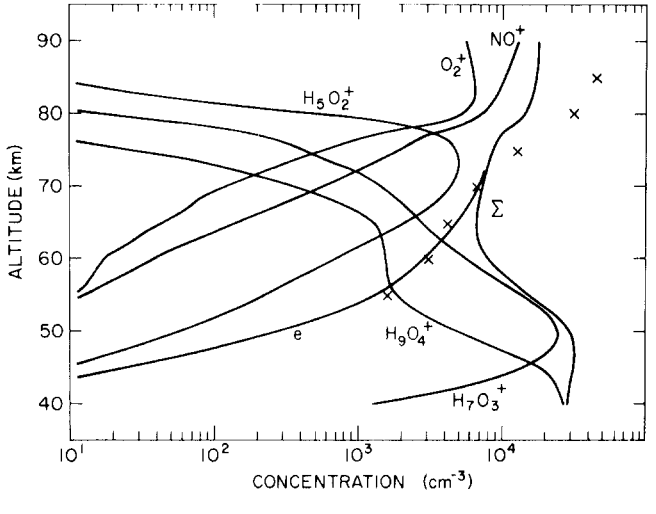

Figure 21-98. Theoretical model of the electron and major positive ion profiles in the SPE disturbed D region as compared with the measured (crosses) electron concentrations [Swider et al., 1978].

21.4.3 Negative Ion Distributions

Our understanding of negative ions is poor. They occur only at D-region altitudes and below. Figure 21-99 is a representation of the negative ion composition computed in conjunction with the positive ions and electron distributions shown in the previous figure. The total negative ion populations calculated appear to be compatible with the calculated and observed electron and total positive ion distributions. However, this match is somewhat misleading since it has been assumed, based upon laboratory evidence (Smith et al., 1976), that all ion-ion recombinations (between positive and negative ions) have a rate coefficient of 6×10^{-8} $cm^3\ s^{-1}$. By definition then, mainly the total negative ion concentration is relevant and not their individual identities. Yet, the individual identities play some role because of their uniquely related ion-molecule interactions with the neutral atmosphere plus photodetachment and photodissociation processes. On the other hand, negative ion profiles computed at night for SPE conditions [Swider et al., 1978] resulted in distributions not unlike those calculated by Arnold and Krankowsky [1971] which were in good agreement

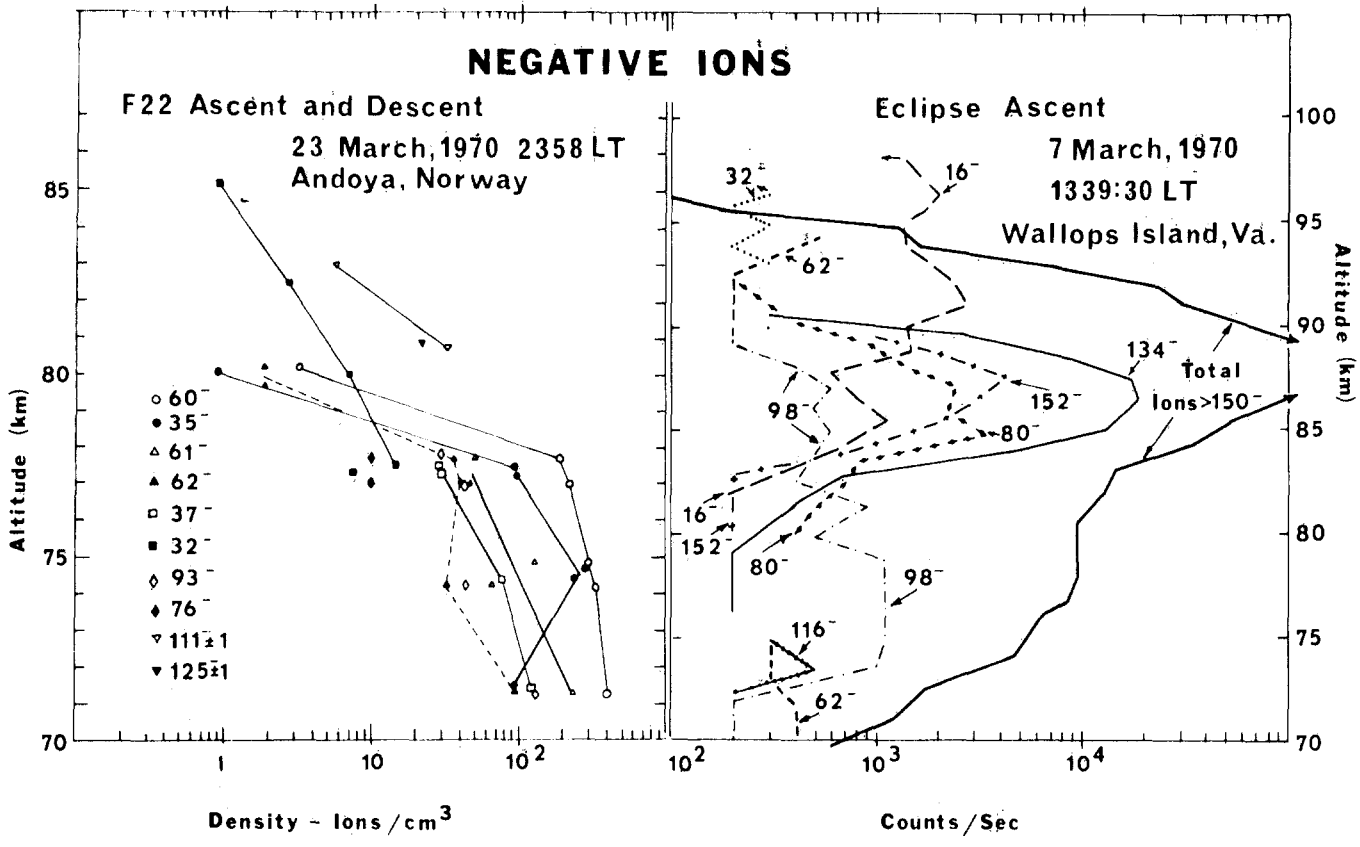

Figure 21-100. D region negative ion observations: Left panel from Arnold et al. [1971]; right panel from Narcisi et al. [1972]. Note the different altitude scales.

with the one observational result (nighttime) they obtained. However, a serious controversy arises over the fact that in fourteen flights to date [upleg and downleg, R.S. Narcisi, private communication, 1981], a layer of heavy negative ions was measured near 85 km. This is illustrated in Figure 21-100 where the Max Planck Institute at Heidelberg results are shown in conjunction with one AFGL result. The AFGL data indicate greater hydration, with mainly NO_3^-(62 amu), $NO_3^-H_2O$ (80 amu) plus higher hydrates than do the Heidelberg group's results. In addition, the AFGL data contain a layer of very heavy negative ions at 85–90 km whose origin cannot be explained by conventional gas-phase theory. During rocket flights into a disturbed and eclipsed D region on 26 February 1979, AFGL [Narcisi et al., 1983] again recorded a layer of heavy negative ions near 85 km as did a University of Bern group [Kopp et al., 1980] in a separate experiment. The Bern results suggest that the principal negative ions may be HCO_3^+ and its hydrates. This conclusion is not incompatible with the AFGL results since such ion identifications are within the mass uncertainty of the AFGL instrument, about ± 1 amu. Reported observations of Cl^- (35 amu and 37 amu) may arise from the interaction of ambient ions with chlorine contaminants [Narcisi, 1973].

CHAPTER 21

REFERENCES

Ackerman, M. and C. Muller, "Stratospheric Methane and Nitrogen Dioxide from infrared spectra," *Pure Appl. Geophys.*, **106–108:**1325–1335, 1973.

Ackerman, M., J.C. Fontanella, D. Frimout, A. Girard, N. Louisnard, and C. Muller, "Simultaneous Measurements of NO and NO_2 in the Stratosphere," *Planet. Space Sci.*, **23:**651–660, 1975.

Ackerman, M., D. Frimout, C. Muller, and D.J. Wuebbles, "Stratospheric Methane Measurements and Predictions," *Pure Appl. Geophys.* **117:**367–380, 1978/79.

Aiken, A.C., and E.J.R. Maier, "Balloon-Borne Photoionization Mass Spectrometer for Measurement of Stratospheric Gases," *Rev. Sci. Instrum.*, **49:**1034–1040, 1978.

Aiken, A.C., B. Woodgate, and H.J.P. Smith, "Atmospheric Ozone Determination by Solar Occulation Using the UV Spectrometer on the Solar Maximum Mission," *Appl. Opt.*, **21:**2421–2424, 1982.

Ainsworth, J.E. and J.R. Hagemeyer, "Measurement of Ozone by a Dasibi Ozone Monitor," in *The Stratcom VIII Effort*, edited by E.I. Reed, NASA Technical Paper 1640, 95–100, 1980.

Allen, M., Y.L. Yung, and J.W. Waters, "Vertical Transport and Photochemistry in the Terrestrial Mesosphere and Lower Thermosphere (50–120 km)," *J. Geophys. Res.*, **86:**3617–3627, 1981.

Allen, M., J.I. Lunine, and Y.L. Yung, "The Vertical Distribution of Ozone in the Mesosphere and Lower Thermosphere," *J. Geophys. Res.*, **89:**484–4872, 1984.

Anderson, G.P., C.A. Barth, F. Cayla, and J. London, "Satellite Observations of the Vertical Ozone Distribution in the Upper Stratosphere," *Ann. Geophys.*, **25:**341–343, 1969.

Anderson, J. G., Rocket-borne Ultraviolet Spectrometer Measurement of OH Resonance Fluorescence with a Diffusive Transport Model for Mesospheric Photochemistry," *J. Geophys. Res.*, **76:**4634–4652, 1971a.

Anderson, J.G., "Rocket Measurement of OH in the Mesosphere," *J. Geophys. Res.*, **76:**7820–7824, 1971b.

Anderson, J.G., "The Absolute Concentration of $O(^3P)$ in the Earth's Stratosphere," *Geophys. Res. Lett.*, **2:**231–238, 1975.

Anderson, J.G., "The Absolute Concentration of OH $(X^2\pi)$ in the Earth's Stratosphere," *Geophys. Res. Lett.*, **3:**165–168, 1976.

Anderson, J.G., "Free Radicals in the Earth's Stratosphere: A Review of Recent Results," *Proc. of the NATO Advanced Study Institute on Atmospheric Ozone*, edited by A.C. Aiken, FAA-EE-80-20, 233–251, 1980.

Anderson, J.G., J.J. Margitan, and D.H. Stedman, "Atomic Chlorine and the Chlorine Monoxide Radical in the Stratosphere: Three in situ Observations," *Science*, **198:**501–503, 1977.

Anderson, J.G., H.J. Grassl, R.E. Shetter, and J.J. Margitan, "Stratospheric Free Chlorine Measured by Balloon-Borne in situ Resonance Fluorescence," *J. Geophys. Res.*, **85:**2869–2887, 1980.

Anderson, J.G., H.J. Grassl, R.E. Shetter, and J.J. Margitan, "HO_2 in the Stratosphere: Three in situ Observations," *Geophys. Res. Lett.*, **8:**289–292, 1981.

Anderson, J.G., N.L. Hazen, B.E. McLaren, S.P. Rowe, C.M. Schiller, M.J. Schwab, L. Solomon, E.E. Thompson, and E.M. Winestock, "Free Radicals in the Stratosphere: A New Observational Technique," *Science*, **228:** 1309–1311, 1985.

Angell, J.K. and J. Korshover, "Global Variation in the Total Ozone and Layer-Mean Ozone: An Update Through 1981," *J. Climate Appl. Meteorol.*, **22:**1611–1627, 1983.

Arnold, F. and D. Krankowsky, "Negative Ions in the Lower Ionosphere: A Comparison of a Model Computation and a Mass-Spectrometric Measurement," *J. Atmos. Terr. Phys.*, **33:**1693–1702, 1971.

Arnold, F., J. Kissel, D. Krankowsky, H. Wieder, and J. Zahringer, "Negative Ions in the Lower Ionosphere: A Mass-Spectrometric Measurement," *J. Atmos. Terr. Phys.*, **33:**1169–1175, 1971.

Arnold, F., D. Krankowsky, K. H. Marien and W. Joos, "A Mass Spectrometer Probe for Composition and Structure Analysis of the Middle Atmosphere Plasma and Neutral Gas," *J. Geophys.*, **44:**125–138, 1977.

Arnold, F., R. Fabian, G. Hepschen, and W. Joos, "Stratospheric Trace Gas Analysis from Ions: H_2O and HNO_3," *Planet. Space Sci.*, **28:**681–685, 1980.

Barnett, J.J., J.T. Houghton, and J.A. Pyle, "The Temperature Dependence of the Ozone Concentration Near the Stratopause," *Quart. J. Roy. Meteorol. Soc.*, **101:**245–257, 1975.

Barth, C.A., D.W. Rusch, R.J. Thomas, G.H. Mount, R.J. Rottman, G.E. Thomas, R.W. Sanders, and G.M. Lawrence, "Solar Mesospheric Explorer: Scientific Objectives and Results," *Geophys. Res. Lett.*, **10:**237–240, 1983.

Biondi, M.A., "The Effects of Ion Complexity on Electron-Ion Recombination," *Comments At. Mol. Phys. Part D*, **4:**85–91, 1973.

Bischof, W., P. Fabian, and R. Borchers, "Decrease in CO_2 Mixing into Ratio Observed in the Stratosphere," *Nature*, **288:**347–348, 1980.

Blatherwick, R.D., A. Goldman, D.G. Murray, G.R. Cook, and J.W. VanAllen, "Simultaneous Mixing Ratio Profiles of Stratospheric NO and NO_2 as Derived from Balloon-Borne Infrared Solar Spectra," *Geophys. Res. Lett.*, **7:**471–473, 1980.

Bloomfield, P., G. Oehlert, M.L. Thompson, and S. Zeger, "A Frequency Domain Analysis of Trends in Dobson Total Ozone Records," *J. Geophys. Res.* **88:**8512–8522, 1983.

Bojkov, R.D., "Tropospheric Ozone, Its Changes and Possible Radiative Effects," WMO Special Environmental Report #16 to be published, World Meteorological Organization. Geneva, 1984.

Brasseur, G., *Physique et Chemie de l'Atmosphere Moyene*, Masson, Paris, 1982.

Brasseur, G., "Coupling Between the Thermosphere and the Stratosphere: The Role of Nitric Oxide," in *Middle Atmosphere Handbook* 10, SCOSTEP, University of Illinois, 1984.

Brasseur, G. and S. Solomon, *Aeronomy of the Middle Atmosphere*, Rydell, New York, 1984.

Brewer, A.W., "Evidence for a World Circulation Provided by the Measurements of Helium and Water Vapour Distribution in the Stratosphere," *Quart. J. Roy. Meteorol. Soc.*, **75:**351–363, 1949.

Burkhardt, E.G., C.A. Lambert, and C.K.N. Patel, "Stratospheric Nitric Oxide: Measurements during Daytime and Sunset," *Science*, **188:**1111–1113, 1975.

Burnett, C.R., "Terrestrial OH Abundance Measurement by Spectroscopic Observation of Resonance Absorption of Sunlight," *Geophys. Res. Lett.*, **3:**319–322, 1976.

Burnett, C.R., "Spectroscopic Measurements of Atmospheric OH Abundance," *Bull. Am. Phys. Soc.*, **22:**539, 1977.

Burnett, C.R. and E.B. Burnett, "Spectroscopic Measurements of the Vertical Column Abundance of Hydroxyl (OH) in the Earth's Atmosphere," *J. Geophys. Res.*, **86:**5185–5202, 1981.

Bush, Y.A., A.L. Schmelekopf, F.C. Fehsenfeld, D.L. Albritton, J.R. McAfee, P.D. Goldan, and E.E. Ferguson, "Stratospheric Measurements of Methane atSeveral Latitudes," *Geophys. Res. Lett.*, **5:**1027–1029,1978.

Calbally, J.E. and C.R. Roy, "Destruction of Ozone at the Earth's Surface," *Quart. J. Roy. Meteorol. Soc.*, **106:**599–620, 1980.

Chaloner, C.P., J.R. Drummond, J.T. Houghton, R.F. Jarnot, and H.K. Roscoe, "Infrared Measurements of Stratospheric Composition I. The Balloon Instrument and Water Vapour Measurements," *Proc. Roy. Soc. London A*, **364:**145–159, 1978.

Chapman, S., "A Theory of Upper Atmosphere Ozone," *Mem. R. Met. Soc.* **3:**103–125, 1930.

CIAP (U.S. Climatic Impact Assessment Program), "The Effects of Stratospheric Pollution by Aircraft," A.J. Grobecker, S.C. Coroniti, and R.H. Cannon, Jr., U.S. Dept. of Transportation, Washington, D.C., 1974.

CIAP "The Natural Stratosphere of 1974," Monograph 1 DOT-TST-74-51, Final Report, U.S. Dept. of Transportation, Washington, D.C., 1975.

Cicerone, R.J., "Minor Constituents in the Stratosphere and Mesosphere," *Rev. Geophys. Space Phys.*, **13:**900, 1975.

Clark, J.H.E. and T.G Rogers, "The Transport of Conservative Trace Gases by Planetary Waves," *J. Atmos. Sci.*, **35:**2232–2235, 1978.

Coffey, M.T., W.G. Mankin, and A. Goldman, "Simultaneous Spectroscopic Determination of the Latitudinal, Seasonal, and Diurnal Variability of Stratospheric N_2O, NO, NO_2, and HNO_3,' *J. Geophys. Res.*, **86:**7331–7341, 1981.

COMESA, *The Report of the Committee on Meteorological Effects of Stratospheric Aircraft (1972–1975)*, Great Britain Meteorological Office, Bracknell, U.K., 1975.

COVOS, *Rapport Final. Activities 1972–1976*, Presente par E.A. Brun, Societe Meteorologique de France, Boulogne, 1976.

CRC Handbook of Toxicology, Cleveland, Ohio, 1969.

Cronn, D. and E. Robinson, "Tropospheric and Lower Stratospheric Vertical Profiles of Ethane and Acetylene," *Geophys. Res. Lett.*, **6:**641–644, 1979.

Crosby, D.S., W.G. Planet, A.J. Miller, and R.M. Nagatani, "Evaluation and Comparison of Total Ozone Fields Derived from TOVS and SBUV," *Proceedings of the Quadrennial International Ozone Symposium*, 1980, Boulder, Colo, edited by J. London, International Ozone Commission, Vienna, Va., 161–167, 1980.

Crutzen, P.J., "Ozone Production Rates in an Oxygen, Hydrogen-Nitrogen Oxide Atmosphere," *J. Geophys. Res.*, **76:**7311–7327, 1971.

Crutzen, P.J., I.S.A. Isakesen, and G.C. Reid, "Solar Proton Events: Stratospheric Sources of Nitric Oxide," *Science*, **189:**457–458, 1975.

Cunnold, D.M., F.N. Alyea, and R.G. Prinn, "Preliminary Calculations Concerning the Maintenance of the Zonal Mean Ozone Distribution in the Northern Hemisphere," *Pure Appl. Geophys.*, **118:**329–354, 1980.

Dandekar, B. S., "Atomic Oxygen Concentration from the [OI] 5577 Å Line Emission at the Auroral Zone Latitude," *Plan. Space Sci.*, **20:**1781, 1972.

Danielsen, E.F. and R.S. Hipskind, "Stratospheric-Tropospheric Exchange at Polar Latitudes in Summer," *J. Geophys. Res.* **85:**393–400, 1980.

Danielsen, E. F., et al., "Observed Distribution of Radioactivity, Ozone, and Potential Vorticity Associated with Tropopause Folding," *J. Geophys. Res.*, **75:**2353–2361, 1970.

Deepak, A. (ed.), *Inversion Methods in Atmospheric Remote Sounding*, Academic Press, New York, 1977.

Dewan, E., "Turbulent Vertical Transport due to Thin Intermittent Mixing Layers in the Stratosphere and Other Stable Fluids," *Science*, **211:**1041–1042, 1981.

Dickinson, P.H.G., R.C. Bolden, and R.A. Young, "Measurements of Atomic Oxygen in the Lower Ionosphere using a Rocket-Borne Resonance Lamp," *Nature*, **252:**289–291, 1974.

Dobson, G.M.B., "Observations of the Amount of Ozone in the Earth's Atmosphere and Its Relation to Other Geophysical Conditions, Part IV," *Proc. Roy. Soc.* **A129:**411–433, 1930.

Dobson, G.M.B., *Exploring the Atmosphere*, Oxford University Press, London, 1963.

Dobson, G.M.B., A.W. Brewer, and B. Cwilong, "Meteorology of the Lower Stratosphere," *Proc. Roy. Soc. London A*, **185:**144–175, 1946.

DOE (Dept. of Environment, Great Britain), "Chlorofluorocarbons and Their Effect on Stratospheric Ozone," (Second Report), Pollution Paper No. 15, *HMSO*, London, 1979.

Drummond, J.R. and R.F. Jarnot, "Infrared Measurements of Stratospheric Composition II. Simultaneous NO and NO_2 Measurements," *Proc. Roy. Soc. London A*, **364:**237–254, 1978.

Drummond, J.W., J.M. Rosen, and D.J. Hoffman, "Balloon-Borne Chemiluminesent Measurement of NO to 45 km," *Nature*, **265:**319–329, 1977.

Dütsch, H.U., "Vertical Ozone Distribution on a Global Scale," *Pure Appl. Geophys.*, **116:**511–529, 1978.

Dütsch, H.U. and C. Ling, "Six Years of Regular Ozone Soundings Over Switzerland," *Pure Appl. Geophys.*, **106–108:**1151–1168, 1973.

Ebel, A. "Eddy Diffusion Models for the Mesosphere and Lower Thermosphere," *J. Atmos. Terr. Phys.*, **42:** 617–628, 1980.

Ehhalt, D.H., "In Situ Measurements of Stratospheric Trace Constituents," *Rev. Geophys. Space Phys.*, **16:**217–224, 1978.

Ehhalt, D.H. and L.E. Heidt, "The Concentration of Molecular H_2 and CH_4 in the Stratosphere," *Pure Appl. Geophys.*, **106–108:**1352–1360, 1973a.

Ehhalt, D.H. and L.E. Heidt, "Vertical Profiles of CH_4 in the Troposphere and Stratosphere," *J. Geophys. Res.*, **78:**5265–5271, 1973b.

Ehhalt, D.H. and U. Schmidt, "Sources and Sinks of Atmospheric Methane," *Pure Appl. Geophys.*, **116:**452–464, 1978.

Ehhalt, D.H. and A. Tonnissen, "Hydrogen and Carbon Compounds in the Stratosphere," *Proc. of the NATO Advanced Study Institute on Atmospheric Ozone*, edited by A.C. Aiken, FAA-EE-80-20, 129–151, 1980.

Ehhalt, D.H., L.E. Heidt, R.H. Lueb, and N. Roper, "Vertical Profiles of CH_4, H_2, CO, N_2O, and CO_2 in the Stratosphere," *Proc. III CIAP Conf.*, Boston, edited by A.J. Broderick and T.M. Hard, DOT-TSC-OST-74-15, U.S. Dept. of Transportation, 153–159, 1974.

Ehhalt, D.H., L.E. Heidt, R.H. Lueb, and E.A. Martell, "Concentrations of CH_4, CO, CO_2, H_2, H_2O, and N_2O in the Upper Stratosphere," *J. Atmos. Sci.*, **32:**163–169, 1975a.

Ehhalt, D.H., L.E. Heidt, R.H. Lueb, and W. Pollock, "The Vertical Distribution of Trace Gases in the Stratosphere," *Pure Appl. Geophys.*, **113:**389–402, 1975b.

Ellsaesser, H.W., J.E. Harries, D. Kley, and R. Penndorf, "Stratospheric H_2O," *Planet. Space Sci.*, **28:**827–835, 1980.

Evans, W.F.J. and E.J. Llewellyn, "Molecular Oxygen Emissions in the Airglow," *Ann. Geophys.* **26:**167–178, 1970.

Evans, W.F.J., H. Fast, J.B. Kerr, C.T. McElroy, R.S. O'Brien, D.I. Wardle, J.C. McConnell, and B.A. Ridley, "Stratospheric Constituent Measurements from Project Stratoprobe," *Proc. WMO Symposium on the Geophysical Aspects and Consequences of Change in the Composition of the Stratosphere*, World Meteorological Organization, **511:**55–60, Geneva, 1978.

FAA (U.S. Federal Aviation Administration), *Second Biennial Report Prepared in Accordance with the Ozone Protection Provision, Section 153(g) of the Clean Air Act Amendments of 1977*, Federal Aviation Administration, U.S. Dept. of Transportation, Washington, D.C., 1979.

Fabian, P., R. Borchers, K.H. Weiler, U. Schmidt, A. Volz, D.H. Ehhalt, W. Seiler, and F. Muller, "Simultaneously Measured Vertical Profiles of H_2, CH_4, CO, N_2O, $CFCl_3$ and CF_2Cl_2 in the Mid-Latitude Stratosphere and Troposphere," *J. Geophys. Res.* **84:**3149–3154, 1979.

Fabian, P., R. Borchers, G. Flentje, W.A. Matthews, W. Seiler, H. Giehl, K. Bunse, F. Muller, U. Schmidt, A. Volz, A. Khedim, and F.J. Johnen, "The Vertical Distribution of Stable Trace Gases at Mid-Latitudes," *J. Geophys. Res.*, **86:**5179–5184, 1981.

Farmer, C.B., O.F. Raper, B.D. Robbins, R.A. Toth, and C. Muller, "Simultaneous Spectroscopic Measurements of Stratospheric Species: O_3, CH_4, CO, CO_2, N_2O, H_2O, HCl, and Hf at Northern and Southern Mid-Latitudes," *J. Geophys. Res.*, **85:**1621–1632, 1980.

Farmer, C.B., O.F. Raper, C. Muller, B.D. Robbins, and R.A. Toth, "Simultaneous Spectroscopic Measurements of Stratospheric Species: O_3, CH_4, CO, CO_2, N_2O, H_2O, HCl and HF at Northern and Southern Mid-Latitudes," *J. Geophys. Res.*, **85:**1621–1632, 1980.

Fels, S.B., J.D. Mahlman, M.D. Schwarzkopf, and R.W. Sinclair, "Stratospheric Sensitivity to Perturbations in Ozone and Carbon Dioxide: Radiative and Dynamical Response," *J. Atmos. Sci.*, **37:**2265–2297, 1980.

Fischer, H., F. Fergg, and D. Rabus, "Radiometric Measurements of Stratospheric H_2O, HNO_3, and NO_2 Profiles," *Proc. Intl. Radiation Symposium*, Fort Collins, August 1980.

Fishman, J., "Ozone in the Troposphere," in *Ozone in the Free Atmosphere*, edited by R.C. Whitten and S. Prasad, Von Nostrand Reinhold, New York, 1985.

Fishman, J., S. Solomon, and P.J. Crutzen, "Observational and Theoretical Evidence in Support of a Significant in situ Photochemical Source of Tropospheric Ozone," *Tellus*, **31:**432–446, 1979.

Fontanella, J.C., A. Girard, L. Gramont, and N. Louisnard, "Vertical Distribution of NO, NO_2, and HNO_3 as Derived from Stratospheric Absorption Infrared Spectra," *Appl. Opt.*, **14:**825–839, 1975.

Garcia, R.R. and D.L. Hartmann, "The Role of Planetary Waves in the Maintenance of the Zonally Averaged Ozone Distribution of the Upper Stratosphere," *J. Atmos. Sci.*, **37:**2248–2264, 1980.

Garcia, R.R. and S. Solomon, "A Numerical Model of the Zonally-Averaged Dynamical and Chemical Structure of the Middle Atmosphere *J. Geophys. Res.*, **88:**1379–1400, 1983.

Garcia, R.R., S. Solomon, R.G. Roble, and D.W. Rusch, "Numerical Study of the Response of the Middle Atmosphere to the 11-Year Solar Cycle," *Planet. Space Sci.*, in press, 1984.

Gidel, L.T., P.J. Crutzen, and J. Fishman, "A Two-Dimensional Photochemical Model of the Atmosphere," *J. Geophys. Res.*, **88:**6622–6640, 1983.

Gille, J.C., G.P. Anderson, W.J. Kohri, and P.L. Bailey, "Observations of the Interaction of Ozone and Dynamics," *Proceedings of the Quadrennial International Ozone, Symposium*, 1980. Boulder, Colo, edited by J. London, International Ozone Commission, Vienna Va., 1007–1011, 1980a.

Gille, J.C., P.L. Bailey, and J.M. Russell III, "Temperature and Composition Measurements from the LRIR and LIMS Experiments on Nimbus 6 and 7," *Phil. Trans. Roy. Soc. London*, **A296:**205–218, 1980b.

Gille, J.C., C.M. Smythe, and D.F. Heath, "Observed Ozone Response to Variations in Solar UV," *Science*, accepted for publication in 1984.

Giraud, A., G. Scialom, A. Pokhounkov, S. Poloskov, and

G. Tulinov, "Daytime and Nighttime Ion Composition Between 100 and 400 km Under Solar Maximum Winter Conditions," *Space Res.*, **11**:1057–1062, 1971.

Girard, A., J. Besson, R. Giraudet, and L. Gramont, "Correlated Seasonal and Climate Variations of Trace Constituents in the Stratosphere," *Pure Appl. Geophys.*, **117**:381–394, 1978/79.

Goldan, P.D., F.G. Fernald, W.J. Williams, and D.G. Murcray, "Vertical Distribution of NO_2 in the Stratosphere as Determined from Balloon Measurements of Solar Spectra in the 4500 A Region," *Geophys. Res. Lett.*, **5**:257–260, 1978.

Goldan, P.D., W.C. Kuster, D.L. Albritton, and A.L. Schmeltokopf, "Stratospheric $CFCl_3$, CF_2Cl_2, and N_2O Height Profile Measurements at Several Latitudes," *J. Geophys. Res.*, **85**:413–423, 1980.

Goldan, P.D., W.C. Kuster, A.L. Schmeltekopf, F.C. Fehsenfeld, and D.L. Albritton, "Correction of Atmospheric N_2O Mixing-Ratio Data," *J. Geophys. Res.*, **85**:5385–5386, 1981.

Golomb, J.D. and R.E. Good, "Atomic Oxygen Profiles over Churchill and Hawaii from Chemical Releases," *Space Res.*, **12**:675–683, Akademie-Verlag, Berlin, 1972.

Good, R.E., "Determination of Atomic Oxygen Density from Rocket-Borne Measurements of Hydroxyl Airglow," *Planet. Space Sci.*, **24**:389, 1976.

Goody, R.M., *Atmospheric Radiation I: Theoretical Basis*, Oxford University Press, London, 1964.

Gordley, L.L., and J.M. Russell III, "Rapid Inversion of Limb Radiance Data Using an Emissivity Growth Approximation," *Appl. Opt.*, 20:807–813, 1981.

Gough, M.P., "On the Ultraviolet Source of the Nighttime E-Region," *Planet Space Sci.*, **23**:1236, 1975.

Harries, J.E., "Spectroscopic Observations of Middle Atmosphere Composition," in *The Middle Atmosphere as Observed from Balloons, Rockets and Satellites*, Cambridge University Press, Cambridge, 161–173, 1980.

Harries, J.E., D.G. Moss, N.R.W. Swann, G.F. Neill, and P. Gildwarg, "Simultaneous Measurements of H_2O, NO_2, and HNO_3 in the Daytime Stratosphere from 15 to 35 km," *Nature*, **259**:300–302, 1976.

Harrison, H., J.E. Johnson, and J.D. Cline, "Light Hydrocarbon in the Atmospheric Boundary Layer Over the North Pacific," Unpublished Manuscript, Dept. of Atmos. Sci., Univ. of Washington, Seattle, 1979.

Hartmann, D.L., Comments on "Stratospheric Long Waves: Comparison of Thermal Structure in the Northern and Southern Hemispheres," *J. Atmos. Sci.*, **34**:434–435, 1977.

Hartmann, D.L., "A Note Concerning the Effect of Varying Extinction on Radiative-Photochemical Relaxation," *J. Atmos. Sci.*, **35**:1125–1130, 1978.

Hays, P.B. and J.J. Olivero, "Carbon Dioxide and Monoxide above the Troposphere," *Planet. Space Sci.*, **18**:1729, 1970.

Hays, P.B. and R.G. Roble, "Observations of Mesospheric Ozone at Low Latitudes," *Planet. Space Sci.*, **11**:273, 1973.

Heaps, W.S., T.J. McGee, R.D. Hudson, and L.O. Caudill, "Stratospheric Ozone and Hydroxyl Radical Measurements by Balloon-borne Lidar," *Appl. Optics* **21**:2265–2274, 1982.

Heath, D.F., L.L. Mateer, and A.J. Krueger, "The Nimbus-4 BUV Atmospheric Ozone Experiment: Two Years Operation," *Pure Appl. Geophys.*, **106–108**,1238–1253, 1973.

Heath, D.F., A.J. Krueger, and P.J. Crutzen, "Solar Proton Event: Influence on Stratospheric Ozone," *Science*, **197**:886–889, 1977.

Heidt, L.E. and D.H. Ehhalt, "Correlations of CH_4 Concentrations Measured Prior to 1974," *Geophys. Res. Lett.*, **7**:1023, 1980.

Heidt, L.E., R. Lueb, W. Pollock, and D.H. Ehhalt, "Stratospheric Profiles of CCl_3F and CCl_2F_2," *Geophys. Res. Lett.*, **2**:445–447, 1975.

Heidt, L.E., J.P. Krasnec, R.A. Lueb, W.H. Pollock, B.E. Henry, and P.J. Crutzen, "Latitudinal Distributions of CO and CH_4 Over the Pacific," *J. Geophys. Res.*, **85**:7329–7336, 1980.

Henderson, W.R., "D-Region Atomic Oxygen Measurement," *J. Geophys. Res.*, **76**:3166, 1971.

Herman, J.R., "The Response of Stratospheric Constituents to a Solar Eclipse, Sunrise, and Sunset," *J. Geophys. Res.*, **84**:3701–3710, 1979.

Hesstvedt, E., "On the Water Vapor Content of the High Atmosphere," *Geofys. Publ. Oslo*, **25**:1, 1964.

Hilsenrath, E., "Rocket Observations of the Vertical Distribution of Ozone in the Polar Night and During a Mid-Winter Stratospheric Warming," *Geophys. Res. Lett.*, **7**:581–584, 1980.

Hilsenrath, E. and B. Schlesinger, "The Seasonal and Interannual Variability of Total Ozone as Revealed by the BUV Nimbus-4 Experiment," *Fourth NASA Weather and Climate Program Science Review*, NASA Conference Publication 2976, edited by E.R. Kreins, 277–286, 1979.

Hilsenrath, E., and B. Schlesinger, "Total Ozone Seasonal and Interannual Variations Derived from the 7 Year Nimbus-4 BUV Data Set," *J. Geophys. Res.*, **86**:12087–12096, 1981.

Hoffman, J.H., "A Mass Spectrometric Determination of the Composition of the Nighttime Topside Ionosphere," *J. Geophys. Res.*, **72**:1883–1888, 1967.

Hoffman, J.H., C.Y. Johnson, J.C. Holmes, and J.M. Young, "Daytime Mid-Latitude Ion Composition Measurements," *J. Geophys. Res.*, **74**:6281–6290, 1969.

Holmes, J.C., C.Y. Johnson, and J.M. Young, "Ionospheric Chemistry," *Space Res.*, **5**:756–766, 1965.

Holton, J.R., "The Dynamic Meteorology of the Stratosphere and Mesosphere," *Meteorol. Monographs*, **15**:1980.

Horvath, J.J. and C.J. Mason, "Nitric Oxide Mixing Ratios Near the Stratopause Measured by a Rocket-Borne Chemiluminescent Detector," *Geophys. Res. Lett.*, **5**:1023–1026, 1978.

Howlett, L.C., K.D. Baker, L.R. Megill, A.W. Shaw, and W.R. Pendleton, "Measurement of a Structured Profile of Atomic Oxygen in the Mesosphere and Lower Thermosphere," *J. Geophys. Res.*, **85**:1291–1298, 1980.

Hsu, C.P.F., "A Numerical Study of the Role of Wave-Wave Interactions During Sudden Stratospheric Warmings," *J. Atmos. sci.*, **38:**189–214, 1981.

Hudson, R.D., "Minor Constituents in the Stratosphere and Mesosphere," *Rev. Geophys. Space Phys.*, **17:**467, 1979.

Hunt, B.G., "Photochemistry of Ozone in a Moist Atmosphere," *J. Geophys. Res.*, **71:**1385–1398, 1966.

Inn, E.C.Y., J.F. Vedder, B.J. Tyson, and D. O'Hara, "COS in the Stratosphere," *Geophys. Res. Lett.*, **6:**191–193, 1979.

Jackman, G.H., J.E. Frederick, and R.S. Stolarski, "Production of Odd Nitrogen in the Stratosphere and Mesosphere: An Intercomparison of Source Strengths," *J. Geophys. Res.*, **85:**7495, 7575, 1980.

Johnson, C.Y. "Ionospheric Composition and Density from 90 to 1200 km at Solar Minimum," *J. Geophys. Res.*, **71:**330–332, 1966.

Johnston, H.S., O. Serang, and J. Podolske, "Instantaneous Global Nitrous Oxide Photochemical Rates," *J. Geophys. Res.*, **84:**5077–5082, 1979.

Kebarle, P., S.K. Searles, A. Zolla, J. Scarborough, and M. Arshadi, "The Solvation of the Hydrogen Ion by Water Molecules in the Gas Phase. Heats and Entropies of Solvation of Individual Reactions: $H^+ (H_2O)_{n-1} + H_2O \rightarrow H^+ (H_2O)_n'$," *J. Amer. Chem. Soc.*, **89:**6393–6399, 1967.

Keneshea, T.J. and M.A. MacLeod, "Wind Induced Modification of E Region Ionization Profiles," *J. Atmos. Sci.*, **27:**981–984, 1970.

Keneshea, T.J. and S.P. Zimmerman, "The Effect of Mixing upon Atomic and Molecular Oxygen in the 70–170 km Region of the Atmosphere," *J. Atmos. Sci.*, **27:**831–840, 1970.

Keneshea, T.J., R.S. Narcisi, and W. Swider, "Diurnal Model of the E-Region," *J. Geophys. Res.*, **75:**845–854, 1970.

Keneshea, T.J., S.P. Zimmerman, and C.R. Philbrick, "A Dynamic Model of the Mesosphere and Lower Thermosphere," *Planet. Space Sci.*, **27:**385–401, 1979.

Kerr, J.B. and C.T. McElroy, "Measurement of Stratospheric Nitrogen Dioxide from the AES Stratospheric Balloon Program," *Atmosphere*, **14:**166–171, 1976.

Kirchhoff, V.W.,J.H., B.R. Clemesha, and D.M. Simonich, "The Atmospheric Neutral Sodium Layer: Recent Modeling Compared to Measurements," *J. Geophys. Res.*, **86:**6892–6898, 1981.

Klenk, K.F., P.K. Bhartia, E. Hilsenrath, and A.J. Fleig, "Standard Ozone Profiles from Balloon and Satellite Data Sets," *J. Climate Appl. Meteorol.*, **22:**2012–2022, 1983.

Kley, D. and M. McFarland, "Chemiluminescence Detector for NO and NO_2," *Atmos. Technol.*, **12:**63–68, 1980.

Kley, D., E.J. Stone, W.R. Henderson, J.W. Drummond, W.J. Harrop, A.L. Schmeltekopf, T.L. Thompson, and R.H. Wrinkler, "In Situ Measurements of the Mixing Ratio of Water Vapor in the Stratosphere," *J. Atmos. Sci.*, **36:**2513–2524, 1979.

Kley, D., J.W. Drummond, and A.L. Schmeltekopf, "On the Structure and Microstructure of Stratospheric Water Vapor," in *Atmospheric Water Vapor*, edited by A. Deepak, T.D. Wilkerson, and L.H. Ruhnke, Academic Press, New York, 314–327, 1980.

Kley, J.W., Drummond, M. McFarland, and S.C. Liu, "Tropospheric Profiles of NO," *J. Geophys. Res.*, **86:**3153–3161, 1981.

Komhyr, W.D. and T.B. Harris, "Development of an ECC Ozonesonde," NOAA Technical Report ERL-ARCL18, Boulder, Colo., 1971.

Kopp, E. and C.R. Philbrick, "Wind and Temperature Induced Effects on Mesospheric Ion Composition and Inferred Minor Constituents," Sixth ESA Symposium on European Rocket and Balloon Programs and Related Research (Interlaken, 1983), ESA Report SP-183, European Space Agency, Paris, 1983.

Kopp, E., L. Andre, P. Eberhardt, and U. Herrmann, "Negative Ion Composition of the D-Region during the 1979 Solar Eclipse," *Eos*, **61:**311, 1980.

Krueger, A.J., "The Mean Ozone Distribution from Several Series of Rocket Soundings to 52 km at Latitudes from 58°S to 64°N," *Pure Appl. Geophys.*, **106–108:** 1272–1280, 1973.

Krueger, A.J., "Nimbus 7 Total Ozone Mapping Spectrometer (TOMS) Data during Gap, France Ozone Intercomparison of June 1981," *Planet. Space Sci.*, **31:**773–777, 1983.

Krueger, A.J., and R.A. Minzner, "A Mid-Latitude Model for the 1976 U.S. Standard Atmosphere," *J. Geophys. Res.*, **81:**4477–4481, 1976.

Krueger, A.J., B. Guenther, A.J. Fleig, D.F. Heath, E. Hilsenrath, R. McPeters, and C. Prabakhara, "Satellite Ozone Measurements," *Philos. Trans. Roy. Soc. London*, **A296:**991–204, 1980.

Lazrus, A.L. and B.W. Gandrud, "Distribution of Stratospheric Nitric Acid Vapor," *J. Atmos. Sci.*, **31:**1102–1108, 1974.

Lazrus, A.L., B.W. Gandrud, J. Greenberg, J. Bonelli, E. Mroz, and W.A. Sedlacek, "Midlatitude Seasonal Measurements of Stratospheric Acidic Chlorine Vapor," *Geophys. Res. Lett.*, **4:**587–589, 1977.

Lean, J.L., "Observation of the Diurnal Variation of Atmospheric Ozone," *J. Geophys. Res.*, **87:**4973–4980, 1982.

Lippens, C., and C. Muller, "Atmospheric Nitric Acid and Chlorofluoromethane from Interferometric Spectra Obtained at the Observations du Pic du Midi," *Aeronomica Acta* **A277** Inst. d'Aeronomie Spatiale Belgique, Brussels, 1980.

Liu, S.C., D. Kley, M. McFarland, J.D. Mahlman, and H. Levy II, "On the Origin of Tropospheric Ozone," *J. Geophys. Res.*, **85:**7546–7552, 1980.

Loewenstein, M. and H., Savage, "Latitudinal Measurements of NO and O_3 in the Lower Stratosphere from 5° to 82° North," *Geophys. Res. Lett.*, **2:**448–450, 1975.

Loewenstein, M., H.F. Savage, and R.C. Whitten, "Seasonal Variation of NO and O_3 at Altitudes of 18.3 and 21.3 km," *J. Atmos. Sci.*, **32:**2185–2190, 1975.

Loewenstein, M., H.F. Savage, and J.B. Borucki, "Geographical Variations of NO and O_3 in the Lower Stratosphere," *International Conference on Problems Related to the Stratosphere*, Utah State University, Logan,

JPL Publication 77-12 Pasedena, Jet Propulsion Lab, Calif. Inst. of Tech. 230–233, 1977.

Loewenstein, M., W.J. Starr, and D.G. Murcray, "Stratospheric NO and HNO_3 Observations in the Northern Hemisphere for Three Seasons," *Geophys. Res. Lett.*, **5**:531–534, 1978a.

Loewenstein, M., W.J. Borucki, H.F. Savage, J.G. Borucki, and R.C. Whitten, "Geographical Variations of NO and O_3 in the Lower Stratosphere," *J. Geophys. Res.*, **83**:1874–1882, 1978b.

Logan, J.A., M. Prather, S. Wofsy, and M.B. McElroy, "Atmospheric Chemistry: Response to Human Influence," *Phil. Trans. Roy. Soc. London, A*, **290**:187–234, 1978.

Logan, J.A., M.J. Prather, S.C. Wofsy, and M.B. McElroy, "Tropospheric Chemistry: A Global Perspective," *J. Geophys. Res.*, **86**:7210–7254, 1981.

London, J. and C.A. Reber, "Solar Activity and Total Atmospheric Ozone," *Geophys. Res. Lett.*, **6**:869–872, 1979.

London, J., R. Bojkov, S. Oltmans, and J. Kelley, "Atlas of the Global Distribution of Total Ozone July 1957–July 1967," NCAR Technical Report NCAR/TN/**113**, National Center for Atmospheric Research, Boulder, Colo., 1976.

Lordi, N.J., A. Kasahara, and S.K. Kao, "Numerical Simulation of Sudden Warmings with a Primitive Equation Spectral Model," *J. Atmos. Sci.*, **37**:3746–2767, 1980.

Louisnard, N., G. Fergant, A. Girard, L. Gramont, O. Lado-Brodowsky, J. Laurent, S. LeBoiteux, and M.P. Lemitre, "Infrared Absorption Spectroscopy Applied to Stratospheric Profiles of Minor Constituents,", *J. Geophys. Res.*, **28**:5365–5377, 1983.

Louisnard, N., G. Fergant, and A. Girard, "Simultaneous Measurements of Methane and Water Vapor Vertical Profiles in the Stratosphere," *Proceedings of the Quadrennial International Ozone Symposium*, 1980, Boulder, Colo, edited by J. London, International Ozone Commission, Vienna, Va, 797–802, 1980a.

Louisnard, N., A. Girard, and G. Eichen, "Mesures du Profil Vertical de Concentration de la Vapeur d'eau Stratospherique," *Comptes Rendus Acad. Sci. Paris, Ser. B*, **290**:385–388, 1980b.

Lovill, J.E., et al., "Total Ozone Retrieval from Satellite Multichannel Filter Radiometer Measurements," *UCRL-52473*, Lawrence Livermore Laboratory, University of California/Livermore, 1978.

Maeda, K., "Semiannual Oscillation of Stratospheric Ozone," *Geophys. Res. Lett.*, **11**:583–586, 1984.

Maier, E.J. A.C. Aiken, and J.E. Ainsworth, "Stratospheric Nitric Oxide and Ozone Measurements Using Photoionization Mass Spectrometer and UV Absorption," *Geophys. Res. Lett.*, **5**:37–40, 1978.

Mason, C.J. and J.J. Horvath, "The Direct Measurement of Nitric Oxide Concentration in the Upper Atmosphere by a Rocket-Borne Chemiluminescent Detector," *Geophys. Res. Lett.*, **3**:391–394, 1976.

Mastenbrook, H.J., "Water Vapor Distribution in the Stratosphere and High Troposphere," *J. Atmos. Sci.*, **25**:299–311, 1968.

Mastenbrook, H.J. and R.E. Daniels, "Measurements of Stratospheric Water Vapor Using a Frost Point Hygrometer," in *Atmospheric Water Vapor*, edited by A. Deepak, T.W. Wilkerson, and L.H. Ruhnke, Academic Press, New York, 329–342, 1980.

Mateer, C.L., "On the Information Content of Umkehr Observations," *J. Atmos. Sci.*, **22**:370–381, 1965.

Mateer, C.L., J.J. DeLuisi, and C.C. Porco, "The Short Umkehr Method, Part 1: Standard Ozone Profiles for use in the Estimation of Ozone Profiles by the Inversion of Short Umkehr Observations," NOAA Technical Memorandum ERL ARL-86, 1980.

Mauersberger, K., "Measurement of Heavy Ozone in the Stratosphere," *Geophys. Res. Lett.*, **8**:935–937, 1981.

Mauersberger, L., and R. Finstad, "Carbon Dioxide Measurements in the Stratosphere," *Geophys. Res. Lett.*, **7**:873–876, 1980.

Mauersberger, K., R. Finstad, S. Anderson, and D. Robbins, "A comparison of Ozone Measurements," *Geophys. Res. Lett.*, **8**:361–364, 1981.

Maugh, T.H. II, "What is the Risk from Chlorofluorocarbons?" *Science*, **223**:1051–1052, 1984.

McPeters, R.D., D.F. Heath, and P.K. Bhartia, "Average Ozone Profiles for 1979 from the NIMBUS 7 SBUV Instrument," *J. Geophys. Res.*, **89**:5199–5214, 1984.

Megie, G., J.Y. Allain, M.L. Chanin, and J.E. Blamont, "Vertical Profile of Stratospheric Ozone by Lidar Sounding from the Ground," *Nature*, **270**:329–331, 1977.

Megie, G., F. Bos, J.E. Blamont, and M.L. Chanin, "Simultaneous Nighttime Lidar Measurement of Atmospheric Sodium and Potassium," *Planet. Space Sci.*, **26**:27, 1978.

Mentall, J.E., J.P. Herman, and B. Zak, "Ozone Profile and Solar Fluxes from a Grating Spectrometer," *The Stratcom VIII Effort*, NASA Technical Paper 1640, edited by E. Reed, 117–123, 1980.

Mihelcic, D., D.H. Ehhalt, G.F. Kulessa, J. Klomfass, M. Trainer, U. Schmidt, and H. Rohrs, "Measurements of Free Radicals in the Atmosphere by Matrix Isolation and Electron Paramagnetic Resonance," *Pure Appl. Geophys.*, **116**:530–536, 1978.

Miller, A.J., R.M. Nagatani, J.D. Laver, and B. Korty, "Utilization of 100 mb Midlatitude Height Fields as an Indicator of Sampling Effect on Total Ozone Varia ions," *Mon. Wea. Rev.*, **107**:782–787, 1979.

Miller, A.J., R.M. Nagatani, T.G. Rogers, A.J. Fleig, and D.F. Heath, "Total Ozone Variations 1970–74 Using Backscattered Ultraviolet (BUV) and Ground-Based Observations," *J. Appl. Meteorol.*, **21**:621–630, 1982.

Millier, F., B.A. Emery, and R.G. Roble, "OSO-8 Lower Mesospheric Ozone Number Density Profiles," in *Proceedings of the Quadrennial International Ozone Symposium*, 1980, Boulder, Colo., edited by J. London, International Ozone Commission, Vienna Va., **1**:572–575, 1981.

Molina, M.J. and F.S. Rowland, "Stratospheric Sink for Chlorofluoromethanes: Chlorine Atomcatalysed Destruction of Ozone," *Nature*, **249**:810, 1974.

Murcray, D.G., A. Goldman, W.J. Williams, F.H. Mur-

cray, J.N. Brooks, J. Van Allen, R.N. Stocker, J.J. Kosters, D.B. Barker, and D.E. Snider, "Recent Results of Stratospheric Trace Gas Measurements from Balloon-Borne Spectrometers," Proc. Third CIAP Conf., edited by A.J. Broderick and T.M. Hard, DOT-TSC-OST-74-15, U.S. Dept. of Transportation, Washington, D.C., 184–192, 1974.

Murcray, D.G., D.B. Barker, J.N. Brooks, A. Goldman, and W.J. Williams, "Seasonal and Latitudinal Variation of the Stratospheric Concentration of HNO_3," *Geophys. Res. Lett.*, **2**:223–225, 1975.

Murcray, D.G., A. Goldman, F.H. Murcray, F.J. Murcray, and W.J. Williams, "Stratospheric Distribution of $ClONO_2$," *Geophys. Res. Lett.*, **6**:856–859, 1979.

Murcray, D.G., W.J. Williams, D.B. Barker, A. Goldman, C. Bradford, and G. Cook, "Measurements of Constituents of Interest in the Chemistry of the Ozone Layer Using IR Techniques," *Proceedings WMO Symposium on the Geophysical Aspects and Consequences of Change in the Composition of the Stratosphere,"* WMO NO. 511, 61–68, Toronto, Canada, June 1978.

Murgatroyd, R.J., "Recent Progress in Studies of the Stratosphere," *Q. J. Roy. Meteorol. Soc.*, **108**:271–312, 1982.

Nagatani, R.M. and A.J. Miller, "Stratospheric Ozone Changes During the First Year of SBUV Observations," *J. Geophys. Res.*, **89**:519–5198, 1984.

Narcisi, R.S., "Processes Associated with Metal-Ion Layers in the E Region of the Ionosphere," *Space Res.*, **8**:360–369, 1968.

Narcisi, R.S., "Discussion, in Meteorological and Chemical Factors in D-Region Aeronomy - Record of the Third Aeronomy Conference," *Aeronomy Rep. 34*, University of Illinois, 284, 1969.

Narcisi, R.S., "Composition Studies of the Lower Ionosphere," in *Physics of the Upper Atmosphere*, edited by F. Verniani, Editrice Compositori, Bologna, 1971.

Narcisi, R.S., "Mass Spectrometer Measurements in the Ionosphere," 171–183 in *Physics and Chemistry of the Upper Atmosphere*, edited by B.M. McCormac, D. Reidel, Dordrecht, Holland, 1973.

Narcisi, R.S. and A.D Bailey, "Mass Spectrometric Measurements of Positive Ions at Altitudes from 64 to 112 Kilometers," *J. Geophys. Res.*, **70**:3687–3700, 1965.

Narcisi , R.S., A.D. Bailey, L.E. Wlodyka, and C.R. Philbrick, "Ion Composition Measurements in the Lower Ionosphere during the November 1966 and March 1970 Solar Eclipse," *J. Atmos. Terr. Phys.*, **34**:647–668, 1972.

Narcisi, R.S., A. Bailey, G. Frederico, and L. Wlodyka, "Positive and Negative Ion Composition Measurements in the D- and E-Regions During the 26 Fegruary 1979 Solar Eclipse," *J. Atmos. Terr. Phys.*, **45**:461–478, 1983.

National Academy of Sciences, *Environmental Impact of Stratospheric Flight*, National Academy Press, Washington, D.C., 1975.

National Academy of Sciences, *Stratospheric Ozone Depletion by Halocarbons: Chemistry and Transport*, National Academy Press, Washington, D.C., 1979.

National Academy of Sciences. *Causes and Effects of Stratospheric Ozone Reduction: An Update*, National Academy Press, Washington, D.C., 1982.

National Academy of Sciences, *Causes and Effects of Stratospheric Ozone: Update, 1983*, National Academy Press, Washington, D.C., 1984.

NASA (U.S. National Aeronautics and Space Administration), *Chlorofluoromethanes and the Stratosphere*, Reference Publication 1010, edited by R.D. Hudson, 1977.

NASA (U.S. National Aeronautics and Space Administration), *The Stratosphere: Present and Future*, Reference Publication 1049, edited by R.D. Hudson and E.I. Reed, 1979.

NASA (U.S. National Aeronautics and Space Administration), *Present State of Knowledge of the Upper Atmosphere: An Assessment Report*, NASA/GSFC, Greenbelt, Md., 1984.

NASA/JPL, "Chemical Kinetics and Photochemical Data for Use in Stratospheric Modeling," Eval. Number 5, JPL Publ. 82-54, Jet Propulsion Laboratory, Calif. Inst. of Tech, Pasadena, Calif., 1982.

Naudet, J.P., R. Rigaud, and D. Huguenin, "Stratospheric NO_2 at Night from Stellar Spectra in the 440 nm Region," *Geophys. Res. Lett.*, **7**:701–703, 1980.

Naudet, J.P., D. Huguenin, P. Rigaud, and D. Cariolle, "Stratospheric Observations of NO_3 and its Experimental and Theoretical Distribution Between 20 and 40 km," *Planet. Space Sci.*, **29**:707–712, 1981.

Nicolet, M., "Solar Radio Flux and the Temperature of the Upper Atmosphere," *J. Geophys. Res.*, **68**:6121–6144, 1963.

Nicolet, M., "Stratospheric Ozone; An Introduction to Its Study," *Rev. Geophys. Space Phys.*, **13**:593, 1975.

Nicolet, M. and W. Swider, "Ionospheric Conditions," *Planet. Space Sci.*, **11**:1459–1482, 1963.

Niple, E., W.G. Mankin, A. Goldman, D.G. Murcray, and F.J. Murcray, "Stratospheric NO_2 and H_2O Mixing Ratio Profiles from High Resolution Infrared Solar Spectra Using Nonlinear Least Squares," *Geophys. Res. Lett.*, **7**:489–492, 1980.

Noxon, J.F., "Atomic Nitrogen Fixation by Lightning," *Geophys. Res. Lett.*, **3**:463–465, 1976.

Noxon, J.F., "Stratospheric NO_2 in the Antarctic Winter," *Geophys. Res. Lett.*, **5**:1021–1022, 1978.

Noxon, J.F., "Stratospheric NO_2, Global Behavior," *J. Geophys. Res.*, **84**:5067–5076, 1979.

Noxon, J.F., "Correction," *J. Geophys. Res.*, **85**:4560–4561, 1980.

Noxon, J.F., E.C. Whipple, Jr., and R.S. Hyde, "Stratospheric NO_2, 1. Observational Method and Behavior at Mid-Latitude," *J. Geophys. Res.*, **84**:5047–5065, 1979.

O'Brien, R.S. and W.F.J. Evans, "Rocket Measurements of the Distribution of Water Vapor in the Stratosphere at High Latitudes," *J. Geophys. Res.*, **86**:12,101–12,107, 1981.

Offermann, D. and A. Drescher, "Atomic Oxygen Densities in the Lower Thermosphere as Derived from in situ 5577 Å Night Airglow and Mass Spectrometer Measurements," *J. Geophys. Res.*, **78**:6690, 1973.

Offermann, D. and K.U. Grossmann, "Thermospheric Density and Composition as Determined by a Mass Spectrometer with Cryo Ion Source," *J. Geophys. Res.*, **78**:8296, 1973.

Offermann, D. and U. von Zahn, "Atomic Oxygen and Carbon Dioxide in the Lower Thermosphere," *J. Geophys. Res.*, **76:**2520, 1971.

Offermann, D., V. Friedrich, P. Ross, and U. von Zahn, "Neutral Gas Composition Measurements Between 80 and 120 km," *Planet. Space Sci.*, **29:**747, 1981.

Ogawa, T., K. Shibasaki, and K. Suzuki, "Balloon Observation of the Stratospheric NO_2 Profile by Visible Absorption Spectroscopy," *J. Meteorol. Soc. Japan*, **59:**410–416, 1981.

Parent, R.A., "A Review of Ozone Toxicology Studies, Air Quality Meteorology and Atmospheric Ozone," SSTM STP 653, edited by A.L. Morris and R.C. Barnes, American Society for Testing and Materials, Philadelphia, 575–396, 1978.

Parrish, A., R. deZafra, and P. Solomon, "Groundbased MM-Wave Emission Spectroscopy for the Detection and Monitoring of Stratospheric Ozone," in *Proceedings of the Quadrennial International Ozone Symposium*, edited by J. London, IAMAP, NCAR, Boulder, Colo., 122–130, 1981.

Patel, C.K., N.E.G. Burkhardt, and C.A. Lambert, "Spectroscopic Measurements of Stratospheric Nitric Oxide and Water Vapor," *Science*, **184:**1173–1176, 1974.

Pelon, J. and G. Megie, "Ozone Monitoring in the Troposphere and Lower Stratosphere: Evaluation and Operation of a Ground-Based Lidar Station," *J. Geophys. Res.*, **87:**4947–4955, 1982.

Penkett, S.A., K.A. Brice, R.G. Derwent, and A.E.J. Eggleton, "Measurement of CCl_3 and CCl_4 at Harwell Over the Period January 1975–November 1977," *Atmos. Environ.*, **13:**1011–1019, 1979.

Penner, J.E., "Trend Prediction of O_3: An Analysis of Model Uncertainty with Comparison to Detection Thresholds," *Atmos. Environ.*, **16:**1109–1115, 1982.

Persson, R., "World Forest Resources," *Res. Notes 17*, Dept. of Forestry Surv., Royal Coll. of Forestry, Stockholm, 1974.

Peters, R.D., C.H. Jackman, and E. G. Stassinopoulous, "Observations of Ozone Depletion Associated with Solar Proton Events," *J. Geophys. Res.*, **86:**12071–12081, 1981.

Phelps, A.V., "Laboratory Studies of Electron Attachment and Detachment Processes of Aeronomic Interest," *Can. J. Chem.*, **47:** 1783–1793, 1969.

Philbrick, C.R., G.A. Faucher, and R.A. Wlodyka, "Neutral Composition Measurements of the Mesosphere and Lower Thermosphere," AFCRL-71-0602, AD739169, 1971.

Philbrick, C.R., G.A. Faucher, and E. Trzcinski, "Rocket Measurements of Mesospheric and Lower Thermospheric Composition," *Space Res.*, **13:**255–260, Akademie Verlag, Berlin, 1973.

Pollock, W., L.E. Heidt, R. Lueb, and D.H. Ehhalt, "Measurement of Stratospheric Water Vapor by Cryogenic Collection," *J. Geophys. Res.*, **85:**5555–5568, 1980.

Pommereau, J.P. and A. Hauchecorne, "Observations Spectroscopiques Depuis le Sol du Dioxyde d'Azote Atmospherique," *Comptes Rendus, Acad. Sci. Paris, Ser. B.*, **288:**135–138, 1979.

Prabhakara, C., B.J. Conrath, R.A. Hanel, and E.J. Williamson, "Remote Sensing of Atmospheric Ozone Using the 9.6 Micron Band," *J. Atmos. Sci.*, **27:**689–697, 1970.

Profitt, M.H. and R.J. McLaughlin, "Fast-Response Dual-Beam UV-Absorption Ozone Parameter Suitable for Use on Stratospheric Balloons," *Rev. Sci. Instrum.* **54:**1983.

Radford, H.E., M.M. Litvak, C.A. Gottlieb, E.W. Gottlieb, S.K. Rosethal, and A.E. Lilley, "Mesospheric Water Vapor Measured from Ground-Based Microwave Observations," *J. Geophys. Res.*, **82:**472–478, 1977.

Ramseyer, H., P. Eberhardt, and E. Kopp, "Silicon Chemistry and Inferred Water Vapor in the Lower Ionosphere," Sixth ESA Symposium on European Rocket and Balloon Programs and Related Research (Interlaken, 1983), ESA Report SP-183, European Space Agency, Paris, 1983.

Reed, R.J. and K.E. German, "A Contribution to the Problem of Stratospheric Diffusion by Large-Scale Mixing," *Mon. Weather Rev.*, **93:**313–321, 1965.

Regener, V.H., "On a Sensitive Method for the Recording of Atmospheric Ozone," *J. Geophys. Res.*, **65:**3975, 1960.

Reid, G.C., "The Production of Water-Cluster Positive Ions in the Quiet Daytime D Region," *Planet. Space Sci.*, **25:**275–290, 1977.

Reinsel, G.C.,"Analysis of Total Ozone Data for the Detection of Recent Trends and the Effects of Nuclear Testing During the 1960's," *Geophys. Res. Lett.*, **8:**1227–1230, 1981.

Remsberg, E.E. and L.L. Gordley, "Analysis of Differential Absorption Lidar from the Space Shuttle," *Appl. Opt.*, **17:**624, 1978.

Remsberg, E.E., J.M. Russel III, J.C. Gille, L.L. Gordley, P.L. Bailey, W.G. Planet, and J.E. Harries, "The Validation of NIMBUS 7 LIMS Measurements of Ozone," *J. Geophys. Res.*, **89:**5161–5178, 1984.

Richter, E.S., J.R. Rowlett, C.S. Gardner, and C.F. Sechrist, "Lidar Observation of the Mesospheric Sodium Layer Over Urbana, Illinois," *J. Atmos. Terr. Phys.* **43:**327–337, 1981.

Ridley, B.A. and D.R. Hastie, "Stratospheric Odd-Nitrogen: NO Measurements at 51°N in Summer," *J. Geophys. Res.*, **86:**3162–3166, 1981.

Ridley, B.A. and L.C. Howlett, "An Instrument for Nitric Oxide Measurements in the Stratosphere," *Rev. Sci. Instr.*, **45:**742–746, 1974.

Ridley, B.A. and H.I. Schiff, "Stratospheric Odd-Nitrogen: Nitric Oxide Measurements at 32°N in Autumn," *J. Geophys. Res.*, **86:**3167–3172, 1981.

Ridley, B.A., M. McFarland, J.T. Bruin, H.I. Schiff, and J.C. McConnell, "Sunrise Measurements of Stratospheric Nitric Oxide," *Can. J. Phys.*, **55:**212–221, 1977.

Rigaud, P., J.P. Naudet, and D. Huguenin, "Etude de la Repartition Verticale de NO_2 Stratospherique Durant la Nuit," *Comptes Rendus Academie des Sciences, Paris, Ser. B*, **284:**331–334, 1977.

Rishbeth, H., "On Explaining the Behavior of the Ionospheric F Region", *Rev. Geophys.*, **6:**33–71, 1968.

Robbins, D.E., "NASA-JSC Ozone Observations for Validation of NIMBUS-7 LIMS Data," NASA Tech Memo 58227, 1980.

Robbins, D.E. and J.G. Carnes, "Variations in the Upper Stratosphere's Ozone Profile," *WMO Symposium on the Geophysical Aspects and Consequences of Changes in the Composition of the Stratosphere*, Toronto, Canada, June, 1978, 511, World Meteorological Organization, Geneva, WMO Publ. No. 131–137, 1978.

Robinson, G.D., "The Transport of Minor Atmospheric Constituents Between Troposphere and Stratosphere," *Quart. J. Roy. Meteorol. Soc.*, **106:**227–253, 1980.

Rodgers, C.D., "Retrieval of Atmospheric Temperature and Composition from Remote Measurements of Thermal Radiation," *Rev. Geophys. Space Phys.*, **14:**609–624, 1976.

Roe, J.M., "A Climatology of a Newly-Defined Tropopause Using Simultaneous Ozone-Temperature Profiles: Final Report," AFGL TR-81-0190, ADA106399 1981.

Rogers, J.W., A.T. Stair, Jr., T.C. Degges, C.L. Wyatt, and D.J. Baker, Rocketborne Measurement of Mesospheric H_2O in the Auroral Zone," *Geophys. Res. Lett.*, **4:**366–368, 1977.

Rowland, F.S., and M.J. Molina, "Chlorofluoromethanes in the Environment," *Rev. Geophys. Space Phys.*, **13:**1, 1975.

Roscoe, H.K., J.R. Drummond, and R.F. Jarnot, "Infrared Measurements of Stratospheric Composition III. The Daytime Changes of NO and NO_2," *Proc. Roy. Soc. London, A*, **375:**507–528, 1981.

Roy, C.R., I.E. Galbally, and B.A. Ridley, "Measurements of Nitric Oxide in the Stratosphere of the Southern Hemisphere," *Quart. J. Roy. Meteorol. Soc.*, **106:**887–894, 1980.

Rudolph, J., D.H. Ehhalt, and G. Gravenhorst, "Recent Measurements of Light Hydrocarbons in Remote Areas," *Proceedings of the First European Symposium on Physico-Chemical Behavior of Atmospheric Pollutants*, Ispra, Italy, Oct 16–18, 1979, D. Reidel, Dordrecht, Holland 41–51, 1979.

Rudolph, J., D.H. Ehhalt, and A. Tonnissen, "Vertical Profiles of Ethane and Propane in the Stratosphere," *J. Geophys. Res.*, **86:**7267–7272, 1981.

Rusch, D.W., G.H. Mount, C.A. Barth, G.J. Rottman, R.J. Thomas, G.E. Thomas, R.W. Sanders, G.M. Lawrence, and R.W. Eckman, "Ozone Densities in the Lower Mesosphere Measured by Limb Scanning Ultraviolet Spectrometer," *Geophys. Res. Lett.*, **10:**241–244, 1983.

SCEP, "Man's Impact on the Global Environment," *Report of the Study of Critical Environmental Problems*, MIT Press, Cambridge, Mass., 1970.

Shapiro, M.A., A.J. Krueger, and P.J. Kennedy, "Nowcasting the Position and Intensity of Jet Streams Using a Satellite-Borne Total Ozone Mapping Spectrometer," in *Nowcasting*, edited by K.A. Browning, Academic Press, New York, 1982.

Shapiro, M.A. E.R. Reiter, R.D. Cadle, and W.A. Sedlacek, "Vertical Mass and Trace Constituent Transport in the Vicinity of Jet Streams," *Arch. Met. Geoph. Biokl, B*, **28:**193–206, 1980.

Singh, H.B. and P.L. Hanst, "Peroxyacetyl Nitrate (PAN) in the Unpolluted Atmosphere: An Important Reservoir for Nitrogen Oxides," *Geophys. Res. Lett.*, **4:**453–456, 1981.

Singh, H.B., L.J. Salas, H. Shigeishi, and E. Scribner, "Atmospheric Halocarbons and Sulfur Hexafluoride: Global Distributions, Sources, and Sinks," *Science*, **203:**899–903, 1979.

Smith, E.K. Jr., and S. Matsushita (eds.), *Ionospheric Sporadic E*, Pergamon Press, New York, 1962.

Smith, D., N.G. Adams, and M.J. Church, "Mutual Neutralization Rates of Ionospherically Important Ions," *Planet. Space Sci.*, **24:**697–703, 1976.

Soloman, S. "Minor Constituents in the Stratosphere and Mesosphere," *Rev. Geophys. Space Phys.*, **21:**276–283, 1983.

Solomon, S., P.J. Crutzen, and R. G. Roble, "Photochemical Coupling Between the Thermosphere and Lower Atmosphere," *J. Geophys. Res.*, **87:**7206, 1982.

Solomon, S., G.C. Reid, D.W. Rusch, and R.J. Thomas, "Mesospheric ozone depletion during the solar proton event of July 13, 1982: Part II," *Geophys. Res. Lett.*, **10:** , 1983.

Stair, A.T. Jr., J.C. Ulwick, K.D. Baker, and D.J. Baker, *Atmospheres of Earth and Planets*, edited by B.M. McCormac, D. Reidel, Dordrecht, Holland, 1975.

Stair, A.T. Jr., R.D. Sharma, R.M. Nadile, D.J. Baker, and W.F. Grieder, "Observations of Limb Radiance with Cryogenic Spectral Infrared Rocket Experiment (SPIRE)," *J. Geophys Res.*, 1984.

Stolarski, R.S. and R.J. Cicerone, "Stratospheric Chlorine: A Possible Sink for Ozone," *Can J. Chem.*, **52:** 1610–1615, 1974.

Strobel, D.F., "Nitric Oxide in the Upper Atmosphere," *J. Geophys. Res.*, **76:**2442–2452, 1971.

Strobel, D.F., "Minor Neutral Constituents in the Mesosphere and Lower Thermosphere," *Radio Sci.*, **7:**1–21, 1972.

Strobel, D.F., T.R. Young, R.R. Meier, T.P. Coffey, and A.W. Ali, "The Nighttime Ionosphere: E Region and Lower F Region," *J. Geophys. Res.*, **79:**3171–3178, 1974.

Swider, W., "Ionization Rates Due to the Attenuation of 1-100 Å Nonflare Solar X Rays in the Terrestrial Atmosphere," *Rev. Geophys.*, **7:**573–594, 1969.

Swider, W., and R.S. Narcisi, "Auroral E-Region: Ion Composition and Nitric Oxide," *Planet. Space Sci.*, **25:**103–116, 1977.

Swider, W., T.J. Keneshea, and C.I. Foley, "An SPE-Disturbed D-Region Model," *Planet. Space Sci.*, **26:**883–892, 1978.

Swider, W., R.S. Narcisi, T.J. Keneshea, and J.C. Ulwick, "Electron Loss During a Nighttime PCA Event," *J. Geophys. Res.*, **76:**4691–4694, 1971.

Sze, N.D., M.K.W. Ko, R. Specht, and M. Livshits, "Modeling of Chemical Processes in the Troposphere and Stratosphere: Final Report," AFGL TR-80-0251, ADA092704, 1980.

Thomas, L., and M.R. Bowman, "The Diurnal Variations of Hydrogen and Oxygen Constituents in the Mesosphere and Lower Thermosphere," *J. Atmos. Terr. Phys.* **34:**1843, 1972.

Thomas, R.J., C.A. Barth, G.J. Rottman, D.W. Rusch, G.H. Mount, G.M. Lawrence, R.W. Sanders, G.E. Thomas, and L.E. Clemens, "Ozone Density Distribution in the Mesosphere (50–90 km) Measured by the SME Limb Scanning Near Infrared Spectrometer," *Geophys. Res. Lett.*, **10:**249–252, 1983.

Thompson, A.M., "The Effects of Clouds on Photolysis Rates and Ozone Formation in the Unpolluted Troposphere," *J. Geophys. Res.*, **89:**134–1349, 1984

Thrush, B.A., "Chemistry of the Stratosphere," *Philos. Trans. Roy. Soc. London*, **296**, 149–160, 1980.

Trinks, H. and K.H. Fricke, "Carbon Dioxide Concentrations in the Lower Thermosphere," *J. Geophys. Res.*, **84:** 3883, 1978.

Trost, T.F., "Electron Concentrations in the E and Upper D Region at Arecibo," *J. Geophys. Res.*, **84:** 2736–2742, 1979.

Twomey, S., B. Herman, and R. Rabinoff, "An Extension to the Chahine Method of Inverting the Radiative Transfer Equation," *J. Atmos. Sci.*, **34:**1085, 1977.

Tyson, B.J., J.F. Vedder, J.C. Arvesen, and R.B. Brewer, "Stratospheric Measurements of CF_2Cl_2 and N_2O," *Geophys. Res. Lett.*, **5:**369–372, 1978.

UNEP, *Report of the 3rd Session*, United Nations Environmental Programme, Coordinating Committee on the Ozone Layer, United Nations, New York, 1979.

UNEP, *Report on the 4th Session*, United Nations Environmental Programme, Coordinating Committee on the Ozone Layer, New York, 1980.

Vedder, J.F., B.J. Tyson, R.B. Brewer, C.A. Boitnott, and E.C.Y. Inn, "lower Stratosphere Measurements of Variation with Latitude of CF_2Cl_2, $CFCl_3$, CCl_4, and N_2O Profiles in the Northern Hemisphere," *Geophys. Res. Lett.*, **5:**33–36, 1978.

Vedder, J.F., E.C.Y. Inn, B.J. Tyson, C.A. Boitnott, and D. O'Hara, "Measurements of CF_2Cl_2, $CFCl_3$, and N_2O in the Lower Stratosphere between 2°S and 73°N Latitude," *J. Geophys. Res.*, **86:**7363–7368, 1981.

Volz, A., U. Schmidt, J. Rudolph, D.H. Ehhalt, F.J. Johnson, and A. Khedim, "Vertical Profiles of Trace Gases at Mid-Latitudes," Jul-Report No. 1742, Kernforschungsanlage, Julich, Federal Republic of Germany, 1981.

von Zahn, U., "Neutral Air Density and Composition," *Physics and Chemistry of the Upper Atmosphere*, D. Reidel, Dordrecht, Holland, 1973.

Voss, H.D., and L.G. Smith, "Global Zones of Energetic Particle Precipitation," *J. Atmos. Terr. Phys.*, **42:**227–239, 1980.

Wang, P., M.P. McCormick, and W.P. Chu, "A Study on the Planetary Wave Transport of Ozone During the Late February 1979 Stratospheric Warming Using the SAGE Ozone Observation and Meteorological Information," *J. Atmos. Sci.*, **40:**2419–2431, 1983.

Waters, J.W., J.J. Gustincic, P.N. Swanson, and A.R. Kerr, "Measurements of Upper Atmospheric H_2O Emission at 183 GHz," *Atmospheric Water Vapor*, edited by A. Deepak, T.D. Wilderson, and L.H. Ruhnke, Academic Press, New York, 229–440, 1980.

Waters, J.W., J.C. Hardy, R.F. Jarnot, and H.M. Pickett, "Chlorine Monoxide Radical, Ozone, and Hydrogen Peroxide: Stratospheric Measurements by Microwave Limb Sounding," *Science*, **214:**61–64, 1981.

Weeks, L.H. R.E. Good, J.S. Randhawa, and H. Trinks, "Ozone Measurements in the Stratosphere, Mesosphere, and Lower Thermosphere During Aladdin 74," *J. Geophys. Res.*, **83:**978–982, 1978.

Weinrab, M.P., W.A. Morgan, I-L. Chang, L.D. Johnson, P.A. Bridges, and A.C. Neverdoffer, "High Altitude Balloon Test of Satellite Solar Occultation Instrument for Monitoring Stratospheric O_3, H_2O, and HNO_3," *J. Atmos. Oceanic Tech.*, **1:**87–100, 1984.

Weinstock, E.M., M.J. Phillips, and J.G. Anderson, "*In situ* Observations of ClO in the Stratosphere: A review of Recent Results," *J. Geophys. Res.*, **86:**7273–7278, 1981.

Whitten, R.C. and S. Prasad (eds). *Ozone in the Free Atmosphere*, Von Nostrand Reinhold, New York, 1985.

Wilcox, R., "Total Ozone Trend Significance from Space and Time Variability of Daily Dobson Values," *J. Appl. Meteorol.*, **17:**1569–1591, 1978.

Wilcox, R., G. Nastrom, and A. Belmont, "Periodic Variations of Total Ozone and Its Vertical Distribution," *J. Appl. Meteorol.*, **16:**290–298, 1977.

WMO (World Meteorological Organization), *Assessment of Performance Characteristics of Various Ozone Observing Systems*, Report of the meeting of Experts, Boulder, July 1980, WMO Global Ozone Research and Monitoring Project Report No. 9, 1981.

WMO (World Meteorological Organization), *The Stratosphere 1981, Theory and Measurements*, WMO Global Ozone Research and Monitoring Project Report No. 11, NASA/GSFC, Greenbelt, Md., 1982.

Wofsy, S.C. and M.B. McElroy, "HO_x, NO_x and ClO_x: Their Role in Atmospheric Photochemistry," *Can. J. Chem.*, **52:**1582–1592, 1974.

Wuebbles, D.J., F.M. Luther, and J.E. Penner, "Effect of Coupled Anthropogenic Perturbations on Stratospheric Ozone," *J. Geophys. Res.*, **88:**1444–1456, 1983.

Zander, R., H. Leclercq, and L.D. Kaplan, "Concentration of Carbon Monoxide in the Upper Stratosphere," *Geophys. Res. Lett.*, **8:**365–368, 1981a.

Zimmerman, P.R., R.B. Chatfield, J. Fishman, P.J. Crutzen, P.L. Hanst, "Estimates of the Production of CO and H_2 from the Oxidation of Hydrocarbon Emissions from Vegetation," *Geophys. Res. Lett.*, **5:**679–682, 1978.